DEVELOPMENT AND EVALUATION OF MAGNETIC AND ELECTRICAL MATERIALS CAPABLE OF OPERATING IN THE 800° TO 1600°F TEMPERATURE RANGE

Second Quarterly Report

by

P. E. Kueser et al

prepared for

NATIONAL AERONAUTICS AND SPACE ADMINISTRATION
LEWIS RESEARCH CENTER
UNDER CONTRACT NAS3-6465

Westinghouse Electric Corporation
AEROSPACE ELECTRICAL DIVISION
LIMA, OHIO

Report No. 65.42E

June 1965

DEVELOPMENT AND EVALUATION OF MAGNETIC AND ELECTRICAL MATERIALS CAPABLE OF OPERATING IN THE 800° TO 1600°F TEMPERATURE RANGE

SECOND QUARTERLY REPORT
(MARCH 1, 1965 - MAY 31, 1965)

sponsored by

NATIONAL AERONAUTICS AND SPACE ADMINISTRATION
CONTRACT NAS3-6465

Project Management
NASA - Lewis Research Center
Space Power Systems Division
R. A. Lindberg

Prepared by: Approved by:

P. E. Kueser, et al   N. W. Bucci, Jr.,
Manager, NASA Materials Study   Manager, Engineering
and Research Program   Systems Research and
                                                Development Department

Westinghouse Electric Corporation
Aerospace Electrical Division
Lima, Ohio

PREFACE

In a program of this magnitude a large group of engineers and scientists are involved in its progress. An attempt to recognize those who are contributing directly, together with their area of endeavor, follows:

Program I - Magnetic Materials for High Temperature Operation

Task 1 - Optimized Precipitation Hardened Magnetic Materials for Application in the 1000 to 1200°F Range

Dr. K. Detert (WR&D); J. W. Toth (WAED)

Task 2 - Investigation for Raising the Alpha to Gamma Transformation Temperature in Cobalt-Iron Alloys

Dr. K. Detert (WR&D); J. W. Toth (WAED)

Task 3 - Dispersion-Strengthened Magnetic Materials for Application in the 1200 to 1600°F Range

Dr. R. J. Towner (WAED)

Task 4 - Creep Testing

M. Spewock (WR&D); D. H. Lane (WAED)

Program II - High Temperature Capacitor Feasibility

R. E. Stapleton (WAED)

Program III - Bore Seal Development and Combined Material Investigation Under a Space Simulated Environment

Task 1 - Bore Seal Development

R. C. McRae, Dr. L. Reed (EIMAC); J. W. Toth (WAED)

Tasks 2, 3, 4 - Stator and Bore Seal, Transformer and Solenoid

W. L. Grant, H. E. Keneipp, D. H. Lane, R. P. Shumate, J. W. Toth (WAED)

Dr. A. C. Beiler (WAED) and Dr. G. W. Wiener (WR&D) are acting as consultants on Program I.

SUMMARY

This is the Second Quarterly Report on Contract NAS3-6465 for the Development and Evaluation of Magnetic and Electrical Materials Capable of Operating in the Temperature Range from 800°F to 1600°F. Advanced space electric-power systems are the area of eventual application.
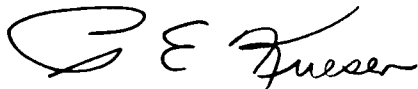
Program I is directed at developing high-temperature magnetic material with satisfactory strength for rotor use. Additions of tungsten and niobium markedly increased the stability at 1025°F of martensitic type alloys over conventional systems. As yet, no cobalt-base alloys evaluated have exhibited strength properties superior to Nivco alloy (23Ni, 2Ti, 1Zr, Bal. Co). The prealloyed powders and composite powders to be used in dispersion strengthening of magnetic materials are being prepared. The 5000 hour creep test on Nivco alloy were initiated and pressures of 4×10^{-8} torr have been realized at 1100°F in capsules.

Program II will determine the feasibility of a high-temperature capacitor using high-quality dielectric materials. Pyrolytic boron-nitride has been prepared in thicknesses of 1.12 mils, electroded with platinum, and exhibited electrical strengths of 10,400 volts/mil at room temperature. Its dielectric constant changed less than one percent when tested from room temperature to 1100°F.

Program III incorporates developments on alkali metal compatible ceramic-to-metal seals on combinations of materials designed into a stator with a bore seal, a transformer, a solenoid for investigations of compatibility under electrical and magnetic stress, at elevated temperature and high vacuum. The vacuum loading chamber for alkali-metal loading has been completed. The thermal vacuum chamber for evaluating the stator, transformer, and solenoid has been tested at the subcontractor at 10^{-11} torr under clean, dry and empty conditions.

TABLE OF CONTENTS

TABLE OF CONTENTS - Continued

TABLE OF CONTENTS - Concluded

LIST OF FIGURES

LIST OF FIGURES - Continued

LIST OF FIGURES - Concluded

LIST OF TABLES

SECTION I

INTRODUCTION

This is the second quarterly report on Contract NAS3-6465 for the Development and Evaluation of Magnetic and Electrical Materials Capable of Operating in the Temperature Range from 800°F to 1600°F. The period of performance is from March 1, 1965 through May 31, 1965. The program consists of three Programs with their related tasks as follows:

Program I - Magnetic Materials for High-Temperature Operation

    Task 1 - Optimized Precipitation Hardened Magnetic Materials for Application in the 1000 to 1200°F Range

    Task 2 - Investigation for Raising the Alpha to Gamma Transformation Temperature in Cobalt-Iron Alloys.

    Task 3 - Dispersion-Strengthened Magnetic Materials for Application in the 1200 to 1600°F Range

    Task 4 - Creep Testing

Program II - High-Temperature Capacitor Feasibility

Program III - Bore Seal Development and Combined Material Investigations Under a Space Simulated Environment

    Task 1 - Bore Seal Development

    Task 2 - Stator and Bore Seal

    Task 3 - Transformer

    Task 4 - Solenoid

In Program I, limitations in magnetic material performance at elevated temperature have been recognized from Contract NAS3-4162 and the development of materials incorporating improved magnetic and mechanical properties is being pursued. In most cases, high-strength compromises the magnetic properties; therefore, a balance between these two variables is sought.

Program II is directed at determining the feasibility of applying high-quality dielectric materials and their processes to a high-temperature (1100°F) capacitor which is lightweight and suitable for static power conditioning apparatus used in space applications.

Program III incorporates development on ceramic-to-metal seals, on combinations of materials previously evaluated under Contract NAS3-4162 into a stator with a bore seal, a transformer, and a solenoid for investigations of compatibility under electrical and magnetic stress at elevated temperature and high vacuum.

The three Programs will be reported consecutively in Sections II, III and IV. Section II and Section IV are further divided into their respective tasks. Each task is reported separately and includes a summary of technical progress, a discussion, and the program for the next quarter so the reader may obtain an understanding of each task.

The First Quarterly Report was issued as NASA-CR-54354 and contains information referenced in this report.

SECTION II

PROGRAM I - MAGNETIC MATERIALS FOR
HIGH-TEMPERATURE OPERATION

Program I is directed at magnetic material improvement and a further understanding of existing magnetic materials suitable for application in the rotor of an alternator or motor in advanced space electric power systems.

Task 1 is concerned with precipitation-hardened magnetic materials in the 1000 to 1200°F range. These materials are of the iron-cobalt-nickel ternary system. The two specific areas of interest are the iron and cobalt corners of the ternary system.

Task 2 is a small research investigation for determining the feasibility of raising the alpha to gamma transformation temperature in the iron-cobalt system; thereby increasing the useful magnetic temperature of this system.

Task 3 is directed at applying dispersion-strengthening mechanisms to magnetic materials to achieve useful and invariant mechanical and magnetic properties in the 1200 to 1600°F range. Because both variables are influenced differently by particle size and spacing, a compromise is sought thereby tailoring the materials to the need of dynamic electric machines.

Task 4 is a creep program on Nivco alloy (approximately 72% cobalt, 23% nickel and certain other elements) which will generate 5000 hour design data in a vacuum environment (1×10^{-6} torr or less). This material represents a presently available magnetic material with the highest useful application temperature.

A. TASK 1 - OPTIMIZED PRECIPITATION HARDENED MATERIALS FOR HIGH TEMPERATURE APPLICATION

1. Summary of Technical Progress

A total of 35 alloys have been tested in the screening program. Twenty alloys consisted of martensitic type. Fifteen alloys were of the cobalt-base type.

The alloys were melted by the levitation melting technique. Dilatometer tests, magnetic saturation measurements and aging tests with hardness and coercivity measurements, and microstructure observations have been conducted. The results obtained show that a base composition of Fe-15Ni-25Co with the single addition of tantalum, molybdenum, tungsten, niobium, beryllium or titanium, when properly aged, produce high hardness in excess of 500 VHN and high magnetic saturation with B_S above 15,000 gauss at 1112°F (600°C). The structure stability appears sufficient at 1022°F (550°C) when tantalum, molybdenum, tungsten or niobium is added. No substantial change in hardness and coercivity can be measured after aging at 1022°F (550°C) up to 100 hours. This is a substantial improvement compared to commercial steels; however, some grain boundary precipitate may influence creep properties.

In the cobalt-base alloys, none of the mechanical properties which were checked appear superior to those of commercially available Nivco (23Ni, 1Zr, 2Ti, Balance Co) material. Structural stability appears to be no problem even at 1292°F (700°C).

2. Discussion

a. BACKGROUND

The objective of this program is to find and evaluate an alloy composition which displays high creep strength at elevated temperature together with useful ferromagnetic properties. The target ultimate tensile strength for the alloy at 1100°F is 125,000 psi or better. The target stress to produce 0.40 percent creep strain in 1000 hours at 1100°F is 76,000 psi or greater. The 10,000 hour stress target at 1100°F is 80 to 90 percent of that at 1000 hours. The target magnetic saturation for the developmental alloy is 13,000 gauss or better at 1100°F and a coercive force less than 25 oersteds. A screening program must be conducted as the first step in attaining this target.

The purpose of this screening program is to find a certain region of alloy composition, where the combination of desired mechanical and magnetic properties can be expected. The screening program must

4

cover a broad variety of alloy compositions using simple test methods. The levitation melting technique is suitable for producing small ingots in the range of 10 to 25 grams. Contamination of the ingot is held at a low level because the molten material does not come into contact with a crucible. The only possibility of contamination is the melting environment. Therefore, melting is done in an inert atmosphere (99.995% argon). The contact of the molten metal with the mold can be neglected because the small volume of metal solidifies and cools rapidly in the cold mold.

A large variety of tests cannot be performed on these small ingots. Therefore, a complete evaluation of mechanical and magnetic properties is not possible. However, several simple tests are adequate for the alloy screening program. The measurement of coercive force and magnetic saturation may be made on small samples and are sufficient for characterizing magnetic properties. The magnetic saturation measurements are made at elevated temperature 1112°F (600°C) as well as at room temperature. Coercivity tests are performed at room temperature only. In most cases, coercivity will be less at higher test temperatures than at room temperature. Table II-1 shows a comparison of saturation, coercive force and induction at 100 oersteds for several commercially available alloys. If, in the course of testing new alloys on the screening program, higher values for magnetic saturation and lower values of coercivity are determined, then the permeability of the new alloy will be better than that listed for the commercial alloys in Table II-1.

Unfortunately, there exists no simple method of testing to predict creep properties, for creep strength is a very complex property. High yield stress is a desirable though insufficient requirement for high creep strength. Hardness measurements allow prediction of yield strength within certain limits. Vickers pyramid hardness data can be multiplied by 450 to get a rough estimate of the 0.2 percent offset yield strength.

In order to obtain a high yield strength, precipitation hardening is being evaluated on this project. Isochronal aging with successive increments in temperature is being used to determine whether age-hardening by a precipitation reaction will occur in a specific alloy. After a homogenization annealing treatment, the samples will be aged for one hour at a temperature which will increase by 90°F (50°C) after each aging step. The room temperature Vickers hardness will be measured after each aging step. If precipitation hardening does occur, a certain temperature will be found at which a maximum hardness can be obtained. This temperature represents the best range for age hardening. The obtained hardness value represents the level of strength which may be achieved in this alloy.

TABLE II-1. Magnetic Properties of Several High-Strength Commercial Alloys

Material	Test Temperature	Induction at 100 Oersteds (gauss)	Coercivity (oersteds)	Saturation (gauss)	Hardness (VHN)
H-11 (Fe-5Cr-1.3Mo-0.5V-0.40C)	Room 792°F(425°C) 1112°F(600°C)(a)	16,400 14,800 12,500	23.9 18.4 14.1	18,000 15,000 13,500	560
15% Ni Maraging Steel (Fe-9Co-5Mo-0.70Ti-0.70Al-15Ni)	Room 792°F(425°C) 1112°F(600°C)(b)	16,500 14,400 10,000	22.6 19.6 38.1	18,500 15,800 13,000	580
Nivco (Co-23Ni-1Zr-2Ti)	Room 792°F(425°C) 1112°F(600°C)	10,800 10,200 9,800	11.46 8.43 6.31	12,500 12,000 11,000	360

(a) - Carbide precipitate not stable at 600°C.
(b) - Matrix not stable at 600°C.

If creep strength at a certain temperature is required, one can postulate as a second necessary but insufficient requirement that the age-hardened structure must stay stable so that yield strength does not decrease during service at this temperature. The temperature range where one can expect structure stability may be estimated by determining the temperature range where overaging occurs. Overaging is a definite indication that the structure is changing. In many cases the temperature range at which overaging is likely to occur is somewhat higher than the temperature range of maximum hardness determined by the isochronal testing method. However, many instances are known in which a decrease in yield strength occurs at a very low or negligible rate after some initial rearrangement of structure. A better indication of the rate of overaging may be obtained by isothermal aging at a specified temperature. The sample is aged at a constant temperature at varying periods of time. The intervals are commonly chosen to resemble a logarithmic sequence. The Vickers hardness is measured at room temperature. It is expected that a maximum hardness will be attained in the initial stages of the aging. The hardness when plotted on a logarithmic time scale gives an indication of the drop in hardness that can be expected at extrapolated times. The extrapolated values may be considered reliable estimates for periods which are more than 10 times larger than measured periods.

Coercivity as a structure sensitive property will also be influenced by the change of structure during overaging. Therefore, it will be useful to measure coercivity during the aging schedules. In most cases overaging is caused by coagulation of precipitate particles. However, it may also be caused, in some instances as in maraging steel, by a diffusion controlled decomposition of the ground matrix when phase transformation is to be expected. A dilatometer test may be applied to establish the temperature range where a phase transformation may occur. If the heating rate is rather low during the dilatometer test, a good estimate of the transformation temperature can be obtained even when the transformation reaction is rather sluggish.

The alloy selections for this program are based on the following concept:

The basic composition must provide magnetic saturation which is still adequate between 1022°F (550°C) and 1212°F (650°C). From the known data in the literature, which are best reviewed in Bozorth, "Ferromagnetism" (ref. 1)[a] it may be seen that there are two areas of general interest.

(a) - See Section V

7

1)   a ferritic or martensitic iron-cobalt alloy
2)   a cobalt alloy

Iron-Cobalt alloys with cobalt between 30 and 50 percent appear to be the most suitable as far as a high value of magnetization is concerned. In Figure II-1, the magnetization dependence of iron-cobalt on cobalt content is plotted as remeasured at the Westinghouse Laboratories. The values differ slightly from earlier results in the literature (refs. 2, 3 & 4). However, it might be necessary to keep the cobalt content well below 30 percent to avoid embrittling effects. For a similar reason compositions in which the phase transformation results in a hexagonal phase, as in pure cobalt, must be avoided. This may be accomplished by the addition of at least five percent iron.

The basic alloy compositions which provide the required magnetic saturation at service temperature do not possess the required strength. Therefore, suitable alloying elements must be added to provide a useful precipitation hardening reaction. R. F. Decker recently presented a review of potent precipitation hardening reactions in high temperature alloys and in steel (refs. 5 & 6). It is generally accepted that a precipitation process involving intermetallic compounds is preferred to carbide formation when stability at temperature is required. Of all known precipitate phases which occur, only precipitation of an A_3B phase appears to lead to a potent precipitation strengthening process. This process, however, never occurs in ferritic iron-cobalt or in face-centered cubic cobalt alloys unless a substantial amount of nickel is present. A discussion of the strengthening possibilities in martensitic alloys will be presented first.

It has been shown that in martensitic alloys with nickel content between 12 and 25 percent, the so called maraging treatment can be applied. This gives very high strength and good toughness (refs. 7, 8, 9 & 10). The limitation of the commercial maraging steels, as far as service temperatures concerned, is caused by the instability of the parent phase which will revert into austenite at temperatures exceeding 662° to 932°F (350° to 500°C) depending on the alloy composition.

The purpose of the screening program is, therefore, to select a suitable composition, which fulfills the following requirements.

1)   Magnetic saturation is high enough at service temperature (target line B_s = 13,000 gauss   or σ = 130 emu/g at 1112°F (600°C))

8
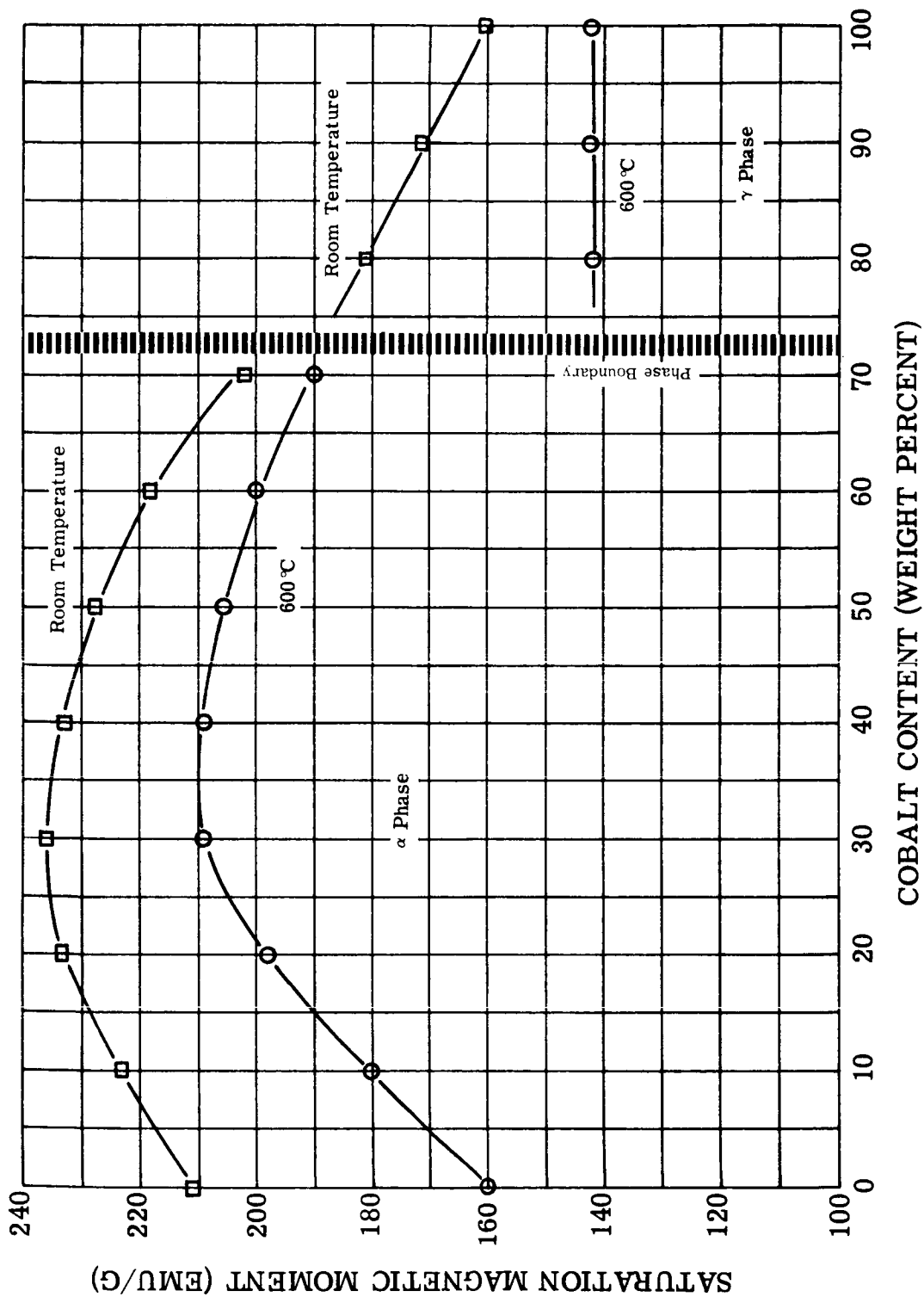
FIGURE II-1. Influence of Cobalt Content on the Saturation Magnetic Moment in the Iron-Cobalt System

Figure II-1. Magnetic Saturation Vs. Cobalt Content in the Fe-Co System

2) Alpha to gamma transformation starts during slow heating ($\leqq$ 90°F (5 °C)/min) above 1112°F (600°C)

3) A precipitation reaction occurs such that a hardness of more than 500 VHN can be achieved during aging at 1022°F (550°C) to 1112°F (600°C).

Previous work has shown (refs. 11 & 12) that 15% Ni Maraging steel, which contains 8% Co, 15% Ni, does not possess sufficient temperature stability. The phase diagram of Fe-Co-Ni (ref. 13) indicates that lowering the nickel content and increasing the cobalt content increases the transformation temperature of the alpha phase and hence the stability of the alpha phase.

Previous studies at the Westinghouse Research Laboratories indicated that an alloy containing 15% Ni, 25% Co, Balance Fe might provide sufficient thermal stability with substantially increased saturation as compared to maraging steel. The measured data are listed in Table II-2.

In the first series of martensitic type alloys on this program (alloys 1-A-1 to 1-A-10, Table II-3), the influence of an addition of a single element to this composition was to be checked; that is, whether precipitation hardening could be obtained and whether the transformation temperature was changed compared to Fe-15Ni-25Co. The list of elements chosen were based on the results of Floreen's work on Fe-18Ni (ref. 14). Floreen showed that titanium beryllium, tantalum, aluminum, niobium, molybdenum, manganese and silicon produced age hardening in Fe-18Ni. The list of elements used for the present program did not contain titanium, molybdenum and tantalum. Experiments performed in 1964 at the Westinghouse Research Laboratories confirmed that these latter elements induce precipitation hardening in Fe-15Ni-25Co. The elements vanadium, tungsten, chromium, antimony and tin were included for investigation on this program. A study of the binary systems (ref. 15) indicates that intermetallic phases with melting points above 1832°F (1000°C) might be formed with at least one of the components iron, nickel, or cobalt so that one can not rule out the possibility that precipitation hardening might occur. The amount added was arbitrarily set to permit the total amount to go into solution at the heat treatment temperature of 1832°F (1000°C).

The second series of alloys, 1-A-11 to 1-A-20, does not contain an element to produce age hardening. Only transformation temperature and saturation had to be checked in order to establish a suitable composition with 12Ni-iron containing cobalt in the required amount to insure adequate temperature stability and magnetic saturation.

TABLE II-2. Properties of Fe-15Ni-25Co Alloy

Transformation Temperature		
Heating	$\alpha \longrightarrow \gamma$	$\gamma \longrightarrow \alpha$
54°F/min (30°C/min)	1319-1553°F (715-845°C)	--
9°F/min (5°C/min)	1300-1560°F (704-849°C)	--
Cooling	$\alpha \longrightarrow \gamma$	$\gamma \longrightarrow \alpha$
54°F/min (30°C/min)	--	977-743°F (525-395°C)
9°F/min (5°C/min)	--	1011-745°F (544-396°C)
Magnetic Saturation		
	Room Temperature	1112°F (600°C)
Specific magnetic moment σ/g in centimeter-gram-second (cgs)	216 emu/g[a]	174 emu/g[a]
(a) - Saturation in gauss can be estimated by multiplying cgs units by 100		

TABLE II-3. Composition of Martensitic Alloys 1-A-1 to 1-A-20
Investigated During the Second Quarter

Alloy Number	Nominal Alloy Composition (weight percent)	Remarks
	(Group 1)	
1-A-1	55Fe-15Ni-25Co-5W	two remelts
1-A-2	58Fe-15Ni-25Co-2Nb	
1-A-3	58Fe-15Ni-25Co-2V	
1-A-4	58Fe-15Ni-25Co-2Cr	
1-A-5	59.5Fe-15Ni-25Co-0.5Al	one remelt
1-A-6	58Fe-15Ni-25Co-2Be	
1-A-6V	59Fe-15Ni-25Co-1Be	modification of 1-A-6
1-A-6W	59.5Fe-15Ni-25Co-0.5Be	modification of 1-A-6
1-A-7	58Fe-15Ni-25Co-2Sb	
1-A-7V	59Fe-15Ni-25Co-1Sb	modification of 1-A-7
1-A-8	58Fe-15Ni-25Co-2Sn	
1-A-8V	59Fe-15Ni-25Co-1Sn	modification of 1-A-8
1-A-9	58Fe-15Ni-25Co-2Si	one remelt
1-A-9V	59Fe-15Ni-25Co-1Si	modification of 1-A-9
1-A-10	58Fe-15Ni-25Co-2Mn	
	(Group 2)	
1-A-11	88Fe-12Ni	
1-A-12	83Fe-12Ni-5Co	
1-A-13	78Fe-12Ni-10Co	
1-A-14	73Fe-12Ni-15Co	
1-A-15	68Fe-12Ni-20Co	
1-A-16	63Fe-12Ni-25Co	
1-A-17	58Fe-12Ni-30Co	
1-A-18	53Fe-12Ni-35Co	
1-A-19	48Fe-12Ni-40Co	
1-A-20	43Fe-12Ni-45Co	

A large variety of cobalt base alloys have been developed as high-temperature materials (refs. 16 & 17). These alloys are either non-magnetic or have very poor magnetic saturation although the range of service temperature might be well above the 1022° to 1202°F (550° to 650°C) range. A few investigations have been made to study precipitation hardening in ferromagnetic alloys (refs. 17, 18, 19 & 20). It appears that one can expect very potent precipitation hardening in cobalt-base alloys only when a face centered cubic phase in the form A_3B is formed (ref. 6). This again requires a substantial amount of nickel present. To obtain good creep strength, discontinuous precipitation which will be favored in cobalt-base alloys (refs. 20 & 21) must be avoided.

The purpose of the first group of alloys, listed in Table II-4, is to study the influence of the addition of iron and nickel on saturation. The tolerable saturation limit is set at $B_s = 11,000$ gausses at 1112°F (600°C). The second group of alloys is chosen to determine the nickel content required to obtain age hardening. The minimum limit of hardness is set at 350 VHN. The addition of 3Ti+1Al was chosen because these elements in this ratio provide precipitation hardening in super alloys of the Nimonic type (ref. 22).

b. EXPERIMENTAL PROCEDURE

(1) Levitation Melting

The experimental screening alloys were prepared by the levitation melting technique. In general, a cylindrical compaction was made about 5/8 inch diameter and 3/4 inch high with a weight of 20 to 25 grams. A pressure of 220,000 psi was applied for one minute. Tiny chips of electrolytic grade nickel, cobalt, and iron were used. Table II-5 lists the metals used according to supplier, trade name, and analysis when it was available from the supplier. The alloying elements present in smaller percentages were added as small, coarse slugs tightly wrapped in cobalt or nickel foil. The small wrapped package was inserted in the center of the compaction.

The levitation melting was performed in a chamber which was first pumped down to better than 10^{-2} torr. Then pure argon* was added to yield a pressure of 9/10 of atmospheric pressure. The levitation melting technique was recently described in detail by W. A. Pfeifer (ref. 23). For this study, a funnel-shaped coil of five windings was used. The frequency stayed in the range of 550 kilocycles, the input energy in the range of 3 to 5 kilowatts, and the operating voltage was near 750 volts.

*Argon was supplied by Airco with purity 99.95%, -85°F dew point.

13

TABLE II-4. Composition of Cobalt-Base Alloys 1-B-1 to 1-B-15
Investigated During the Second Quarter

Alloy Number	Nominal Alloy Composition (weight percent)
	(Group 1)
1-B-1	95Co-5Fe
1-B-2	90Co-5Fe-5Ni
1-B-3	85Co-5Fe-10Ni
1-B-4	80Co-5Fe-15Ni
1-B-5	75Co-5Fe-20Ni
1-B-6	70Co-5Fe-25Ni
1-B-7	65Co-5Fe-30Ni
1-B-8	85Co-10Fe-5Ni
1-B-9	80Co-15Fe-5Ni
1-B-10	75Co-20Fe-5Ni
1-B-11	70Co-25Fe-5Ni
1-B-12	65Co-30Fe-5Ni
	(Group 2)
1-B-13	86Co-5Fe-5Ni-3Ti-1Al
1-B-14	81Co-5Fe-10Ni-3Ti-1Al
1-B-15	76Co-5Fe-15Ni-3Ti-1Al

TABLE II-5. Analyses of Metals Used in Experimental Alloys (weight percent)

Material	Supplier	Designation	Fe	Co	Ni	Be	V	Ti	
Iron [a]	The Glidden Co.	Electrolytic Iron Alloy	99.9	0.002	0.005	0.0005		0.001	0.0
Cobalt [a]	International Nickel Co.	Electrolytic Cobalt	0.0015	99.61	0.35				
Nickel [a]	International Nickel Co.	Electrolytic Nickel	0.04		99.95				
Beryllium [b]	Brush Beryllium Co.	Beryllium Pebbles				95			
Titanium	Frankel Co.	Titanium Chips	0.25					99.1-99.3	
Aluminum [b]	Alcoa	Pure Aluminum Bar	0.05					0.007	
Manganese [b]	Foote Mineral Co.	Electrolytic Manganese	0.001						

Material	Supplier	Designation	Cr	Sn	Sb	Si	Zn	Ge	
Chromium [a]	Union Carbide Metals Co.	Elchrome HP	99.94			0.004			
Tin [a]	Fisher Scientific Co.	T-124 Tin Shot		99.9					
Antimony [a]	J. T. Baker Chemical Co.	Assay Sb 100			99.97				
Silicon [a]	Electro-Metallurgical Co.	Silicon Metal Low Al				98.64			
Zinc [a]	Fisher Scientific Co.	Granular Zinc Metal					99.97		
Germanium	Westinghouse Electric Corp.	Semiconductor Grade						99.999	
Niobium [a]	Electro-Metallurgical Co.	Roundals							99. min
Tantalum [a]	Electro-Metallurgical Co.	Roundals							

(a) - Lot analysis provided by supplier.
(b) - Typical analysis provided by supplier.

l	Mn	Si	C	Cu	S	V	H	N	O	Other
03	0.001	0.001	0.004	0.001	0.004	0.005				P-0.003
			0.016	0.005	0.001					Pb-0.00026
		Trace	Trace	0.03	Trace					
										Slag 4%
			0.10							Total < 0.6
	0.001	0.04	0.0039	0.011		0.01				Mg-0.002 Ga-0.01
	99.9 min.	Trace	0.004		0.024		0.015 max.	0.001 max.		P-Not detectable Heavy Metals 0.005 max.

b	Ta	Fe	C	As	Cu	Pb	H	N	O	Other
		0.004	0.007				0.0003	0.008	0.0089	S-0.006
		0.005		0.00005	0.001	0.020				Total foreign metals 0.05
		0.002		0.004	0.002	0.004				
		0.75								Al-0.05 Ca-0.01
		0.01		0.000001		0.010				
	99.6 min.									

15 B

The procedure for melting consisted of heating the compac-
tions to the melting temperature within 60 seconds. Within
five seconds, the entire surface appeared molten. The sample
was kept in the molten state for eight seconds more. During
this period, the temperature increased further; an indication
that the sample was completely molten. Then the melted
mass was dropped into a copper mold beneath the coil by
turning the power off. The mold was slightly tapered to pro-
vide a bar-shaped ingot with a 9/32 inch diameter on one end
and 5/16 inch diameter on the upper end. The ingot was
1-7/8 inches long.

The cast structure always shows a homogeneous phase as
shown in a typical photograph in Figure II-2. A dendritic
growth from the outside wall into the center may be noted.
The appearance of rather large dendritic growth even after
casting in a cold mold proves that the purity and homogenity
of the material is very good.

One must anticipate that a fraction of the added elements with
higher vapor pressure such as manganese, chromium, and
those with activity toward oxygen like aluminum, titanium
and beryllium, will be lost during melting. The method of
compaction and the use of inert gas will provide some protec-
tion against evaporation and oxidation. Therefore, one can
expect, based on the experience gained in levitation melting
practice, that less than 20 percent of the total amount of these
elements might be lost during the melting procedure. An
analysis to determine the actual amount of alloying constituent
in the melted ingot was omitted on the screening program.
Analysis becomes necessary, however, when selection of
the better alloys is made for preparation of larger ingots
later in the program.

(2)   Machining

Specimens for saturation measurements were machined from
all ingots except those of the remelts and substitute alloys.
The specimens were 1/10 inch in diameter and 1/10 inch high.
Dilatometer samples were machined to bars 1/4 inch in diam-
eter and one inch long.

(3)   Cold Rolling

The dilatometer rod samples of alloys 1-A-1 to 1-A-15 were
cold rolled (~50% reduction) in a two high mill with eight
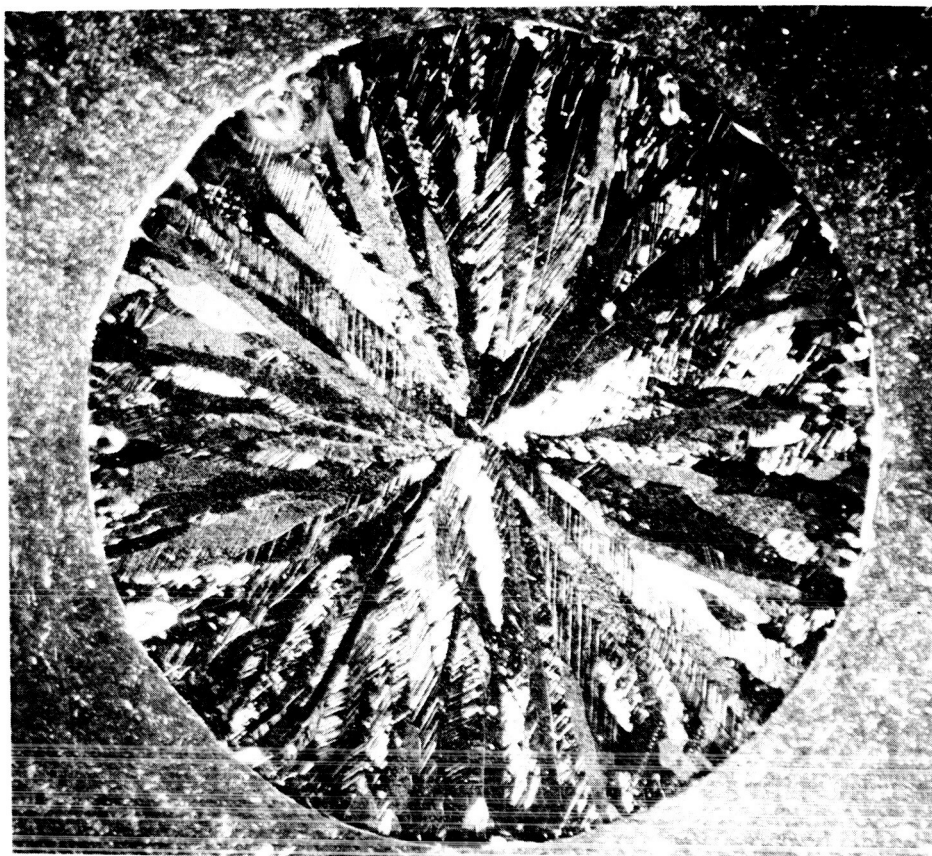
Photograph shows dendritic growth in the levitation
melted ingot.   The grains contain many twins.

FIGURE II-2.   Photograph of As-cast Structure of Cobalt Base
Alloy 1-B-4 (80Co-5Fe-15Ni) 14X

inch diameter rolls at low speed (1 in/sec). All samples, except 1-A-2, 1-A-3, 1-A-4, 1-A-10, 1-A-11 and 1-A-12, broke during the first pass. The alloys 1-A-7 and 1-A-8 were extremely brittle. Alloys 1-A-1, 1-A-5 and 1-A-9 were remelted and the machined bars were annealed at 1832°F (1000°C) for 30 minutes, quenched in oil, and warmed up to 212°F (100°C) before rolling. The dilatometer sample of alloy 1-A-16 was similarly treated. Rolling of these four samples (1-A-1, 1-A-5, 1-A-9 and 1-A-16) was partially successful. Alloy sample 1-A-1 developed cracks on one end. 1-A-9 developed edge cracks completely around the piece but did not break. Substitute alloys with reduced addition of beryllium, tin or antimony were made as shown in Table II-3. After treating and rolling in the same manner as the remelts, the samples with tin and antimony broke again, appearing extremely brittle. The sample with 1% Be also broke, but the sample with 0.5% Be was rolled successfully. The bars of alloys 1-B-13, 1-B-14, 1-B-15, presented in Table II-4, were annealed for two hours at 1832°F (1000°C), cooled in the cooling chamber of the furnace, then cold rolled to flat 25 mil strip.

(4)   Saturation Measurements and Dilatometer Tests

Descriptions of saturation measurements and dilatometer tests were presented in the First Quarterly Report (NASA-CR-54354).

(5)   Aging Tests

The sequence of treatments and tests to obtain change of hardness by isochronal aging with incremental increases in temperature is shown in Figure II-3. The sequence of aging treatment for alloy series B differed slightly from series A in that the lowest temperature of aging was 932°F (500°C), the highest was 1382°F (750°C).

After the isochronal aging the samples were homogenized. The homogenization treatment consisted of two heat treatments with a light reduction pass in between. The change of hardness and coercivity was determined after isothermal aging at 1022°F (550°C) for the martensitic alloys and at 1292°F (700°C) for the cobalt-base alloys. The flow-chart describing the thermal-mechanical treatment and isothermal aging is shown in Figure II-4. The total aging time was 100 hours. The type of salt used in the aging bath depended on the aging temperature (see Table II-6). The austenitizing anneal was done in an argon

18
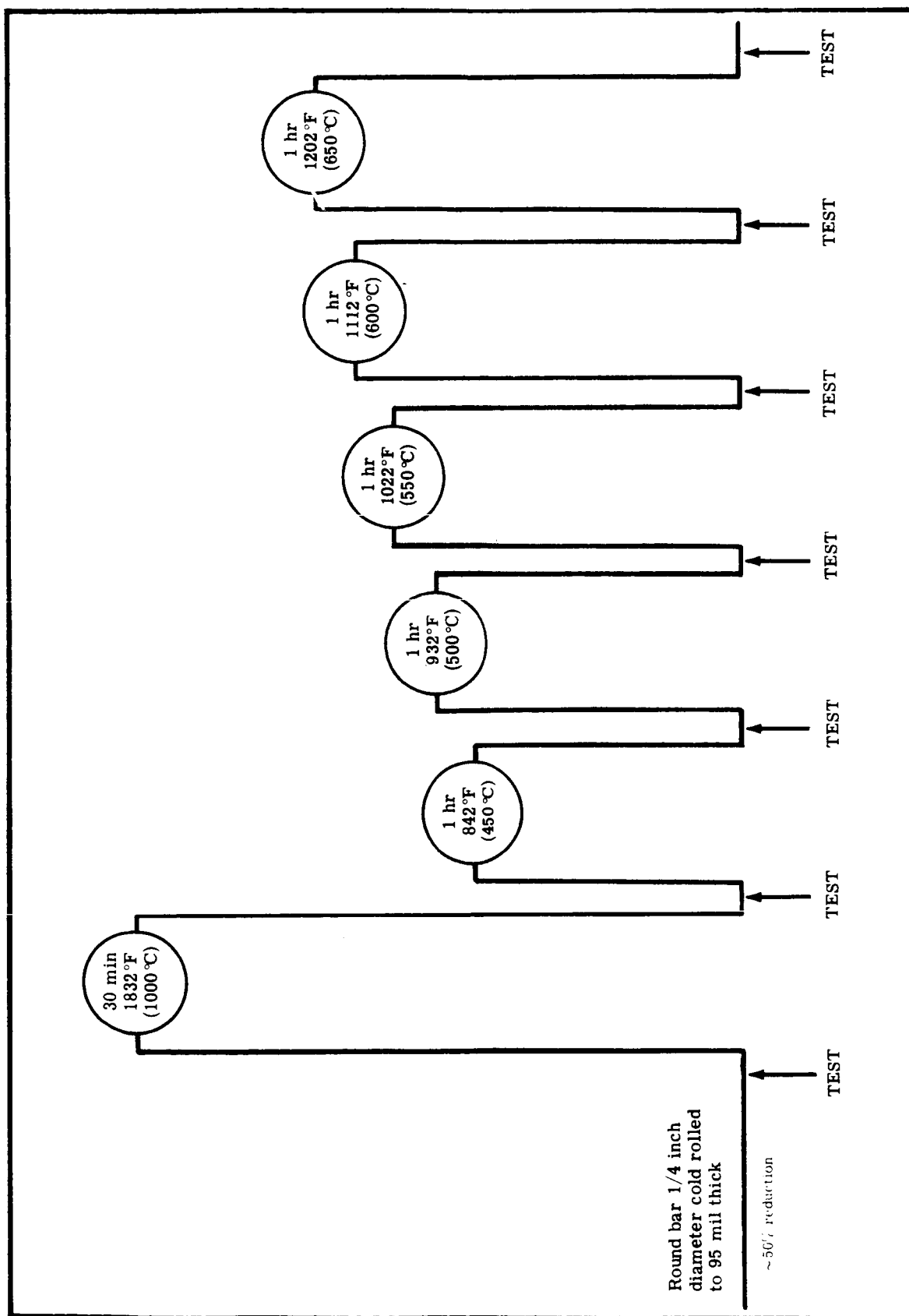
FIGURE II-3. Flow Chart for the Treatment of Martensitic Alloys During Isochronal aging. One Test Consists of Vickers Pyramid Hardness Measurements (3 indentations) and Coercivity Measurements at Room Temperature (4 readings).

19
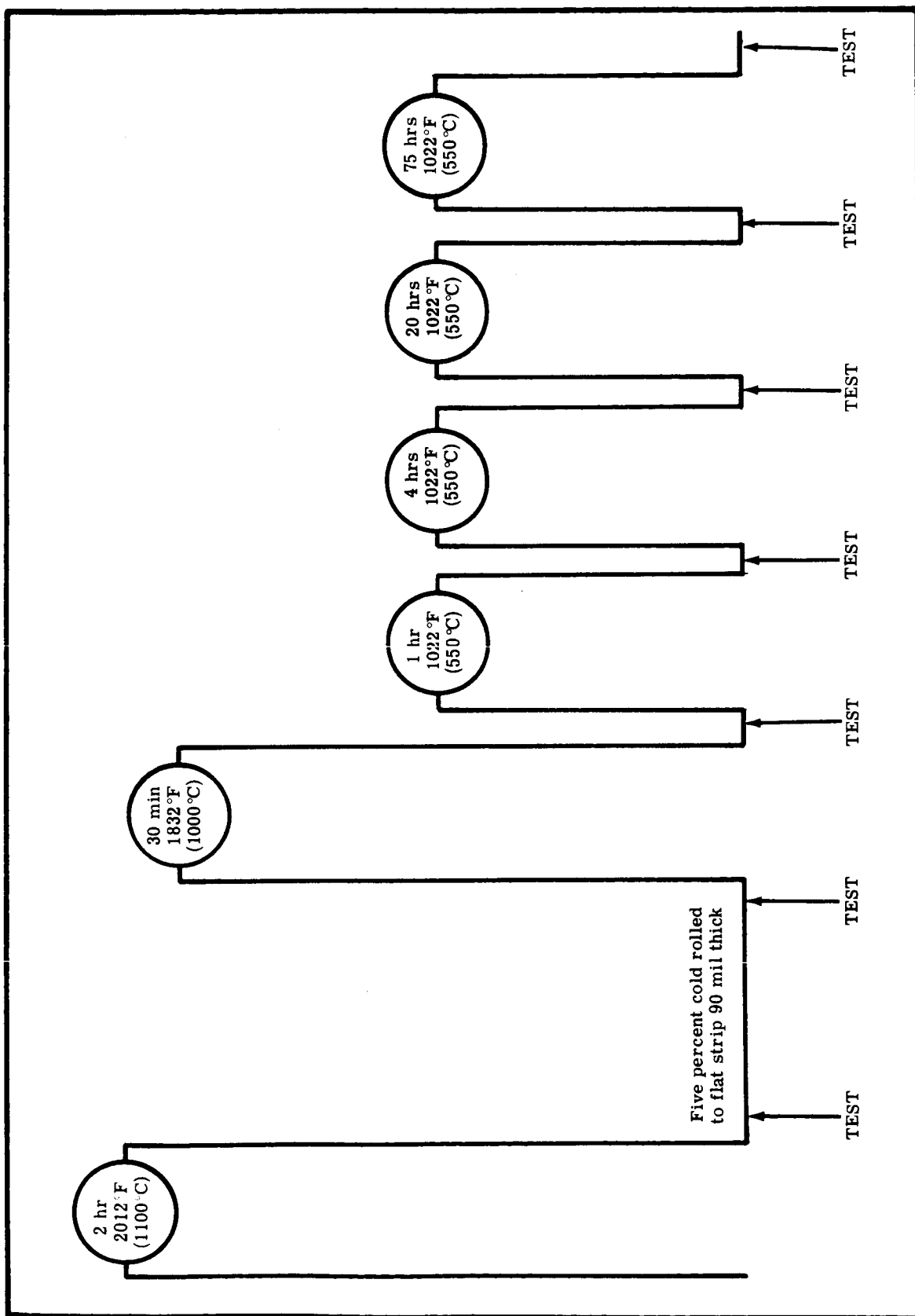
FIGURE II-4. Flow Chart for the Isothermal Aging of Martensitic Alloys.
One Test Consists of Vickers Pyramid Hardness Measurements
(3 indentations) and Coercivity Measurements at Room Temperature
(4 readings).

TABLE II-6. Type of Salt Bath Used for the Aging Treatments

Temperature of Treatment	Salt Designation	Main Constituents	Supplier
842-1022°F (450-550°C)	Thermosalt #311	Blend of Alkali Nitrates and Nitrites	Carmac Chemical Company
1112-1292°F (600-700°C)	Thermosalt #914	Ternary Mixture of Alkali and Alkaline Chlorides	Carmac Chemical Company
1382°F (750°C)	Thermosalt #1018	Eutectic Mixture of Chlorides	Carmac Chemical Company

or helium flushed tube furnace set at temperature. Hardness
was measured by the Vickers pyramid method using a 50 kg
load, 15 second indentation time. Three indentations were
made and the mean value determined. The coercivity was
measured in the Koerzimeter made by the Forster Co.,
Reutlingen, Germany (Figure II-5). This instrument is
capable of measuring the coercive force of samples with
small or unusual geometry. The sample was magnetized in
a large field coil, the magnetizing field being 1300 oersteds.
After switching off the field, the remanent field of the samples
was determined by a very sensitive field probe as seen in Fig-
ure II-6. A reverse field was then applied increasing gradually
from zero until the field probe did not measure any remanent
field from the sample. The measured value of coercivity was
established by four readings. Between each reading the direc-
tion of the applied magnetizing field was reversed.

The samples were mechanically polished in a conventional
way and then etched for observation of microstructure. Buehler
automatic polishing equipment was used. Linde A polishing
powder was applied for the final polishing stage.

The following etchants were used. A mixture of 20 ml HCl,
40 ml HNO_3, 60 ml glycerin was very successful for the
sample 1-B-15. All the other samples which were reported
in this study were electrolytically etched in the Buehler appara-
tus for electrolytic polishing and etching. The surface
was 1/4 inch diameter, the current density was about 1 A/cm^2.

c.   RESULTS

The results of the dilatometer tests for samples 1-A-1 to 1-A-20
were reported in the First Quarterly Report (NASA-CR-54354).
The saturation measurements of samples 1-A-11 to 1-A-20 had
been completed in the first quarter and were reported in the first
quarterly report.

The results of saturation measurements on samples 1-A-1 to 1-A-10
are listed in Table II-7. The measured room temperature values
of samples in the as-cast condition are listed in the first column.
The samples were then subjected to an aging treatment of one hour
at 1112°F (600°C) in a helium flushed tube furnace. The measured
saturation values of samples in the aged condition at room tempera-
ture and at 1112°F (600°C) are listed in the second and third columns
of Table II-7.
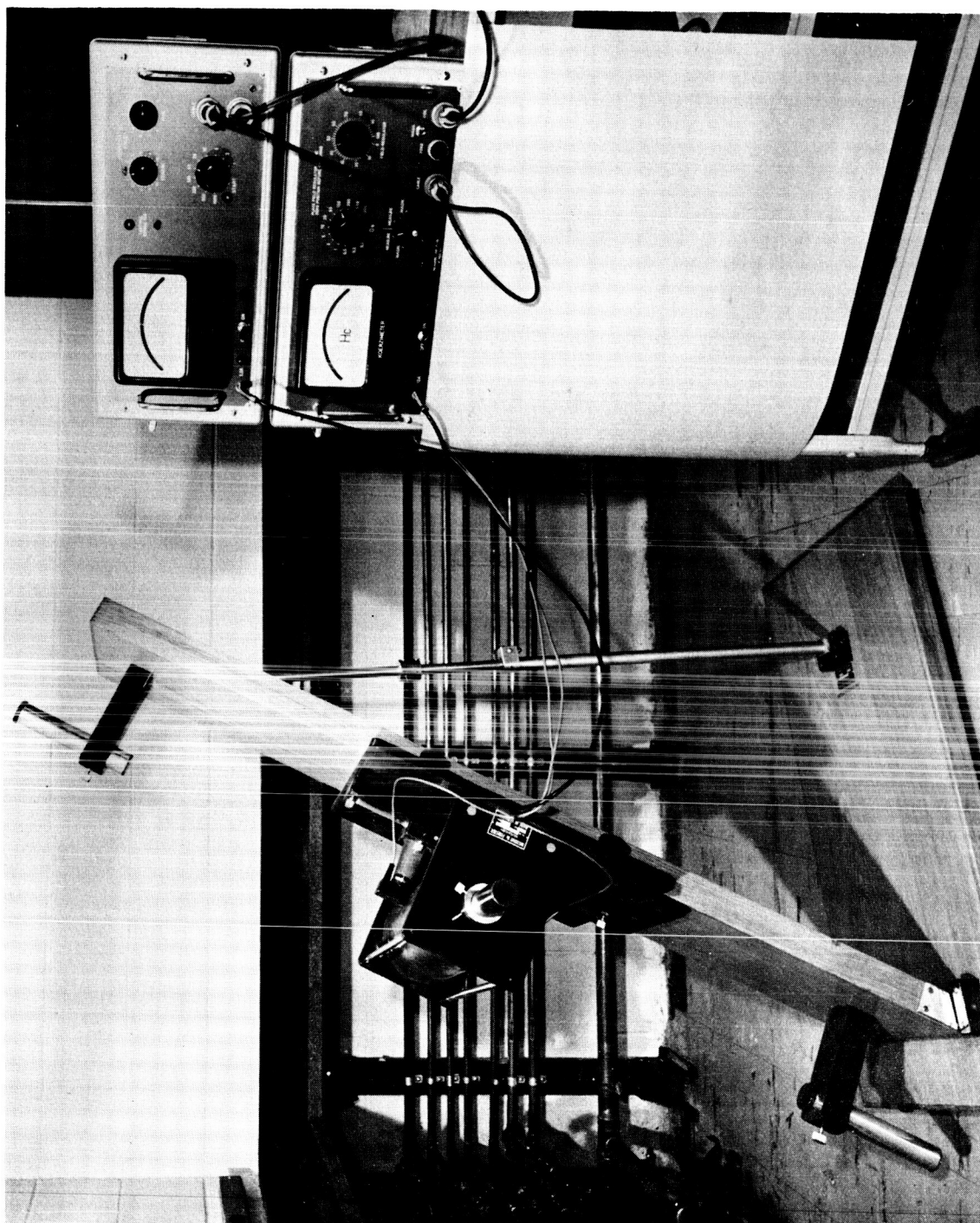
FIGURE II-5. Photograph of the Forster "Koerzimeter"

23
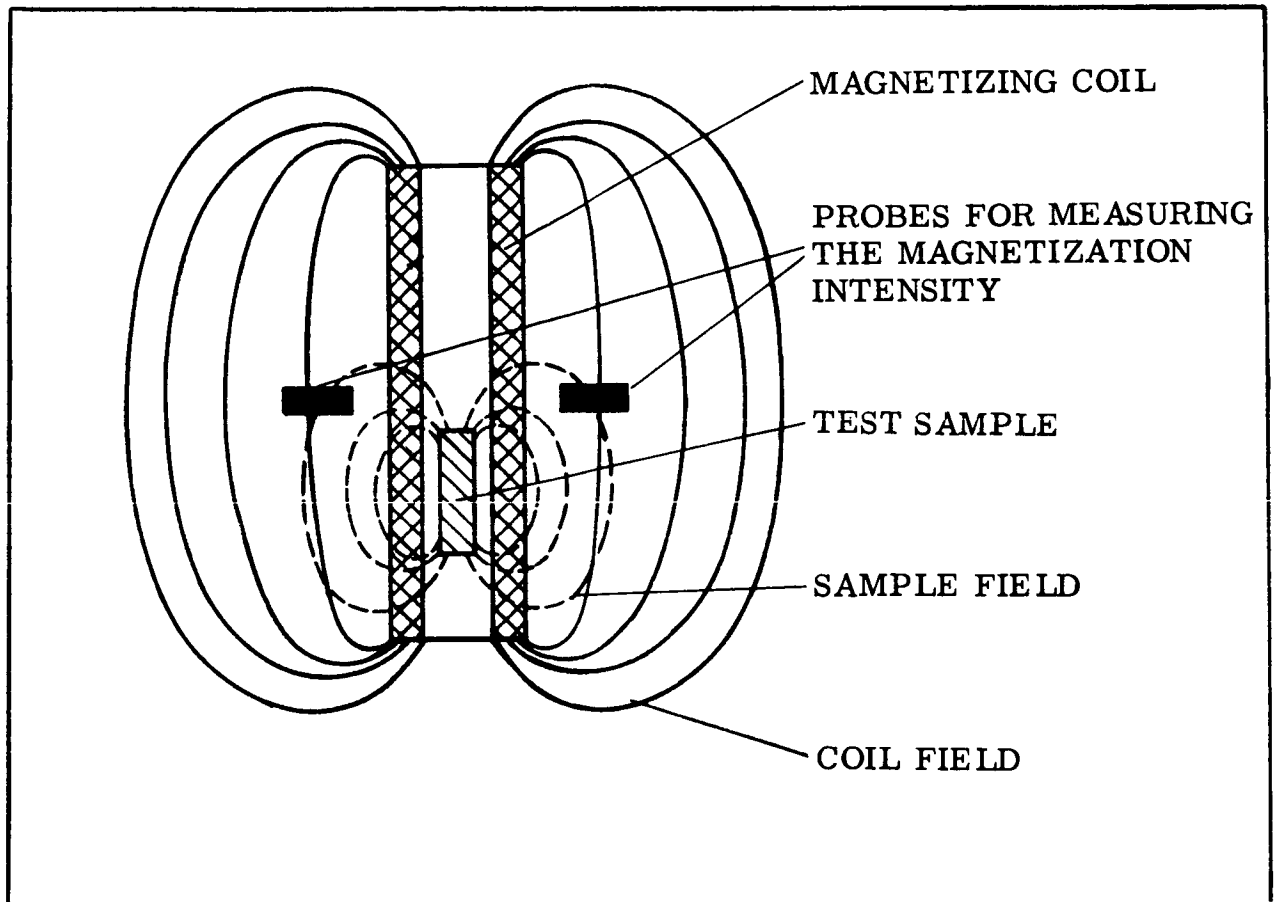
FIGURE II-6. Schematic of Sensitive Field Probe Used in the Coercive
Force Meter Showing Coil and Sample Fields

TABLE II-7. Saturation Magnetic Moment of Alloy Samples 1-A-1 to 1-A-10

Alloy Number	Nominal Alloy Composition (weight percent)	Saturation Magnetic Moment (emu/g)[a]		
		As Cast at Room Temperature	After Aging One Hour at 1112°F(600°C)	
			Tested at Room Temperature	Tested at 1112°F(600°C)
1-A-1	55Fe-15Ni-25Co-5W	197.6	198.9	152.7
1-A-2	58Fe-15Ni-25Co-2Nb	208.4	211.0	167.8
1-A-3	58Fe-15Ni-25Co-2V	206.4	206.5	158.4
1-A-4	58Fe-15Ni-25Co-2Cr	204.8	202.8	149.8
1-A-5	59.5Fe-15Ni-25Co-0.5Al	212.0	204.4	168.9
1-A-6	58Fe-15Ni-25Co-2Be	194.8	195.1	162.2
1-A-7	58Fe-15Ni-25Co-2Sb	210.8	208.1	163.2
1-A-8	58Fe-15Ni-25Co-2Sn	210.8	195.7	166.1
1-A-9	58Fe-15Ni-25Co-2Si	202.0	201.6	154.1
1-A-10	58Fe-15Ni-25Co-2Mn	214.0	205.5	151.0

All specimens were machined from cast ingots.

(a) - To convert Saturation Magnetic Moment to the approximate value in gauss, multiply the listed value by 100.

TABLE II-8. Saturation Magnetic Moment of Alloy Samples 1-B-13 to 1-B-15

Alloy Number	Nominal Alloy Composition (weight percent)	Saturation Magnetic Moment (emu/g)		
		As Cast at Room Temperature	After Aging One Hour at 1292°F(700°C)	
			Tested at Room Temperature	Tested at 1112°F(600°C)
1-B-13	86Co-5Fe-5Ni-3Ti-1Al	146.2	142.0	109.0
1-B-14	81Co-5Fe-10Ni-3Ti-1Al	142.0	137.1	105.9
1-B-15	76Co-5Fe-15Ni-3Ti-1Al	136.4	132.1	102.0

The measured values of saturation of the cobalt alloys 1-B-1 to 1-B-12 are plotted as a function of iron content or nickel content in Figure II-7 at room temperature and at 1112°F (600°C). The measured values of 1-B-13 to 1-B-15 are listed in Table II-8. The samples had been annealed for one hour at 2012°F (1100°C) and saturation was first measured at room temperature in the annealed condition. The samples were then aged for one hour at 1292°F (700°C) and the saturation was measured at room temperature and at 1112°F (600°C).

The change of hardness and coercivity during the isochronal aging (samples held one hour at temperature with intermittent increases of 90°F (50°C) between 842°F (450°C) and 1202°F (650°C)) were measured. Isochronal curves with the parameter of one hour time at temperature as the variable were plotted. Figures II-8, II-9, and II-10 depict aging of the martensitic alloys. Figure II-10 was obtained from previous studies on a Westinghouse program. These results were added for comparison. The maximum values of hardness measured during this aging program are listed in Table II-9 together with the aging temperature for which hardness and the coercivity were measured. The alloys 1-A-7 and 1-A-8 were not tested because they were brittle. The alloy 1-A-6 was replaced by a substitute with lower beryllium content of 0.5 weight percent. The results for alloys with titanium, tantalum, and molybdenum have been included for completeness although these studies had been completed during 1964 on a Westinghouse internally funded program.

Isothermal aging tests were conducted for the alloys which showed considerable increase in hardness. Isothermal aging curves for alloys 1-A-1, 1-A-2, 1-A-3, 1-A-5, and 1-A-6W are shown in Figures II-11, II-12, and II-13. Alloy 1-A-16 also underwent an isothermal aging test at 1022°F (550°C) to check its temperature stability (Figure II-14). The results show that little change in hardness and coercivity occurred in the case of alloys 1-A-1, 1-A-2, 1-A-5 and 1-A-16 during the 100 hour aging time. Additions of molybdenum and tantalum should exhibit similar behavior during isothermal aging.

The temperature stability of 15% Ni Maraging steel is poor at 1022°F (550°C). The change of hardness and coercivity at 1022°F (550°C) (ref. 12) is plotted for comparison in Figure II-13. The large increase of coercivity during 100 hours aging should be noted.

The isochronal and isothermal behavior of the cobalt alloys 1-B-13, 1-B-14 and 1-B-15 are shown in Figures II-15 and II-16. The hardening effect is rather low; the stability even at 1292°F (700°C) is considerable.

26

FIGURE II-7. Influence of Iron and Nickel Content on the Magnetic Saturation of Cobalt-5% Nickel and Cobalt-5% Iron Alloys Respectively (Alloys 1-B-2, 1-B-8 to 1-B-12 and 1-B-1 to 1-B-7)
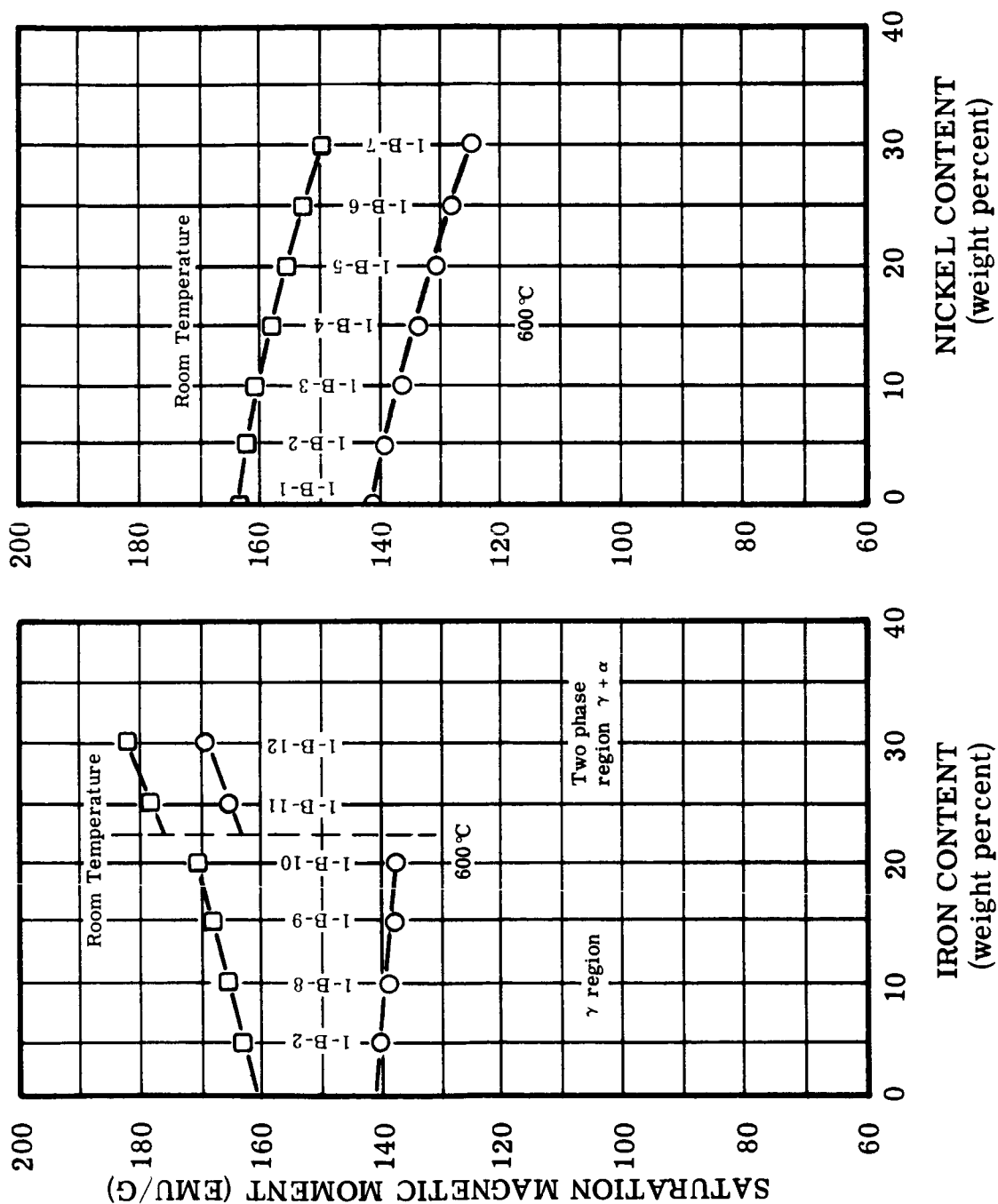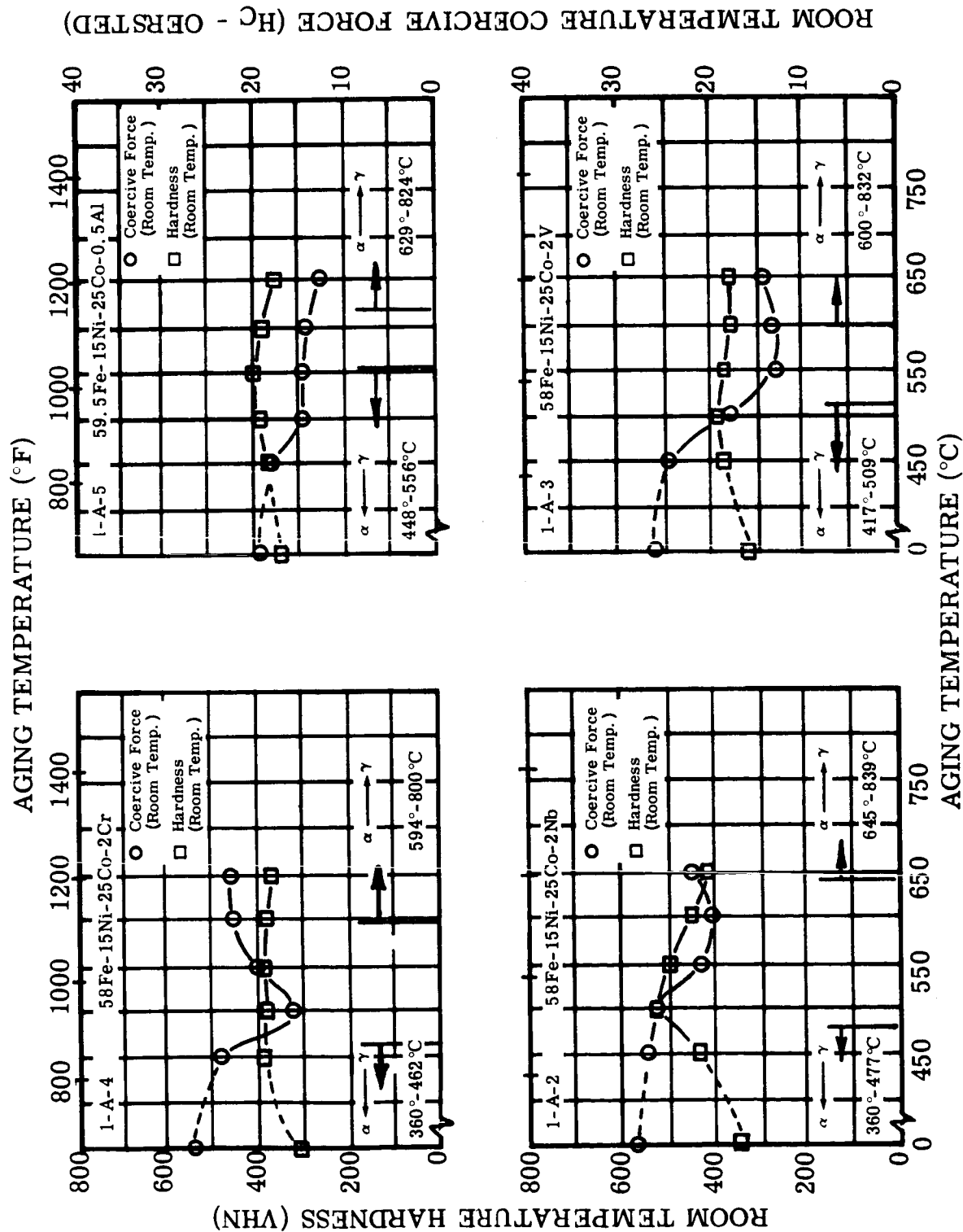
FIGURE II-7. Magnetic Saturation of Cobalt-Base Alloys 1-B-1 to 1-B-12

27

FIGURE II-8. Hardness and Coercive Force of Alloys 1-A-2, 1-A-3, 1-A-4 and 1-A-5 at Room Temperature After Aging One Hour at Temperature
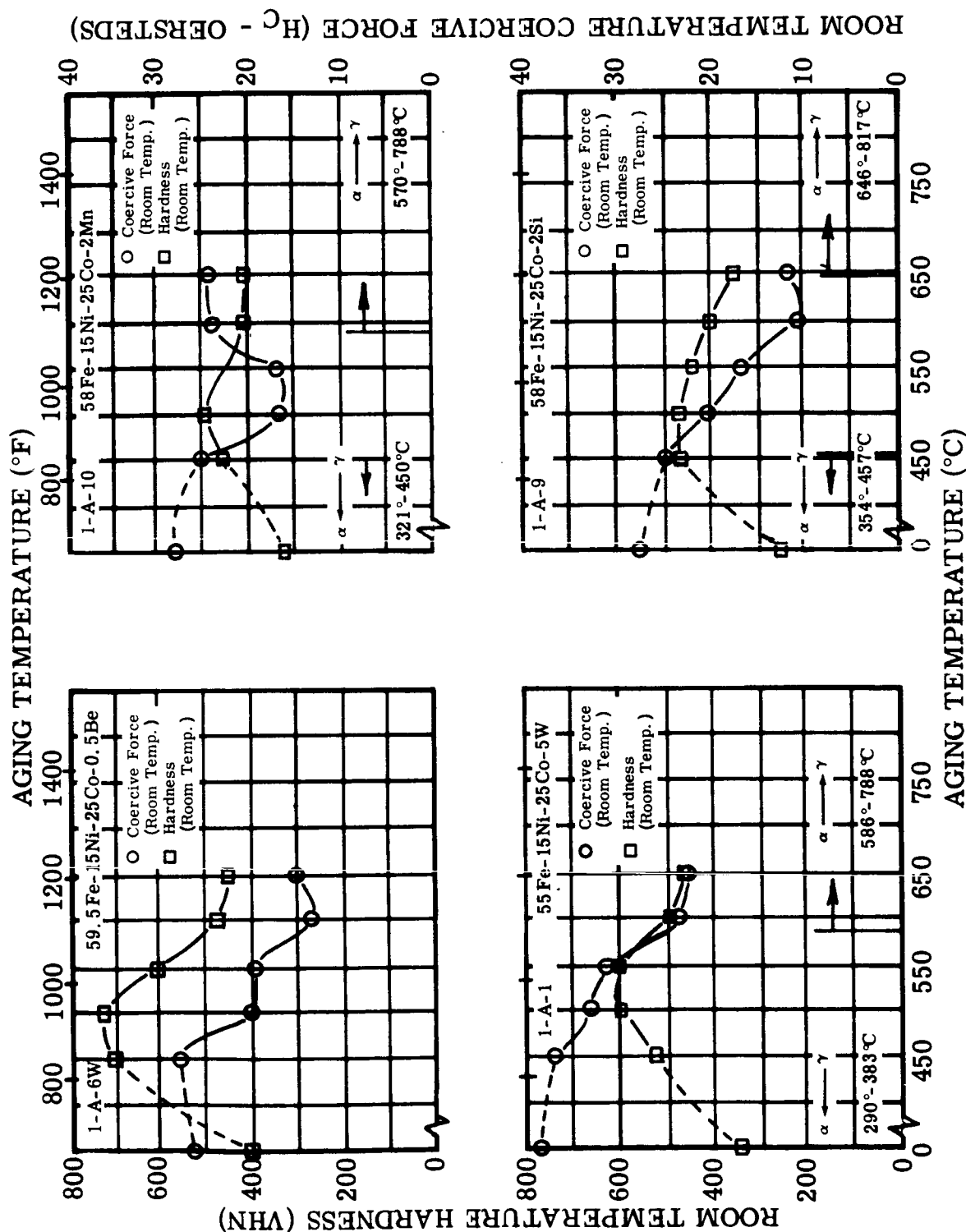
Figure II-8. Hardness and Coercive Force of Alloys 1-A-2, 1-A-3, 1-A-4 and 1-A-5

28

ROOM TEMPERATURE COERCIVE FORCE (H_C - OERSTEDS)

AGING TEMPERATURE (°F)

1-A-10   58Fe-15Ni-25Co-2Mn

○ Coercive Force (Room Temp.)
□ Hardness (Room Temp.)

570°-788°C
321°-450°C
α → γ

1-A-9   58Fe-15Ni-25Co-2Si

○ Coercive Force (Room Temp.)
□ Hardness (Room Temp.)

646°-817°C
354°-457°C
α → γ

AGING TEMPERATURE (°C)

1-A-6W   59.5Fe-15Ni-25Co-0.5Be

○ Coercive Force (Room Temp.)
□ Hardness (Room Temp.)

1-A-1   55Fe-15Ni-25Co-5W

○ Coercive Force (Room Temp.)
□ Hardness (Room Temp.)

586°-788°C
290°-383°C
α → γ

ROOM TEMPERATURE HARDNESS (VHN)

FIGURE II-9.   Hardness and Coercive Force of Alloys 1-A-1, 1-A-6W, 1-A-9 and 1-A-10 at Room Temperature After Aging One Hour at Temperature

Figure II-9.   Hardness and Coercive Force of Alloys 1-A-1, 1-A-6W, 1-A-9 and 1-A-10

29
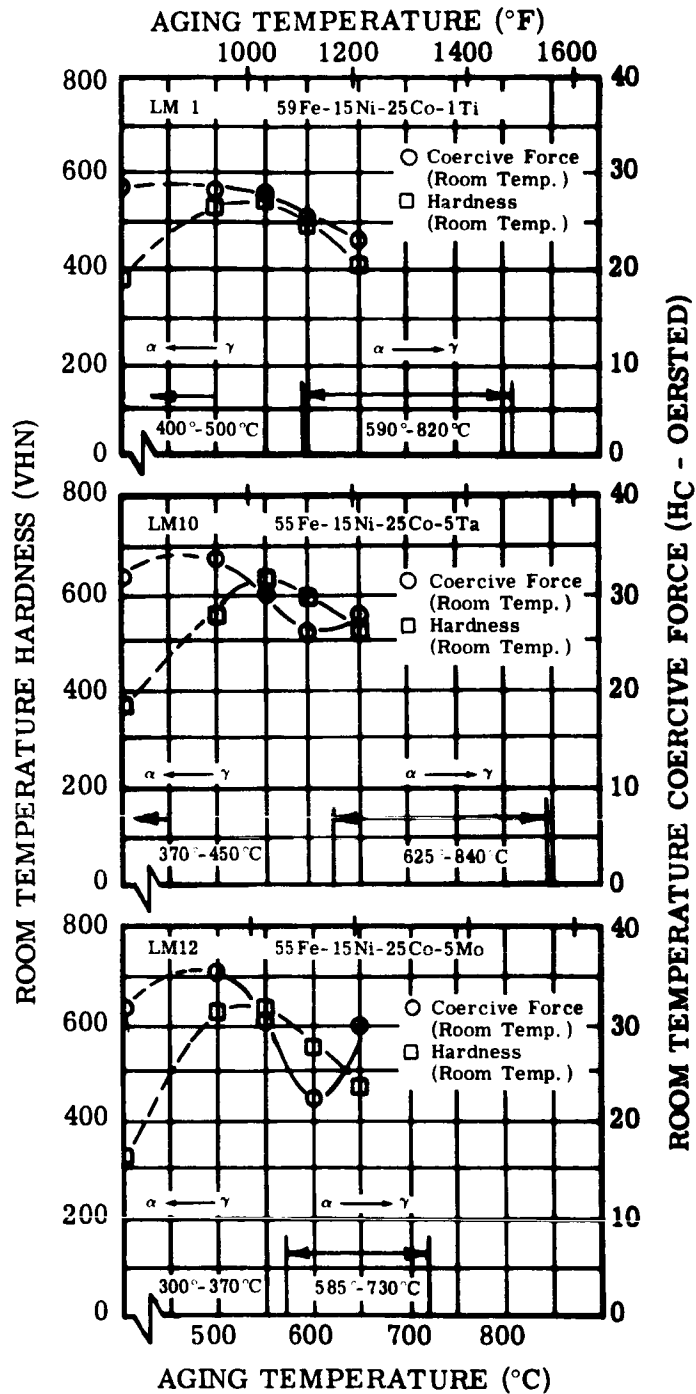
FIGURE II-10. Hardness and Coercive Force of Alloys LM1, LM10
and LM12 at Room Temperature After Aging One Hour
at Temperature (Reference: From Unpublished
Westinghouse Data, 1964)

Figure II-10. Hardness and Coercive Force of Alloys LM1, LM10
and LM12

TABLE II-9. Maximum Hardness Obtained from the Isochronal Aging Sequence(a)

Alloy Number	Nominal Alloy Composition (weight percent)	Aging Temperature at Which Maximum Room Temperature Hardness was Obtained (°F)	(°C)	Total Aging Time(b) (hours)	Maximum Room Temperature Hardness (VHN)	Room Temperature Coercivity at Maximum Hardness (oersteds)
1-A-1	55Fe-15Ni-25Co-5W	932	500	2	610	33.5
1-A-2	58Fe-15Ni-25Co-2Nb	932	500	2	558	27.4
1-A-3	58Fe-15Ni-25Co-2V	932	500	2	390	18.3
1-A-4	58Fe-15Ni-25Co-2Cr	1022	550	3	391	20.1
1-A-5	59.5Fe-15Ni-25Co-0.5Al	1022	550	3	412	14.65
1-A-6W	59.5Fe-15Ni-25Co-0.5Be	932	500	2	717	19.1
1-A-9	58Fe-15Ni-25Co-2Si	842	450	1	468	24.2
1-A-10	58Fe-15Ni-25Co-2Mn	932	500	2	482	16.3
LM 1(c)	59Fe-15Ni-25Co-1Ti	932	500	2	530	28.5
LM 12(c)	55Fe-15Ni-25Co-5Mo	1022	550	3	645	31
LM 10(c)	55Fe-15Ni-25Co-5Ta	1022	550	3	625	30

(a) - See Figures II-8, 9, 10
(b) - Total aging time may be determined by adding one hour aging time for each 90°F(50°C) increment in temperature starting at 842°F(450°C).
(c) - Unpublished data obtained on a Westinghouse sponsored High Temperature Magnetics Program in 1964.
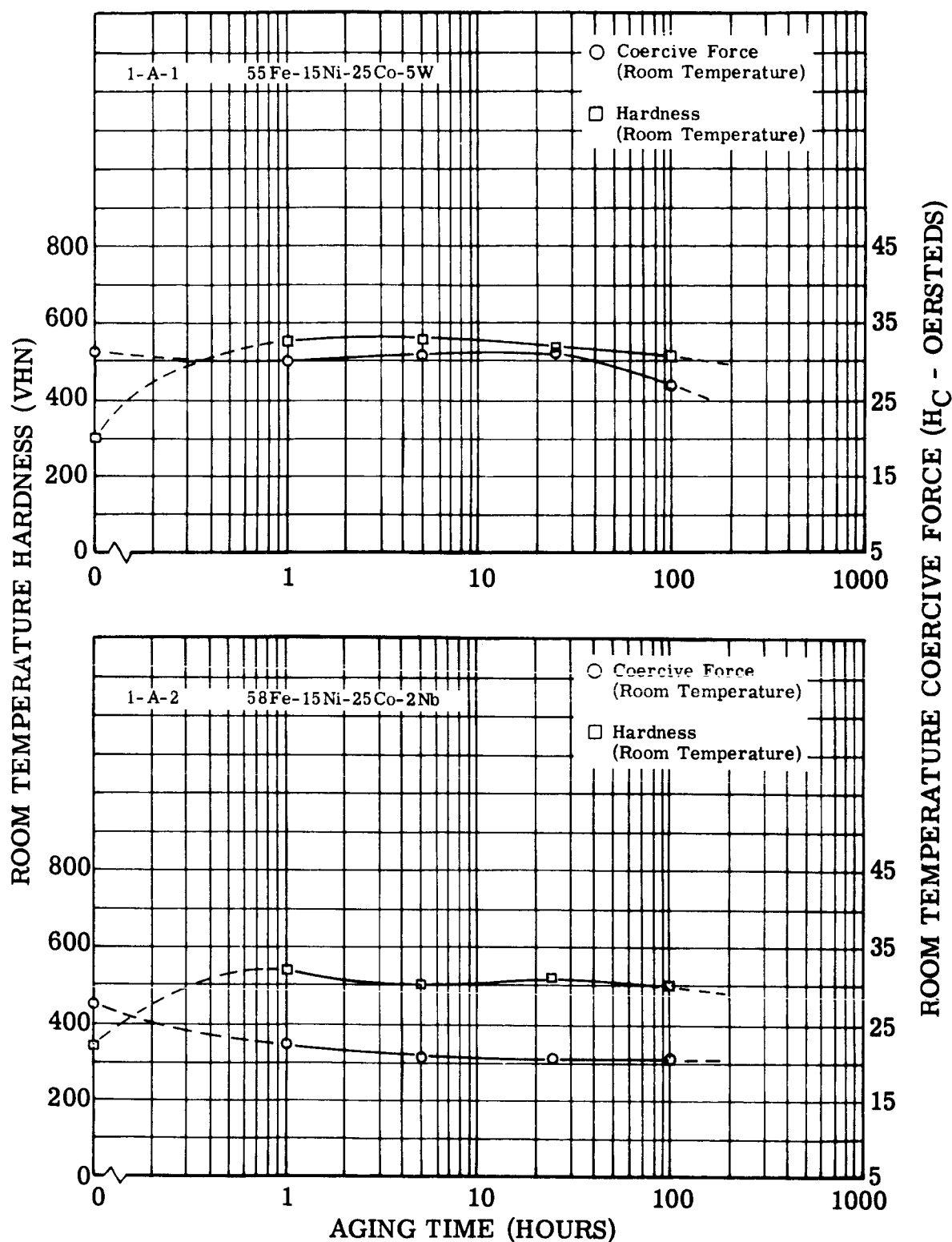
FIGURE II-11. Change in Room Temperature Hardness and Coercive
Force of Alloys 1-A-1 and 1-A-2 During Isothermal
Aging at 1022°F (550℃)

Figure II-11. Hardness and Coercive Force of Alloys 1-A-1 and 1-A-2
During Isothermal Aging
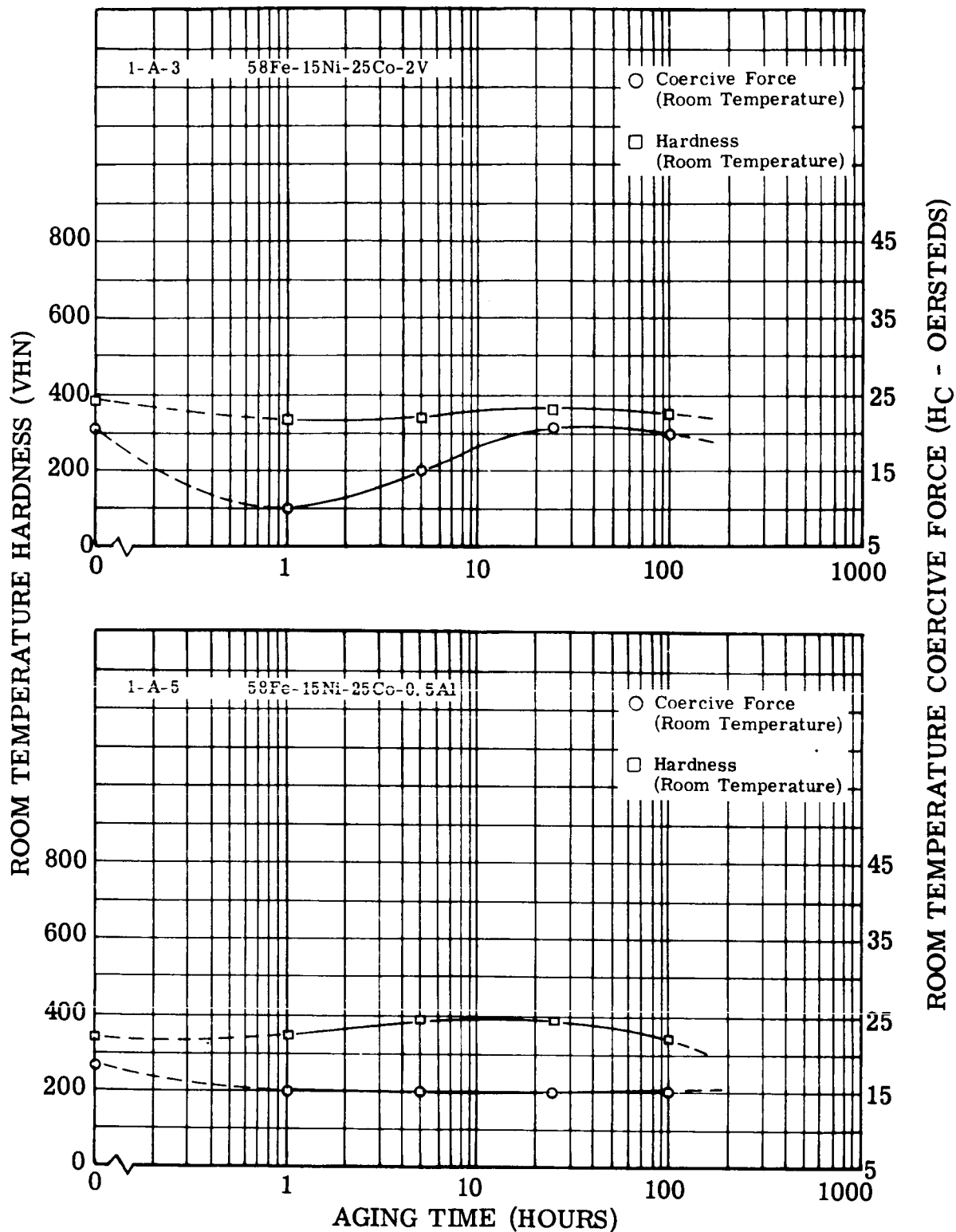
FIGURE II-12. Change in Room Temperature Hardness and Coercive
Force of Alloys 1-A-3 and 1-A-5 During Isothermal
Aging at 1022°F (550°C)

Figure II-12. Hardness and Coercive Force of Alloys 1-A-3 and 1-A-5
During Isothermal Aging
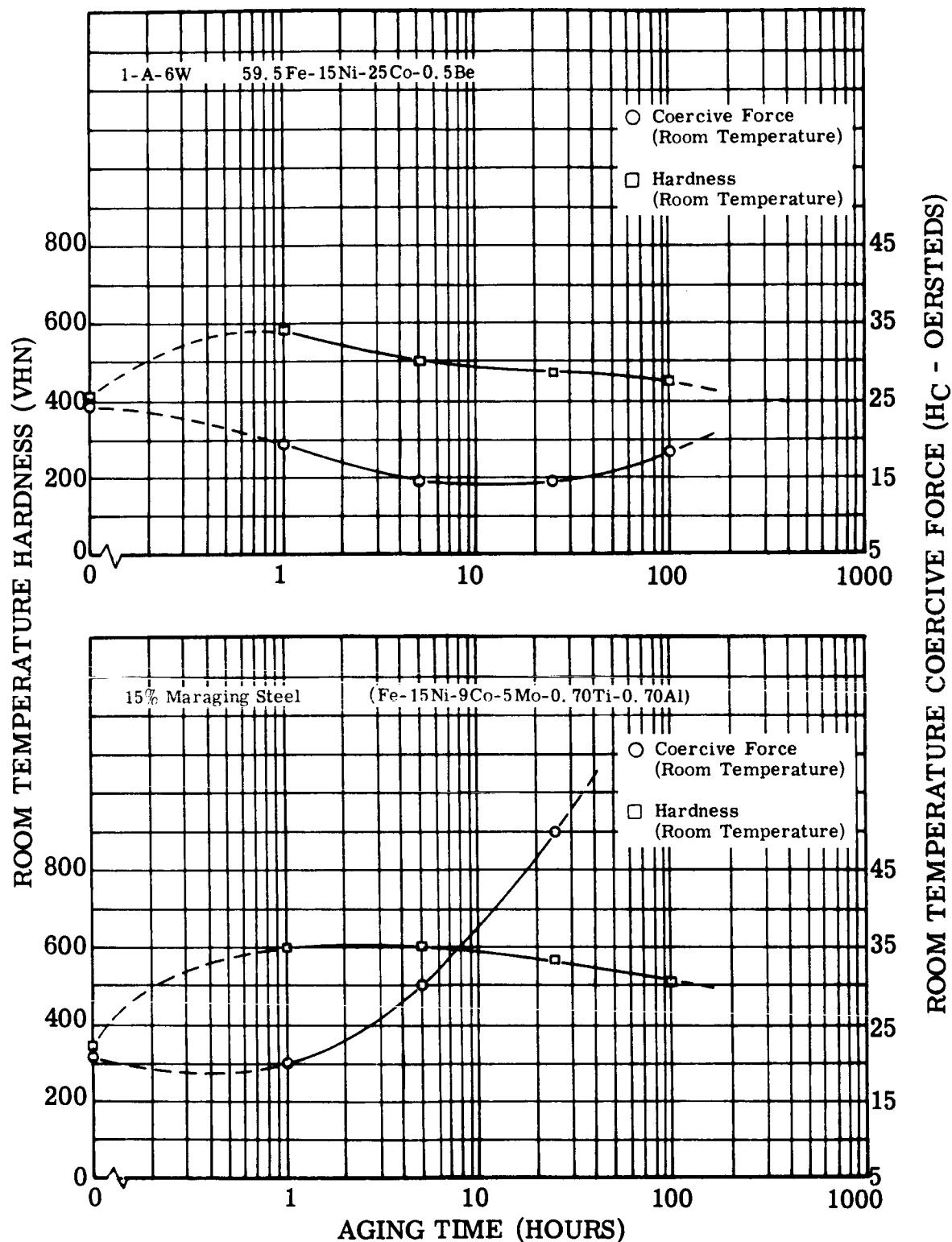
FIGURE II-13. Change in Room Temperature Hardness and Coercive
Force of Alloys 1-A-6W and 15% Ni Maraging Steel
During Isothermal Aging at 1022°F (550°C)

Figure II-13. Hardness and Coercive Force of Alloy 1-A-6W and
15% Ni Maraging Steel During Isothermal Aging
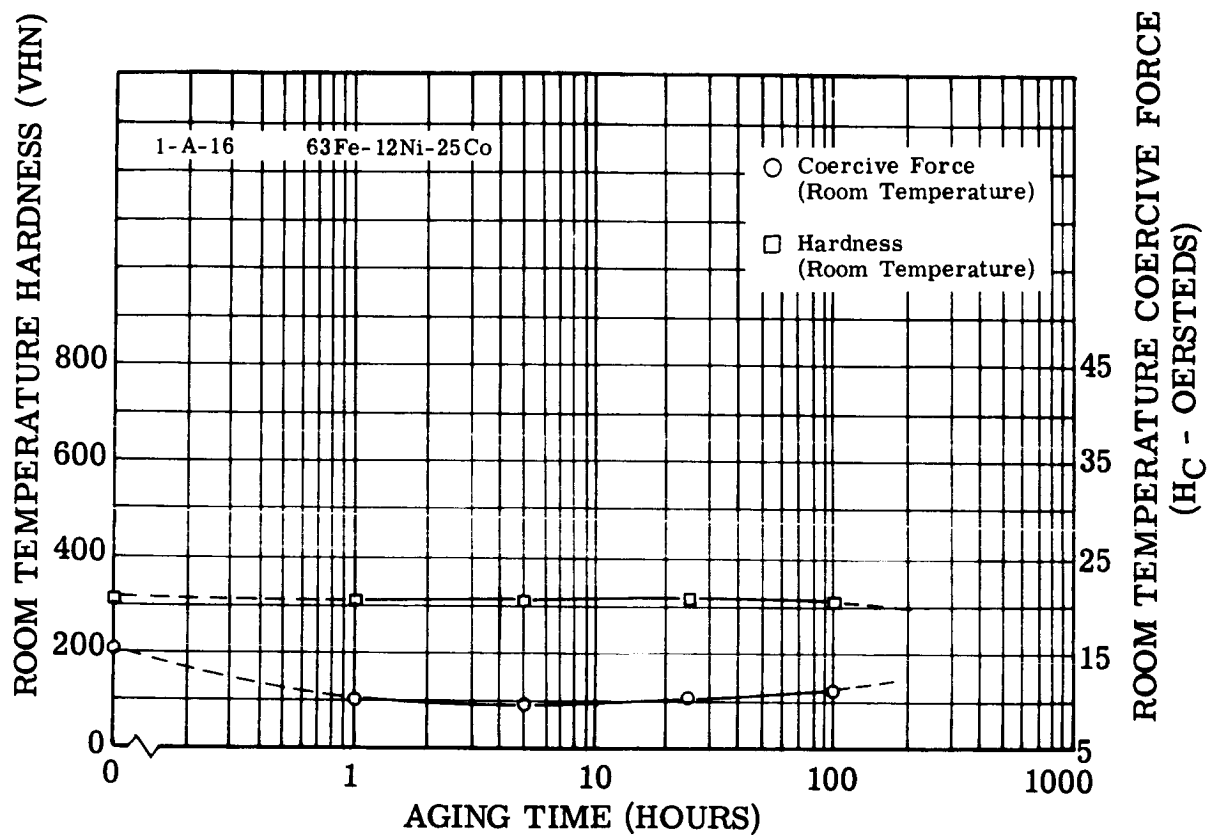
FIGURE II-14.   Change in Room Temperature Hardness and Coercive
Force of Alloy 1-A-16 During Isothermal Aging
at 1022°F (550°C)

Figure II-14.   Hardness and Coercive Force of Alloy 1-A-16
During Isothermal Aging

35
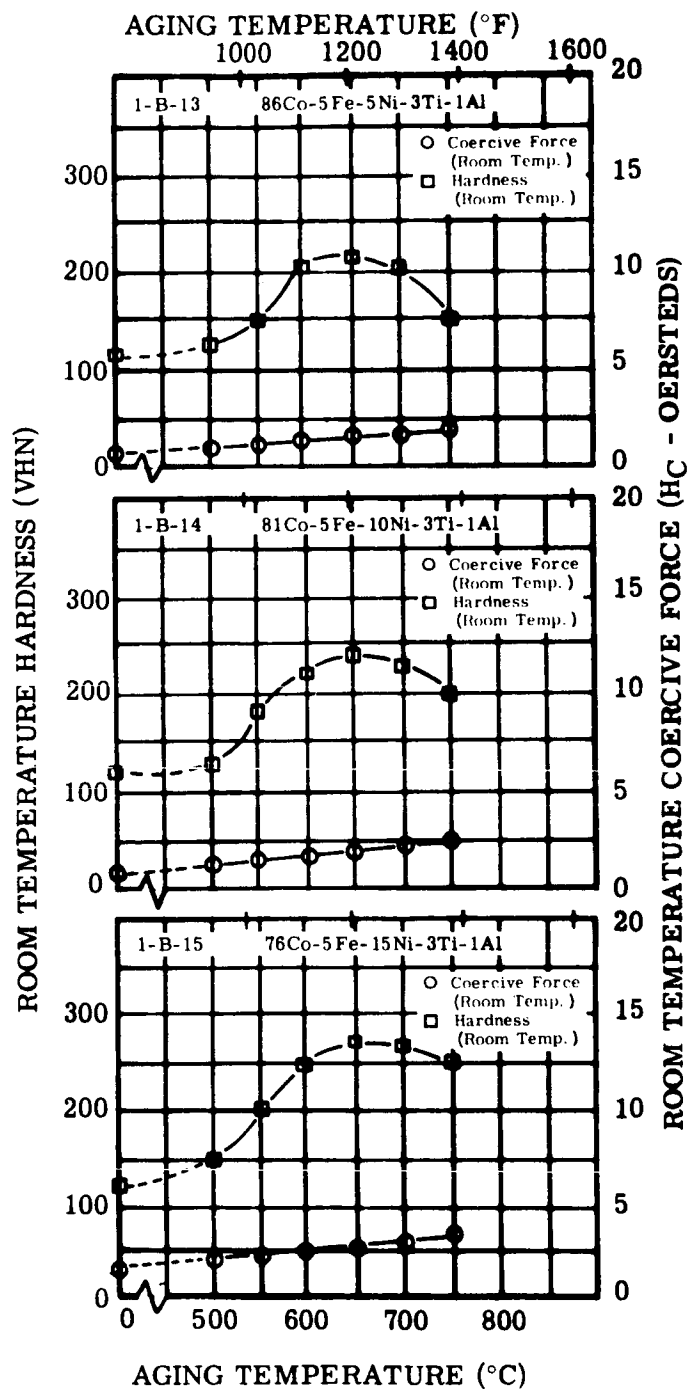
FIGURE II-15. Hardness and Coercive Force of Alloys 1-B-13, 1-B-14
and 1-B-15 at Room Temperature After Aging One Hour
at Temperature

Figure II-15. Hardness and Coercive Force of Alloys 1-B-13, 1-B-14
and 1-B-15

36
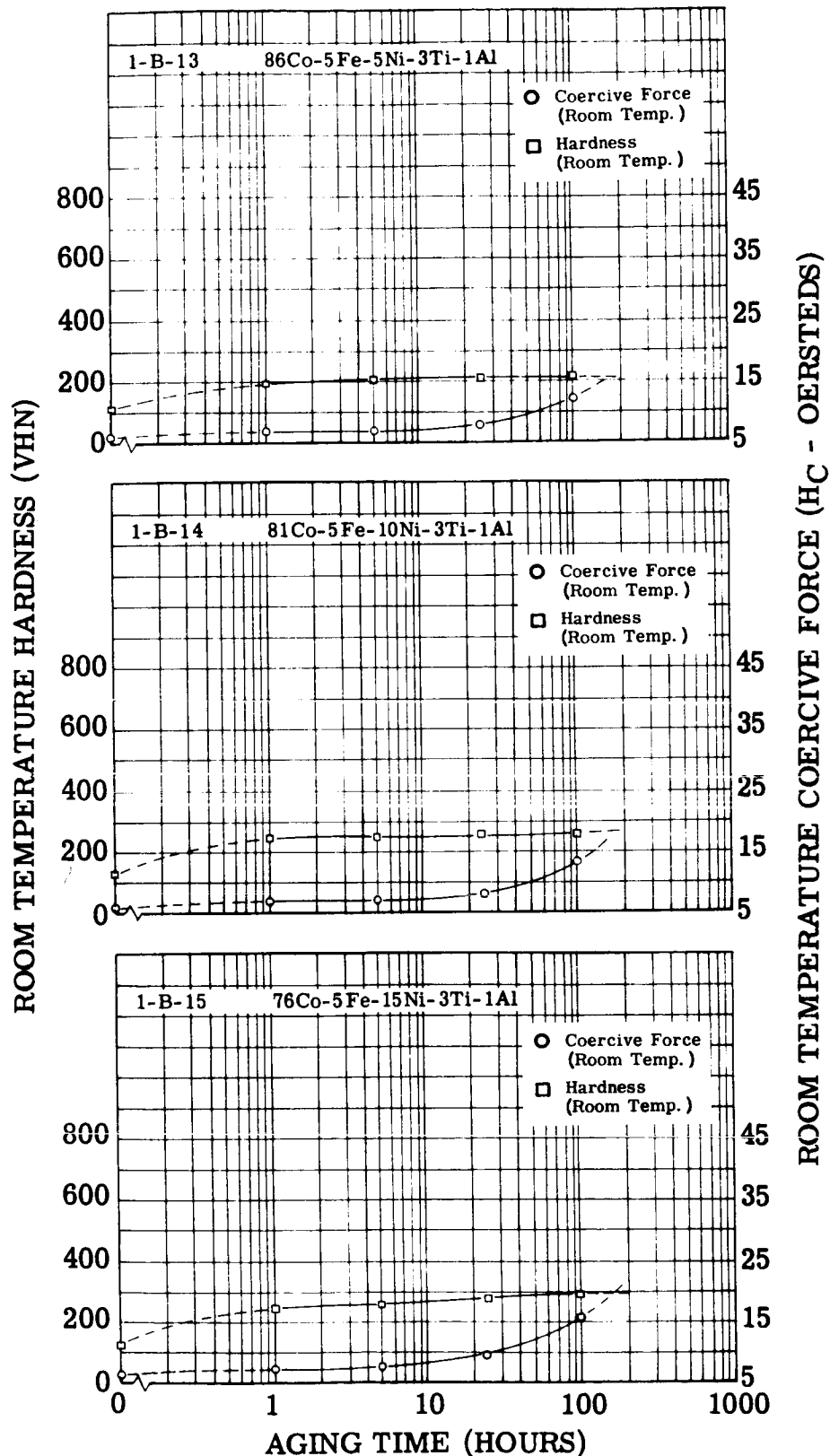
FIGURE II-16. Change in Room Temperature Hardness and Coercive Force of Alloys 1-B-13, 1-B-14 and 1-B-15 During Isothermal Aging at 1292°F (700°C)

Figure II-16. Hardness and Coercive Force of Alloys 1-B-13, 1-B-14 and 1-B-15 During Isothermal Aging

After completion of the isothermal aging treatment with a total aging time of 100 hours, the microstructure was observed. See Figures II-17 through II-21. The martensitic alloys show general grain boundary precipitate and fine precipitate within the grains. A similar structure is seen in all of the age hardened cobalt alloys 1-B-13, 1-B-14 and 1-B-15 (Figure II-22). Except for a few small spots in the interior of the grain, there is no continuous precipitation to be seen. Discontinuous precipitation which started at some of the grain boundaries can be seen. An electron microscope study to identify the phase present in the discontinuous precipitation reaction has been started. This study will be completed in the next quarter.

d.   DISCUSSION OF RESULTS

The behavior of the experimental alloys during cold rolling indicated that the addition of tin and antimony cause severe embrittling so that both of these elements can be ruled out as useful additions to produce age hardening. The addition of tungsten, aluminum, beryllium and silicon resulted in major difficulties during cold rolling. These difficulties might be overcome; however, this behavior indicates a tendency toward grain boundary segregation or precipitate as was confirmed by the micrographs. The addition of cobalt will lead to difficulties during cold rolling when added in excess of ten percent, but these difficulties will be minimized if cobalt is held below 25 percent.

It was stated in the First Quarterly Report (NASA-CR-54354) that addition of beryllium increases the stability of the alpha phase. The addition of 5%W, 2%Cr, 2%Mn, 2%V and 2%Sn are detrimental to the stability of the alpha phase in Fe-15Ni-25Co at 1112°F (600°C). A reduction of the amount added or a change of the basic composition toward a more stable alpha phase may decrease this influence to a tolerable level. Alloys with 12Ni, with a cobalt addition of ten percent or more, balance Fe, will have increased stability of the alpha phase as compared to Fe-15Ni-25Co.

The alloying additions in Fe-15Ni-25Co lower the magnetic saturation especially at 1112°F (600°C). The values obtained, however, are well above the value B_S of 13,000 gauss representing H-11 steel or 15% Ni Maraging steel at 1112°F (600°C). In no case is the value of B_S below 15,000 gauss. An alloy with a basic composition of 12Ni with at least 20Co, Balance Fe may give rise to still better magnetic saturation at 1112°F (600°C).

The measurements in the cobalt series shows that iron addition is not beneficial to saturation at 1112°F (600°C). See Figure II-7.
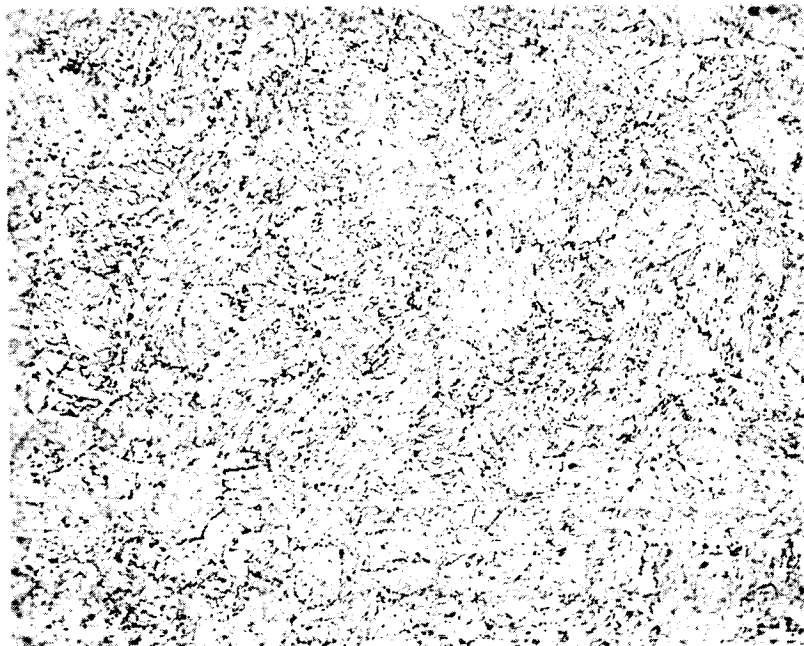
38

Sample electrolytically etched. For thermal-
mechanical treatment prior to aging see flow
chart on page 20.

FIGURE II-17. Microstructure of Alloy 1-A-1 (55Fe-15Ni-25Co-
5W) After 100 Hours Aging at 1022°F (550°C) 500X
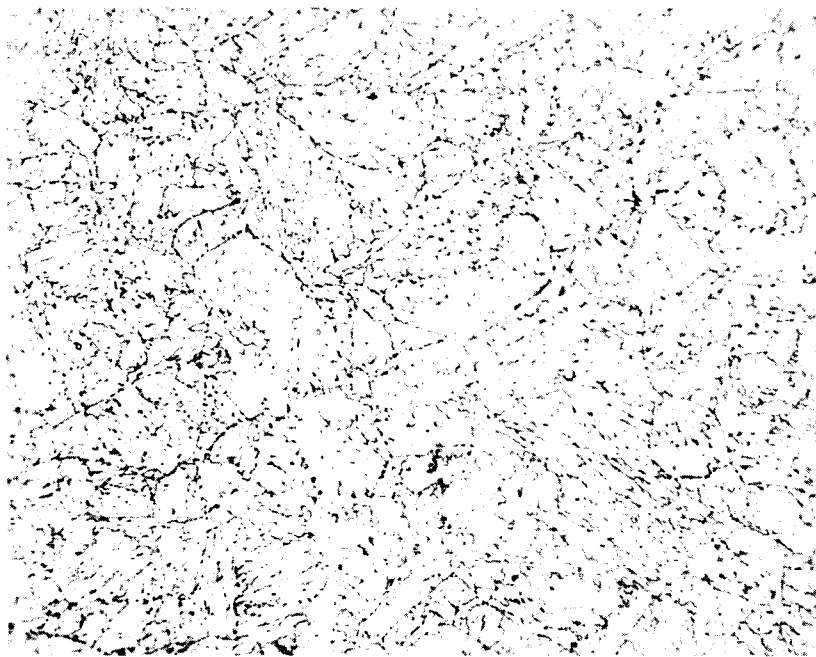
Sample electrolytically etched. For thermal-
mechanical treatment prior to aging see flow
chart on page 20.

FIGURE II-18. Microstructure of Alloy 1-A-2 (58Fe-15Ni-25Co-
2Nb) After 100 Hours Aging at 1022°F (550°C) 500X
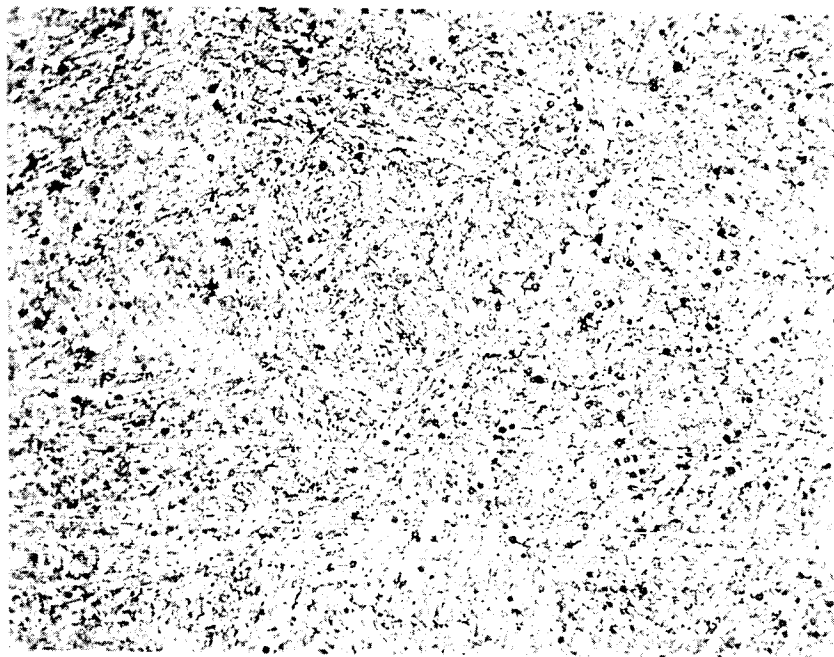
Sample electrolytically etched. For thermal-
mechanical treatment prior to aging see flow
chart on page 20.

FIGURE II-19.   Microstructure of Alloy 1-A-3 (58Fe-15Ni-25Co-
2V) After 100 Hours Aging at 1022°F (550°C) 500X

Sample electrolytically etched. For thermal-
mechanical treatment prior to aging see flow
chart on page 20.

FIGURE II-20. Microstructure of Alloy 1-A-5 (59.5Fe-15Ni-
25Co-0.5Al) After 100 Hours Aging at
1022°F (550°C) 500X
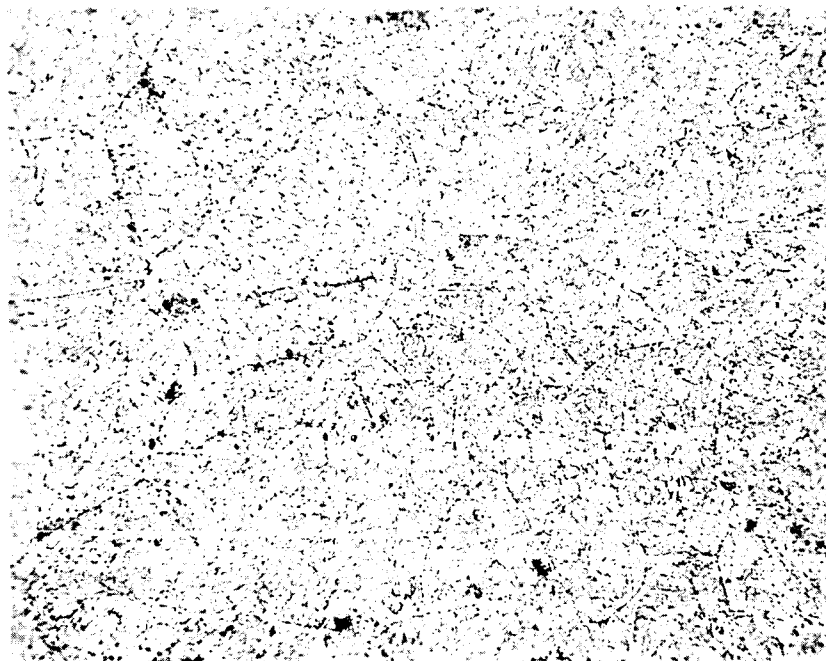
Sample electrolytically etched. For thermal-
mechanical treatment prior to aging see flow
chart on page 20.

FIGURE II-21. Microstructure of Alloy 1-A-6W (59.9Fe-15Ni-
25Co-0.5Be) After 100 Hours Aging at
1022°F (550°C) 500X
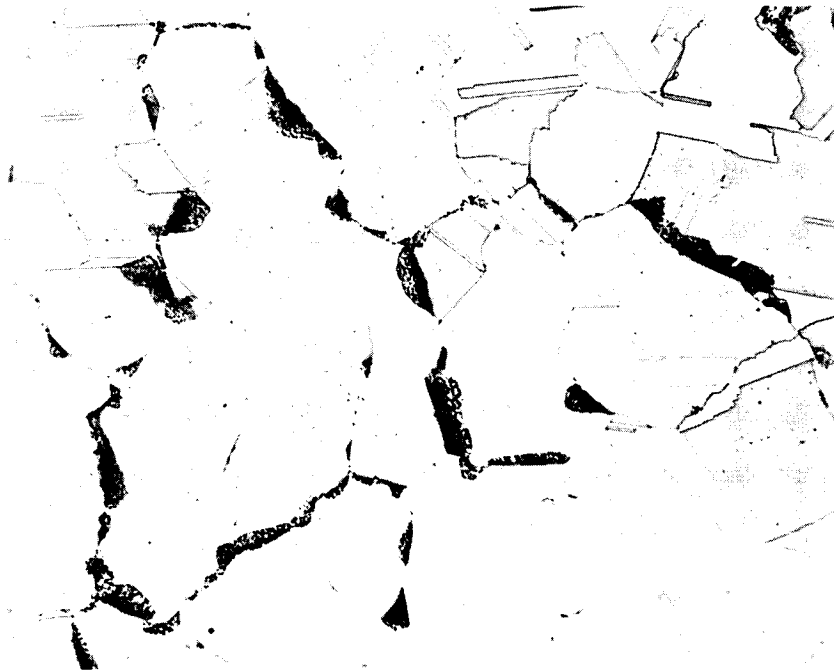
Sample etched in solution of 20ml HCl, 40ml HNO$_3$,
60ml glycerin. Note the formation of discontinuous
precipitate.

FIGURE II-22. Microstructure of Alloy 1-B-15 (76Co-5Fe-15Ni-
3Ti-1Al) After 100 Hours Aging at 1292°F (700°C)
200X

additions which increase the strength of the matrix and the precipitate, and reduce the solubility limit may have such an effect. The thermal stability in the temperature range of 1022 to 1202°F (550 to 650°C) does not pose a real problem if the discontinuous precipitation can be prevented.

3. Program for the Next Quarter

The influence of additions (Ta, Mo, W, Nb, Ti, Be of Al) on an alloy with a higher M_S temperature (e.g. Fe-12Ni-20Co) will be determined. The influence of combinations of two or more modifying elements (Ta, Mo, Nb, Ti and Be) will be determined in the Fe-15Ni-20Co matrix. Several new substitute alloys in the cobalt series will be tested. These will include the addition of 3%Ti and 1%Al to alloys with 20 percent nickel. Evaluation of alloys by electron microscopy will be continued.

B. TASK 2 - INVESTIGATION FOR RAISING THE ALPHA TO GAMMA
    TRANSFORMATION TEMPERATURE IN COBALT-IRON ALLOYS

1. Summary of Technical Progress

Fifteen alloys were melted by the levitation melting technique.

The basic composition consists of iron and cobalt in the ratio 1:1
by weight. Minor amounts of about one weight percent of various
elements were added which are known to raise the alpha to gamma
transformation temperature of iron. The transformation temperature
was measured by dilatometer technique and magnetic saturation was
measured at room temperature, 1112°F (600°C), and at 1652°F (900°C).
The results show that in only a few cases (Be, Ti) the transformation
temperature appeared to be raised slightly (less than 18°F) by addition
of one percent of the modifying element. The saturation was decreased
in all cases.

2. Discussion

    a. BACKGROUND

        Alloys having appreciable magnetic saturation at temperatures of
        1652°F (900°C) and higher can be found only in cobalt and cobalt-
        iron alloys. Figure II-23 shows the dependence of magnetic satura-
        tion on the composition in iron-cobalt alloys at room temperature
        and 1652°F (900°C) (refs. 24 & 25). The highest magnetic saturation
        at 1652°F (900°C) is found in 50%Fe, 50%Co. Unfortunately, in the
        iron-cobalt alloys, the upper temperature limit where ferromagnetism
        disappears is set by the phase transformation (see Figure II-24)(ref.
        26). Figure II-24 also indicates the extrapolated values of the theoreti-
        cal Curie temperature if the body centered cubic structure could per-
        sist above the transformation temperature. The alloy 50Fe, 50Co
        would have a theoretical Curie temperature similar to that of cobalt.
        If some means could be found to prevent the phase transformation in
        this alloy or to increase the transformation temperature slightly, an
        alloy which displays magnetic saturation superior to cobalt could be
        obtained.

        The phase transformation temperature from the body centered cubic
        alpha phase to the gamma phase can be changed by applying hydrostatic
        pressure or by alloying. Increased hydrostatic pressure will increase
        the stability of the gamma phase and hence decrease the transformation
        temperature. It is therefore, not possible to increase the transforma-
        tion temperature in iron-cobalt alloys by applying hydrostatic pressure.
        However, alloying might be a useful tool for increasing the transforma-

47
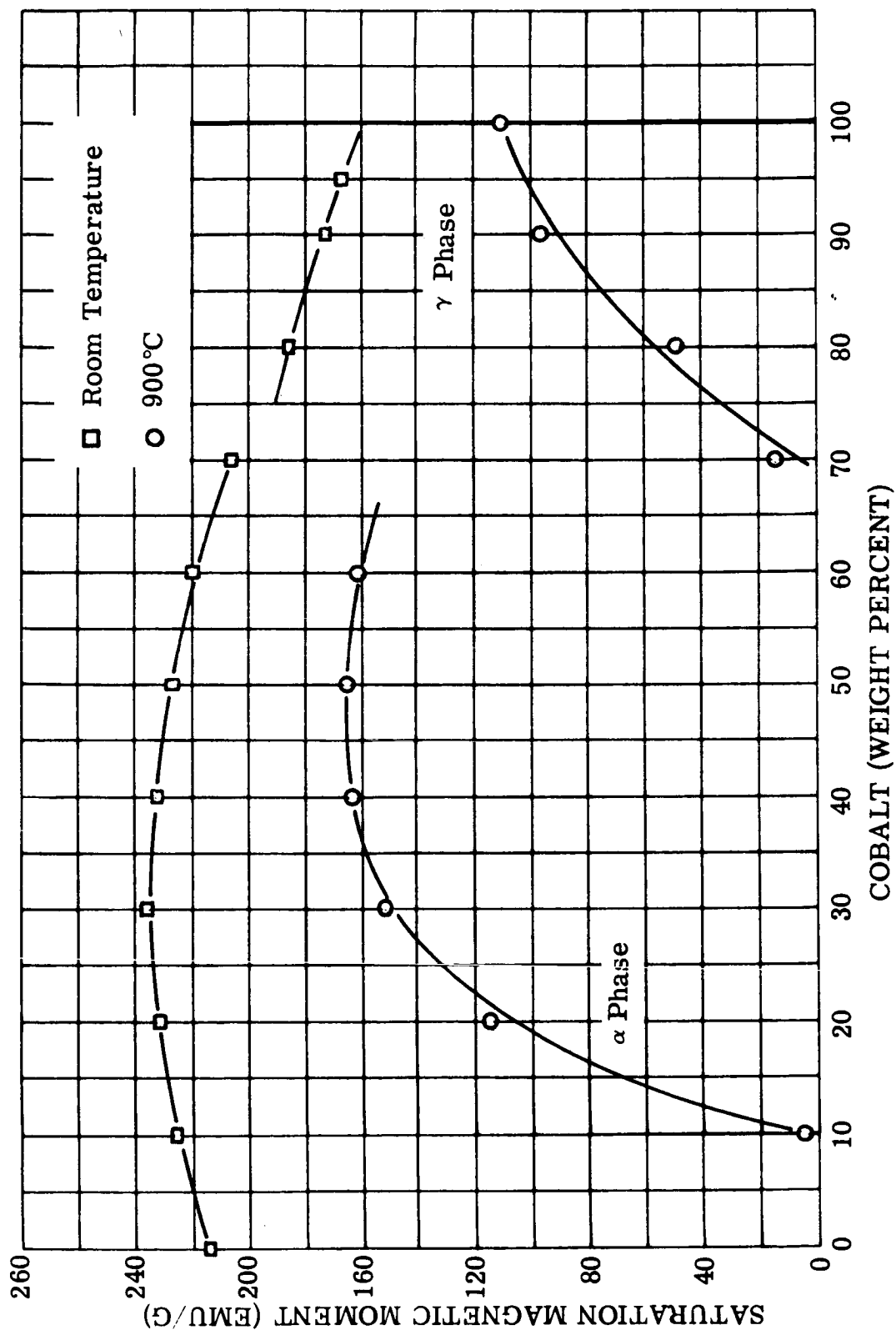
FIGURE II-23. The Influence of Cobalt Content on Saturation Magnetic Moment in Iron-Cobalt Alloys at Room Temperature and 1652°F (900°C). (References 24 and 25)

Figure II-23. Influence of Cobalt in Fe-Co Alloys on Magnetic Saturation

48
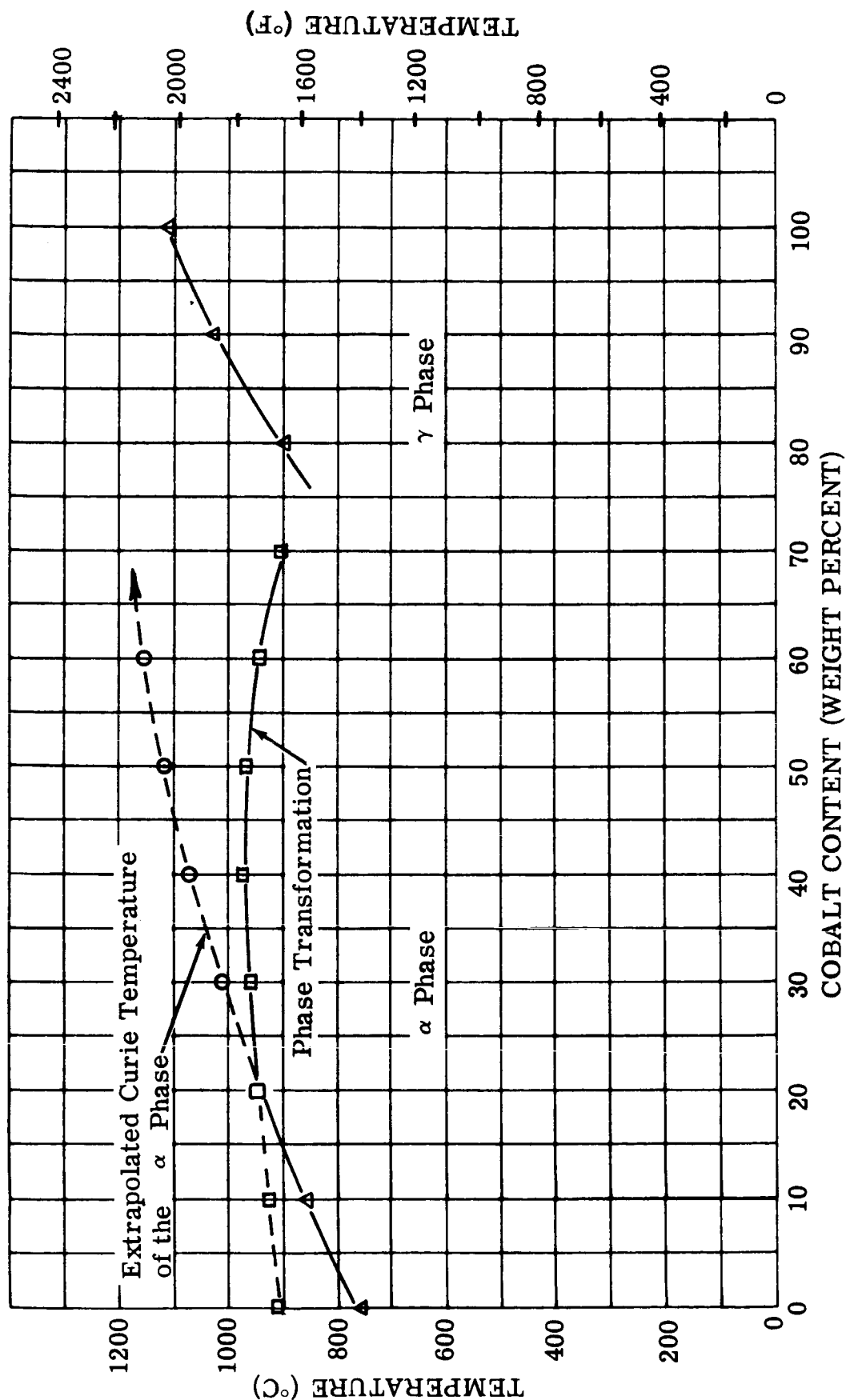
FIGURE II-24. Curie Temperature of the Iron-Cobalt Binary Alloys. (References 26 and 27)

Figure II-24. Curie Temperature of Fe-Co Binary Alloys

49

FIGURE II-25. Saturation Magnetic Moment of Cobalt and Iron-Cobalt Binary Alloys as a Function of Temperature. (Reference 24)
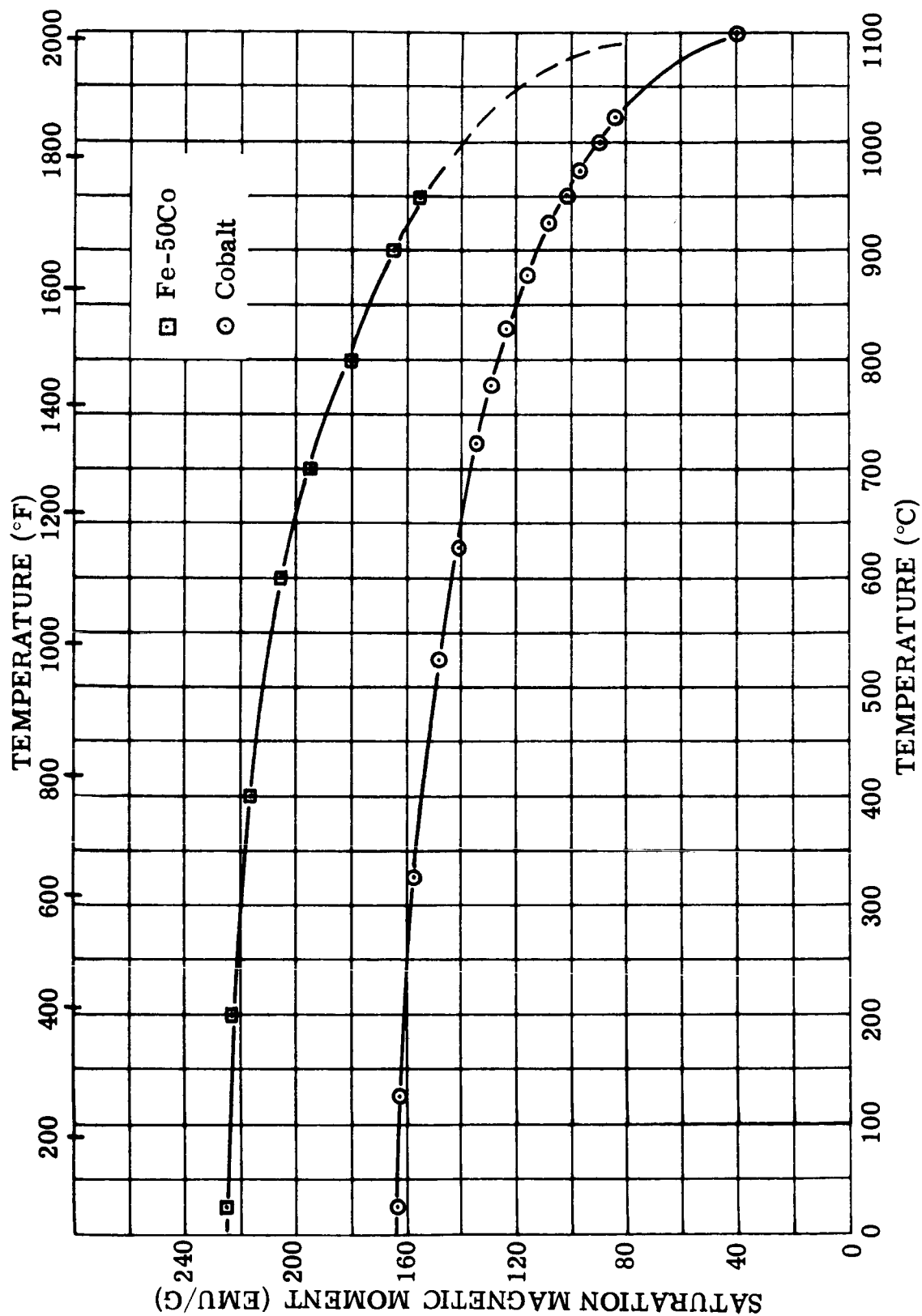
Figure II-25. Magnetic Saturation of Cobalt and Fe-Co Binary Alloys as a Function of Temperature

tion temperature. The alloying additions will also influence the magnetic saturation and the true Curie temperature.

The primary effort on this program will be the preparation of alloys of a basic Fe-50Co composition with some minor constituents added. The transformation temperature and the magnetic saturation of these alloys must then be determined. There have been a number of studies on the change of transformation temperature in ternary systems. However, no specific information can be extracted concerning the influence of additions on iron-cobalt at elevated temperatures. C. Chen determined the influence of additions on the magnetic saturation in iron-cobalt alloys (ref. 26) but the saturation was measured at room temperature only. Chen found that the magnetic saturation of Co-50Fe will be lowered in general by all kinds of added elements except manganese which caused a small increase in saturation.

The melting of a series of alloys with a basic composition of Fe:Co at a ratio of 1:1 with the addition of about one weight percent of other elements was planned on this program. Those elements which are known to raise the transformation temperature of pure iron were chosen (ref. 27). Niobium and tantalum were added in the amount of 0.5 percent because of their anticipated limited solubility in Fe-Co alloys. Furthermore, alloys containing chromium, gold, and zinc were added to the list (see Table II-10). Gold is known to decrease the alpha to gamma transformation temperature of iron only slightly. Chromium and zinc decrease the alpha to gamma transformation temperature in alpha iron when added in small amounts. On the other hand, the gamma loop will be closed by these additions. Therefore, it appeared reasonable to include alloys incorporating these elements on the list because one cannot rule out the possibility that their influence on the transformation temperature in Fe-Co may differ from that in pure iron.

b.   EXPERIMENTAL PROCEDURE

The samples were prepared by levitation melting technique as described in Section II. A. of this report. Typical analysis of the constituents is given in Section II. A. Melting of the alloys listed in Table II-10 was performed with a few exceptions where difficulties were anticipated during melting because of excessive vapor pressure. Melting of these alloys was postponed until a suitable melting method could be established.

A dilatometer specimen and a sample for magnetic saturation measurements were machined from each cast ingot. The dilatometer specimens were one inch long and 1/4 inch in diameter with a hole

TABLE II-10. Alloys for Alpha to Gamma Transformation Study

Alloy Number	Nominal Alloy Composition (weight percent)	Remarks
2-0	50Fe-50Co	Melted - Tested
2-01	55Fe -45Co	Melted - Tested
2-02	60Fe-40Co	Melted - Tested
2-1	49.5Fe-49.5Co-1Al	Melted - Tested
2-2	49.5Fe-49.5Co-1As	Melting postponed
2-3	49.5Fe-49.5Co-1Be	Melted - Tested
2-4	49.5Fe-49.5Co-1Ge	Melted - Tested
2-5	49.5Fe-49.5Co-1Mo	Melted - Tested
2-6	49.5Fe-49.5Co-1P	Melting postponed
2-7	49.5Fe-49.5Co-1Sb	Melted - Tested
2-8	49.5Fe-49.5Co-1Si	Melted - Tested
2-9	49.5Fe-49.5Co-1Sn	Melted - Tested
2-10	49.5Fe-49.5Co-1Ti	Melted - Tested
2-11	49.5Fe-49.5Co-1V	Melted - Tested
2-12	49.5Fe-49.5Co-1W	Melted - Tested
2-13	49.75Fe-49.75Co-0.5Nb	Melted - Tested
2-14	49.75Fe-49.75Co-0.5Ta	Melted - Tested
2-15	49.5Fe-49.5Co-1Cr	Melted - Tested
2-16	49.5Fe-49.5Co-1Zn	Melting was done, Zn was lost
2-17	49.5Fe-49.5Co-1Au	Melted - Tested
2-18	49.5Fe-49.5Co-1Mn	Melted - Tested

to insert the thermocouple. The samples were held in an argon (purity 99.995%) filled quartz tube during the dilatometer test.

The furnace, preheated to 1292°F (700°C), was slid over the tube containing the sample and the extensometer. The samples were then heated at a rate of 5.4°F/min (3°C/min) from 1292°F (700°C) to 1832°F (1000°C) and then cooled at a similar rate from 1832°F (1000°C) to 1292°F (700°C). In order to check the dilatometer, a bureau of standards test specimen was tested before and after making five experimental determinations. The results obtained on the standard sample established an error in measured temperature of ± 9°F (±5°C). The method for performing the saturation measurements on the 1/10 inch diameter by 1/10 inch high samples at room temperature and at elevated temperature is described in the first quarterly report.

c.   RESULTS

The temperatures of transformation measured by the dilatometer test are listed in Table II-11. In a few cases, the samples were re-run to confirm the reproducibility of measurements. The temperature where transformation started and where it ended was read from the dilatometer recorder chart. The measured values of magnetic saturation are listed in Table II-12. Saturation was measured at room temperature, at 1112°F (600°C) and at 1652°F (900°C).

The re-run of several dilatometer tests shows that in the pure iron-cobalt alloys the reproducibility is within 36°F (20°C). In the case of the tertiary alloys, the reproducibility appears to be somewhat better. The values for transformation temperature which were determined on this program for the iron-cobalt alloys appear to be 18-36°F (10-20°C) lower than the data reported in the literature. This discrepancy requires additional investigation. The addition of 1%Be and of 1%Ti causes a rise in the transformation temperature. The increase is between 9 and 18°F (5 and 10°C). Although this increase exceeds the error of the instrument, it is less than the reproducibility limit of the transformation temperature for these alloys. Alloys containing 1%Si, 1%Mo, 1%Mn, and in particular 1%Cr, exhibit a strong influence in decreasing the transformation temperature more than 18°F (10°C).

The magnetic saturation decreased in all cases. The decrease at elevated temperature is larger than at room temperature. The addition of one weight percent of beryllium decreased the saturation at 1832°F (900°C) by about 15 percent. All other elements were less influential.

TABLE II-11. Alpha to Gamma Transformation Temperatures of Alloys During Heating and Cooling in °C (Rate 5.4°F/min or 3°C/min)

Alloy Number	Nominal Alloy Composition (weight percent)	Transformation on Heating (°C)	Transformation on Cooling (°C)	Arithmetic Mean (°F)	Arithmetic Mean (°C)	Change Over 50Fe-50Co (°F)	Change Over 50Fe-50Co (°C)
2-0	50Fe-50Co	948-958	953-935	1740	949	Standard	Standard
		960-973	964-948	1764	961	1755	957
		963-973	960-948	1762	961		
2-01	55Fe-45Co	948-953	948-940	1738	948	+5	+3
		975-980	970-963	1783	973		
2-02	60Fe-40Co	948-958	963-953	1751	955	+14	+8
		973-983	973-967	1787	975		
2-1	49.5Fe-49.5Co-1Al	958-963	950-938	1746	952	-9	-5
2-3	49.5Fe-49.5Co-1Be	973-978	965-953	1774	968	+20	+11
2-4	49.5Fe-49.5Co-1Ge	953-963	953-938	1755	957	0	0
2-5	49.5Fe-49.5Co-1Mo	925-963	933-791	1724	940	-31	-17
2-7	49.5Fe-49.5Co-1Sb	955-968	953-938	1749	954	-6	-3
2-8	49.5Fe-49.5Co-1Si	948-958	938-928	1729	943	-25	-14
2-9	49.5Fe-49.5Co-1Sn	963-970	958-948	1762	961	+7	+4
2-10	49.5Fe-49.5Co-1Ti	968-980	965-950	1773	967	+18	+10
2-11	49.5Fe-49.5Co-1V	963-970	943-958	1760	960	+5	+3
2-12	49.5Fe-49.5Co-1W	953-973	925-948	1742	950	-16	-9
2-13	49.75Fe-49.75Co-0.5Nb	965-980	958-938	1760	960	+5	+3
		960-975	948-932	1751	955	-7	-4
2-14	49.75Fe-49.75Co-0.5Ta	965-975	958-935	1756	958	+2	+1
		963-970	960-953	1764	962	+9	+5
2-15	49.5Fe-49.5Co-1Cr	965-970	960-945	1762	961	+7	+4
		913-970	898-842	1670	910	-84	-47
2-17	49.5Fe-49.5Co-1Au	963-975	963-945	1764	962	+9	+5
		963-978	953-938	1751	955	-7	-4
2-18	49.5Fe-49.5Co-1Mn	965-978	958-943	1762	961	+7	+4
		943-970	938-912	1724	940	-31	-17

54

TABLE II-12. Saturation Magnetic Moment of the Iron Cobalt Alloys 2-0 to 2-18.

Alloy Number	Nominal Alloy Composition (weight percent)	Saturation Magnetic Moment (emu/g)[a]				
		Room Temperature	1112°F (600°C)	Percent Change Relative to Room Temperature Value	1652°F (900°C)	Percent Change Relative to Room Temperature Value
2-0	50Fe-50Co	229.9	214.0	-7.6	172.5	-24.9
2-01	55Fe-45Co	233.0	215.3	-7.6	-	-
		233.4	-	-	-	-
2-02	60Fe-40Co	235.1	214.3	-8.8	-	-
		235.5	-	-	-	-
2-1	49.5Fe-49.5Co-1Al	223.8	206.5	-7.7	162.5	-27.4
2-3	49.5Fe-49.5Co-1Be	217.9	196.7	-9.7	149.8	-31.3
2-4	49.5Fe-49.5Co-1Ge	226.2	207.1	-8.4	163.5	-27.7
2-5	49.5Fe-49.5Co-1Mo	225.0	208.2	-7.5	162.1	-27.9
2-7	49.5Fe-49.5Co-1Sb	225.0	209.9	-6.7	164.8	-26.8
2-8	49.5Fe-49.5Co-1Si	226.2	207.8	-8.1	158.8	-29.8
2-9	49.5Fe-49.5Co-1Sn	225.4	208.8	-7.4	163.6	-27.4
2-10	49.5Fe-49.5Co-1Ti	225.4	210.3	-6.7	167.0	-25.9
2-11	49.5Fe-49.5Co-1V	224.6	209.2	-6.9	165.1	-26.5
2-12	49.5Fe-49.5Co-1W	225.5	209.4	-7.1	166.0	-26.4
2-13	49.75Fe-49.75Co-0.5Nb	227.1	211.3	-6.9	167.6	-26.2
2-14	49.75Fe-49.75Co-0.5Ta	228.6	213.0	-6.8	169.9	-25.7
2-15	49.5Fe-49.5Co-1Cr	224.8	207.8	-7.6	155.0	-31.1
2-17	49.5Fe-49.5Co-1Au	228.9	211.1	-7.8	166.1	-27.4
2-18	49.5Fe-49.5Co-1Mn	229.4	211.3	-7.9	164.5	-28.3

(a) - To convert saturation magnetic moment to the approximate value in gausses, multiply the listed value by 100.

3. Program for the Next Quarter

Melting and testing those alloys which had been postponed will be completed.

C. TASK 3 - DISPERSION-STRENGTHENED MAGNETIC MATERIALS FOR APPLICATIONS IN THE 1200-1600°F RANGE

1. Summary of Technical Progress

a) Purchase Orders for 18 prealloyed cobalt-base and cobalt-iron base atomized powders were placed with two suppliers. Four of these powders have been shipped but have not been received yet by Westinghouse.

b) A total of seven cobalt-base and cobalt-iron base composite powders containing dispersions of alumina and thoria were ordered from three different suppliers.

c) Two hot-extruded rods and one further cold-worked rod of cobalt containing dispersions of thoria were ordered to complement the other methods of producing dispersion-strengthened magnetic material being pursued by Westinghouse.

d) A literature survey was continued for the purpose of identifying the boride compounds which form under equilibrium conditions in cobalt-base and cobalt-iron base alloys containing additions of boron, titanium, zirconium, columbium and tantalum. Boride compounds will be the dispersion strengthening agents in 10 of the 18 compositions being purchased in the form of prealloyed atomized powders for subsequent processing into extrusions.

e) In preparation for applying hydrogen reduction treatments to remove oxides of cobalt and iron from prealloyed atomized powders and composite powders, a literature survey was continued for the characteristics of oxides which might be expected to form on the surface of powders. The hydrogen dew point and temperature requirements for their reduction were surveyed. Construction of retorts for use in hydrogen reduction treatments was initiated.

f) Internal-oxidation conditions pertinent to cobalt and cobalt-iron alloys and powders of various compositions that have been reported in the literature were reviewed. Four of the prealloyed atomized powders ordered for this program contain aluminum and beryllium which will be internally oxidized to form alumina and beryllia.

g) Rubber bags and tooling for the isotatic pressing of powders into compacts for subsequent extrusion into rod have been ordered.

2. Discussion

   a. PREALLOYED ATOMIZED POWDERS

The nominal composition of the 18 prealloyed atomized powders to be used in the program were listed in Table II-8 of the first quarterly report. Fourteen of these powders (Nos. 1-6, 8, 10-15, and 17) are being purchased from the Hoeganaes Sponge Iron Corporation. The other four (Nos. 7, 9, 16, and 18) are being obtained from Domtar Chemicals Ltd. Hoeganaes has shipped to Westinghouse four powders and they are expected to arrive shortly. On May 4, 1965, the project engineer, Dr. R. J. Towner, visited the Hoeganaes plant in Riverton, New Jersey to discuss and observe the processing and testing of these powders. The production equipment and procedures were found in accordance with earlier communications with Hoeganaes and in accordance with the specifications accompanying the Purchase Order. Flowing argon is used as a cover gas over the metal charge and melt. Segregation in the melt and powder product is avoided by the following procedures used in making the powders:

1) The stirring action imposed on the melt by induction heating during melting, superheating, holding, and pouring into hand shank ladle.

2) The short atomizing time required (about 3 minutes) for a 100 pound melt due to the high rate of atomizing.

Ten of the 18 prealloyed atomized powders which are part of this task contain boron. Their compositions are as follows:

Atomized Powder Number	Nominal Composition (weight percent)
2	Co-2.0%B
3	Co-1.0%B-2.2%Ti
4	Co-1.0%B-4.2%Zr
5	Co-1.0%B-4.2%Cb
6	Co-1.0%B-8.3%Ta
11	26.5%Co-71.5%Fe-2.0%B
12	26.1%Co-70.7%Fe-1.0%B-2.2%Ti
13	25.6%Co-69.2%Fe-1.0%B-4.2%Zr
14	25.6%Co-69.2%Fe-1.0%B-4.2%Cb
15	24.5%Co-66.2%Fe-1.0%B-8.3%Ta

58

In calculating the amounts of boron, titanium, zirconium, columbium, and tantalum to be added to the atomized alloys, the ratio of metal to boron was used which is found in the diborides (TiB_2, ZrB_2, CbB_2, and TaB_2) for the respective metal-boron binary systems. Although other boride compounds (binary, ternary and quaternary) probably will be also present in the powder extrusions, the diborides are desirable because of their high melting point and outstanding stability at elevated temperatures.

The atomizing process provides an extremely rapid quench of the molten powder particles to the solid state and insures that the boride constituent particles of high-melting point, which solidify first, will be dispersed and not have time to grow above submicron size before the cobalt or cobalt-iron matrix has solidified. Although the atomizing process produces cooling and solidification under conditions which are far from equilibrium, the boride compounds which have been identified in systems in equilibrium can serve as a valuable guide to the boride phases that will be found in the extrusions fabricated from powder.

A literature survey is continuing for the purpose of identifying boride compounds which form under equilibrium conditions. Results to date are given in Table II-13.

b.   COMPOSITE POWDERS

A meeting was held with the NASA Project Manager concerning selection of composite powders from the group of 12 listed in Table II-9 of the first quarterly report. Each of the composite powders identified in Table II-14 will be obtained in four quantities for the initial evaluation phase of this program.

c.   SUPPLIER EXTRUSIONS OF DISPERSION-STRENGTHENED
       COBALT

Two compositions defined in Table II-15 have been ordered from suppliers for the initial evaluation phase of this program. The compositions of the nine candidate extrusions from which final selection was made were listed in Table II-10 of the first quarterly report. The processes by which the powders will be made by the suppliers for subsequent extrusion are also listed in Table II-15. These processes for producing dispersions in metal are different and will serve to complement those used for the composite powders given in Table II-15 and the atomized powders. Extrusion No. 3 contains ten percent by volume of thoria while extrusion No. 9 contains two percent. In the case of extrusion No. 9, a second rod given an 85 percent reduction by cold working will be obtained as well as the hot-extruded rod. All

TABLE II-13. Some Boride Compounds in Cobalt and Cobalt-Iron Base Alloys

Boride Compound	Boron Content (weight percent)	Crystal Structure	Melting or Decomposition Temperature (°F)	(°C)	Calculated Density (g/cm³)
1. Co-B System					
a. Co_3B	--	Orthorhombic, Fe_3C type (often suppressed)	2030	1110	--
b. Co_2B	8.75	Tetragonal, $CuAl_2$(C16) type	2309	1265	--
c. CoB	15.51	Orthorhombic, FeB type	>2372	>1300	7.25
2. Co-B-Ti System					
a. $Co_{23-m}Ti_mB_n$ ternary [a]	--	Cubic, $Cr_{23}C_6$ type [a]	--	--	--
b. $(Co, Ti)_2B$ [b]		See Co_2B data 1.b			
c. TiB_2	31.12	Hexagonal, AlB_2(C32) type	5054	2790	4.52
d. TiB	18.43	Cubic, $NaCl$(B1) type	4748	2620	5.26
e. Ti_2B	10.15	Tetragonal, $CuAl_2$(C16) type [c]	3992	2200	--
3. Co-B-Zr System					
a. $Co_{23-m}Zr_mB_n$ ternary [a]	--	Cubic, $Cr_{23}C_6$ type [a]	--	--	--
b. ZrB_2	19.18	Hexagonal, AlB_2(C32) type	5504	3040	6.15
c. ZrB	10.59	Cubic, $NaCl$(B1) type	2282	1250	6.7
4. Co-B-Cb System					
a. $Co_{23-m}Cb_mB_n$ ternary [a]	--	Cubic, $Cr_{23}C_6$ type [a]	--	--	--
b. CbB_2	18.89	Hexagonal, AlB_2(C32) type	5432	3000	7.00
c. Cb_3B_4	13.32	Orthorhombic, Ta_3B_4 type	--	--	--
d. CbB	10.44	Orthorhombic, TaB type	3632	2000	7.60
e. Cb_2B	5.50	--	--	--	--
f. Cb_3B	3.74	--	--	--	--
5. Co-B-Ta System					
a. $Co_{21}Ta_2B_6$ ternary [a]	--	Cubic, $Cr_{23}C_6$ type [a]	--	--	--
b. TaB_2 [d]	10.69	Hexagonal, AlB_2(C32) type	5792	3200	12.62
6. Co-Fe-B System					
a. Co-Fe-B ternary(s)	--	--	--	--	--
b. $(Fe, Co)_3B$ [e]		See Co_3B data 1.a			
c. Fe_2B	8.83	Tetragonal, $CuAl_2$(C16) type	2532	1389	--
d. $(Fe, Co)_2B$		See Co_2B and Fe_2B data 1.b, 6.c			
e. FeB	16.25	Orthorhombic	2804	1540	7.15
f. $(Fe, Co)B$		See CoB and FeB data 1.c, 6.e			
7. Co-Fe-B-Ti System					
a. Fe-Co-Ti-B quaternary(s)	--	--	--	--	--
b. Fe-Co-Ti-B ternary(s)	--	--	--	--	--
c. $(Fe, Co, Ti)_2B$ [b]		See Co_2B, Fe_2B data 1.b, 6.c			
d. $(Fe, Co)B$		See CoB and FeB data 1.c, 6.e			
e. TiB_2		See data listed previously 2.c			
f. TiB		See data listed previously 2.d			
8. Co-Fe-B-Zr System					
a. Fe-Co-Zr-B quaternary(s)	--	--	--	--	--
b. Fe-Co-Zr-B ternary(s)	--	--	--	--	--
c. $(Fe, Co)_2B$		See Co_2B and Fe_2B data 1.b, 6.c			
d. $(Fe, Co)B$		See CoB and FeB data 1.c, 6.e			
e. ZrB_2		See data previously listed 3.b			
f. ZrB		See data previously listed 3.c			

TABLE II-13. Some Boride Compounds in Cobalt and Cobalt-Iron Base Alloys - Continued

Boride Compound	Boron Content (Weight percent)	Crystal Structure	Melting or Decomposition Temperature		Calculated Density (g/cm³)
			(°F)	(°C)	
9. Co-Fe-B-Cb System					
a. Fe-Co-Cb-B quarternary(s)	--	--	--	--	--
b. Fe-Co-Cb-B ternary(s)	--	--	--	--	--
c. (Fe,Co)₂B		See Co₂B and Fe₂B data 1.b, 6.c			
d. (Fe,Co)B		See CoB and FeB data 1.c, 6.e			
e. CbB₂		See data previously listed 4.b			
f. Cb₃B₄		See data previously listed 4.c			
g. CbB		See data previously listed 4.d			
h. Cb₂B		See data previously listed 4.e			
i. Cb₃B		See data previously listed 4.f.			
10. Co-Fe-B-Ta System					
a. Fe-Co-Ta-B quaternary(s)	--	--	--	--	--
b. Fe-Co-Ta-B ternary(s)	--	--	--	--	--
c. (Fe,Co)₂B (f)		See Co₂B, Fe₂B, and Ta₂B data 1.a, 6.b, 5.e			
d. (Fe,Co)B		See CoB and FeB data 1.b, 6.d			
e. TaB₂		See data previously listed 5.b.			
f. Ta₃B₄ (a)	7.39	Orthorhombic	--	--	13.69
g. TaB (d)	5.64	Orthorhombic type	3704	2040	14.28
h. Ta₂B (d)	2.90	Tetragonal, CuAl₂(C16) type	3704	2040	--
i. Ta₃B (d)	1.96	--	—	--	--

NOTES:

(a) - Other ternary compounds occur, but structure not identified. One of the ternary compounds (phase called x in Co-Ta-B system) has the same structure in both Co-Cb-B and Co-Ta-B systems, but the structure is unknown (ref. 1).

(b) - Work in progress by H. H. Stadelmaier indicates some small solubility of Ti in Co₂B. Solubility of Ti in (Fe,Co)₂B can be expected to have same order of magnitude (ref. 1).

(c) - May not be C16 type (ref. 2).

(d) - Ta₃B₄, TaB, Ta₂B, and Ta₃B not observed in cobalt-rich alloys (ref. 1).

(e) - Work in progress by H. H. Stadelmaier on (Fe,Co)₃B indicates Co₃B dissolves a large amount of Fe (ref. 1).

(f) - Despite the fact that both Ta₂B and Co₂B have the C16 structure type, there is no solubility of Ta in Co₂B due to an unfavorable size factor. For the same reason, it is highly improbable that (Fe,Co)₂B dissolves Ta (ref. 1).

The following sources, publications and references cited therein were consulted in compiling Table II-13.

1. H. H. Stadelmaier, University of North Carolina at Raleigh, Private Communication, May 22, 1965.
2. B. Aronsson, Arkiv Kemi, v. 16, 1960, p. 379-423.
3. S. Rundqvist, "Two Borides with the Cementite Structure (Co₃B), Nature, v. 181, 1958, p. 259-260.
4. S. Rundqvist, "Crystal Structure of Ni₃B and Co₃B", Acta Chemica Scandinavica, v. 12, 1958, p. 658-662.
5. M.R. Fruchart, "Moments Magnetiques des Borures Ferromagnetiques de Cobalt Co₃B, Co₂B et du Borure de Fer FeB," Compt. Rend. , v. 256, no. 15, April 8, 1963, p. 3304-05.
6. P. T. Kolomytsev, Dokl. Akad. Nauk SSSR, v. 130, 1960, p. 767.
7. H. H. Stadelmaier and R. E. Burgess, "Loslichkeit von Zink in den Boriden Co₂B und CoB und Konstitution der Kobaltreichen Legierungen im System Kobalt-Zink-Bor," Metall, v. 17, no. 8, 1963, p. 781-783.
8. G.V. Samsonov, and Ya. S. Umansky, "Hard Compounds of Refractory Metals," NASA Technical Translation F102, June, 1962.
9. H. H. Stadelmaier and G. Hofer, "Cobalt-Rich Corner of the Cobalt-Tantalum-Boron System and the Co₂₁Ta₂B₆ Phase," Metall, v. 18, no. 5, May, 1964, p. 460-2. (In German).
10. H. W. Lavendel, "Alloys of Tantalum Diboride with Iron, Cobalt, and Nickel," Planseeberichte fur Pulvermetallurgie, v. 9, April, 1961, p. 80-95.
11. H. H. Stadelmaier, "Ternary Borides with the Cubic Chromium Carbide Structure," Met. Soc. AIME, Nuclear Metallurgy, v. X, 1964, p. 159-166.
12. R. Kiessling, "The Borides of Some Transition Elements," J. Electrochem. Soc., v. 98, no. 4, April, 1951 p. 166-170.
13. G. Hagg and R. Kiessling, "Distribution Equilibria in Some Ternary Systems Me₁-Me₂-B and the Relative Strength of the Transition-Metal-Boron Bond," J. Inst. Metals, v. 81, 1952-53, p. 57-60.
14. M. Hansen, Constitution of Binary Alloys, Second Edition, 1958, McGraw-Hill.
15. F. R. Morral, Cobalt and Its Alloys - A Summary of Allotropy and Phase Diagrams, Second Edition, Revised 1958, Cobalt Information Center, Battelle Memorial Institute.
16. N. Fuschillo and R. A. Lindberg, "Electrical Conductors at Elevated Temperatures," ASD-TDR-62-481, January, 1963.

TABLE II-14. Composite Powders

Composite Powder Number	Nominal Composition (weight percent)	Particle Size of Oxide (microns)	Supplier's Process of Manufacture	Supplier
1	$95.2Co+4.75Al_2O_3$	0.01-0.06	Proprietary semi-metallic powder process	Pfizer
2	$95.2Co+4.75Al_2O_3$	0.1-0.6	Proprietary semi-metallic powder process	Pfizer
3	$88.8Co+11.2ThO_2$	0.01-0.06	Proprietary semi-metallic powder process	Pfizer
3	$88.8Co+11.2ThO_2$	0.01-0.06	Coating of suspended oxide core particles by precipitation of metal from aqueous solution	Sherritt Gordon
4	$88.8Co+11.2ThO_2$	0.1-0.6	Proprietary semi-metallic powder process	Pfizer
11	$23.7Co+64.2Fe+12.1ThO_2$	0.01-0.06	Proprietary semi-metallic powder process	Pfizer
11	$23.7Co+64.2Fe+12.1ThO_2$	0.01-0.06	High intensity arc covaporization of mixed oxides of cobalt-iron and throium followed by hydrogen reduction of cobalt-iron oxides to metal.	Vitro Labs.

TABLE II-15. Supplier Extrusions

Extrusion Number	Nominal Composition (weight percent)	Particle Size of Oxide (microns)	Supplier's Process of Manufacture of Powder for Extrusion	Supplier
3	$88.8Co+11.2ThO_2$	0.01-0.06	Thermal decomposition of a thorium salt on cobalt powder.	New England Materials Laboratory
9	$97.74Co+2.26ThO_2$	0.01-0.06	Co-dissolving the desired elements in a volatile solvent, flash-drying grinding and reduction of cobalt oxide to metal.	Curtiss-Wright, Metals Processing Division

material will be 3/8 inch in diameter by 84 inches long. The two percent thoria product will permit a comparison of properties to be made with those of other products made on this program which generally contain 10 percent by volume. The strength and magnetic properties of the two percent thoria in cobalt rod will be compared in both the hot-extruded and cold-worked conditions.

d.   HYDROGEN REDUCTION TREATMENT

Although processing conditions used by the suppliers are controlled to minimize oxidation of cobalt and cobalt-iron in the powders obtained for this program, there is opportunity for contact of powders with water and air during collection, mixing, screening, packing, shipping and weighing. Furthermore, four prealloyed atomized powders containing aluminum or beryllium additions will be internally oxidized intentionally to produce oxides of aluminum and beryllium. After such treatment, cobalt and iron oxides which formed will require hydrogen reduction. Therefore, a hydrogen reduction treatment (less than -60°F dew point) at 1220°F for six hours will be applied to the powders to reduce oxides of cobalt and iron that may have formed before the powders are compacted, sintered and extruded. It is planned to perform the hydrogen reduction treatment on the powders while they are spread out in shallow trays (150 mm long x 65 mm wide x 19 mm high) of 99% alumina (Coors AD99) inside Inconel 600 retorts through which purified and dried hydrogen is flowing. The water pumped, 99.95% purity hydrogen will flow from a cylinder through an attached Deoxo Hydrogen Catalytic Purifier (Model 10-50) and thence through a Drierite Drying Apparatus before entering the retort. Argon of 99.995% minimum purity will be used for flushing and back-filling. The Inconel 600 retorts are being constructed of 1/8 inch thick sheet and have inside dimensions of approximately 14-3/4 inch wide x 7-3/4 inch high x 21-1/4 inch long. The retort pan has welded joints and a one inch wide flange around the outside at the top to which will be fastened the retort lid by means of machine screws and nuts made of 18-8 stainless steel spaced at approximately 2 inch intervals around the periphery. A soft copper gasket 1/16 inch thick x 1 inch wide will be interposed between retort pan and lid. In addition, a refractory cement may be applied to seal the lid further, if required. The hydrogen gas inlet line will be 1/4 inch O.D. x 0.035 inch wall and the outlet line 3/8 inch O.D. x 0.035 inch wall Inconel 600 tubing. Provision will be made for dew point measurements. The retorts will be heated in a Pereco Model FGO-7800 furnace 18 inches wide x 18 inches high x 24 inches deep equipped with Globar heating elements, saturable core reactor with magnetic amplifier, strip chart controller-recorder and high-limit safety cut-off switch.

An electron diffraction study of the oxide films formed on cobalt at 0. 1 atmosphere of oxygen over the temperature range of 392-932°F (200-500°C) has been reported in the literature (ref. 28). After 50 minutes at 392°F (200°C), both CoO and Co_3O_4 were detected. The oxidation of cobalt was later investigated at temperatures of 392-1292°F (200-700°C) for oxygen pressures of 0. 1 to 0. 005 atmospheres (ref. 29). Oxidation of cobalt at higher temperatures 1472-2192°F (800-1200°C) and 1112-2192°F (600-1200°C) has also been explored (refs. 30 & 31). Co_3O_4 has been variously reported to be unstable above 1742°F (950°C) in air (ref. 30), above 1688°F (920°C) in air (ref. 31), above 1752°F (900°C) in 0. 013-27. 2 atmospheres oxygen pressure (ref. 32), and above 1688°F (920°C) in oxygen pressure of less than one atmosphere (ref. 33). Summaries of oxidation studies are readily available (ref. 34 & 35).

A thirty percent Co-Fe alloy oxidized at 572°F (300°C) for 30 minutes in 0. 1 atmosphere of oxygen showed the presence of Fe_3O_4 on the surface and a spinel, which may have been either Fe_3O_4, $CoO \cdot Fe_2O_3$ spinels or a mixture of the two (ref. 36). CoO was not observed on the surface or in the body of the oxide even though the weight percentage of cobalt was as high as 30. There may have been a solid phase reaction between CoO and Fe_2O_3 to form the spinel, $CoO \cdot Fe_2O_3$. Also it was reported that oxide films formed at 1112°F (600°C) and one millimeter oxygen pressure on 5, 30, and 40 percent Co-Fe all gave Fe_3O_4 type patterns (ref. 37). The standard free energy of formation of the spinel cobalt ferrite, $CoFe_2O_4$, from the oxide components CoO and Fe_2O_3 has been calculated (ref. 38). Also, the stabilities of Co and CoO as a function of oxygen activity and temperature, and the activity of CoO in contact with a Co-Fe alloy as a function of oxide composition in the system CoO-FeO at 2192°F (1200°C) have been determined (ref. 39).

Thermodynamic calculations have shown that the oxides of cobalt (CoO and Co_3O_4) are reduced by hydrogen even in atmospheres containing large amounts of water vapor (ref. 29). Furthermore, a graphical presentation of the thermodynamic requirements in regard to temperature and dew point on the oxidation of metals and reduction of their oxides in hydrogen indicated that a dew point of well above +65°F at 1220°F was sufficient for reduction of CoO to Co, and FeO and Fe_3O_4 to Fe (ref. 40). However, it should be mentioned that spinels might respond to a given hydrogen atmosphere in a manner unlike that shown by the individual oxides (refs. 40 & 41).

e.   INTERNAL OXIDATION TREATMENT

The compositions of the four prealloyed atomized powders which will be internally oxidized are as follows:

Atomized Powder Number	Nominal Composition (weight percent)
8	Co-2.5%Al
9	Co-1.3%Be
17	26.3%Co-71.0%Fe-2.7%Al
18	26.6%Co-72.0%Fe-1.4%Be

The amounts of aluminum and beryllium present were calculated to give ten percent by volume of oxide in the form of Al_2O_3 and BeO. The internal oxidation treatments will be applied at an elevated temperature where the aluminum and beryllium are in solid solution. Internal oxidation will occur over a period of six hours at 1830°F in oxygen of 99.5 percent minimum purity at a pressure of one atmosphere.   Inconel 600 retorts of similar size to those previously described containing a ceramic insert will be used.

It has been reported that internal oxidation began at 1652°F (900°C) and became more intense at higher temperatures in a Co-5%Al alloy specimen cut from a vacuum-melted ingot and exposed to air for 50 hours (ref. 42).   The 5%Al present had little effect on the scaling rate of cobalt above 1652°F (900°C).   Also, Co-32%Cr-0.41%Al and Co-32%Cr-0.39%Be alloys were oxidized for 50 hours.   In both alloys internal oxidation was evident at 1652°F (900°C) and became deeper with increasing temperature.   The oxidation of cobalt-aluminum alloys at 1112-2462°F (600-1350°C) in low-pressure oxygen was reported to result in the formation of gamma alumina on the surface below about 1652°F (900°C) which did permit the passage of cobalt ions through the layer, becoming oxidized to Co_3O_4.   The transformation from gamma alumina to alpha alumina occurs between 1652-2012°F (900-1100°C) and is accompanied by volume changes which can cause fissuring of the scale (refs. 43 & 44).

The internal oxidation of Ni-Al alloy specimens from castings at 1830°F for times of 6.25, 25, and 100 hours has been studied at four levels of oxygen pressure ranging from 10^{-4} to 10 atmospheres. The extent of the subscale formation was generally independent of oxygen pressure, as were subscale particle characteristics and hardnesses (ref. 45).   Powders of dilute Cu-Si, Cu-Al, Ni-Al, and Ni-Cr alloys were internally oxidized, hydrogen reduced, compacted, sintered and extruded.   A substantial strengthening effect was

achieved with the Al_2O_3 dispersions (ref. 46). The internal oxidation of dilute alloys of Cu-Si and Cu-Al in the form of minus 20 mesh powder has been reported (ref. 47). Powder compacts of Cu-0.38% Be, Cu-0.19%Al, Ni-1.9%Al and Ni-1.0%Cr alloys have been internally oxidized (ref. 48). Furthermore, Al_2O_3 dispersions in Fe-Al alloy powders (-100 mesh) have been produced by internal oxidation treatments (ref. 49).

3. <u>Program for Next Quarter</u>

a) As prealloyed atomized and composite powders are received, chemical and particle size analyses will be obtained. Metallographic examination of powder particle shape and size, and the fineness and uniformity of the dispersion within powder particles will be conducted.

b) Hydrogen reduction treatments will be applied to powders, and preparations made for internal oxidation treatments of four powders.

c) The isostatic pressing of hydrogen reduced powders into compacts will be started.

D. TASK 4 - CREEP TESTING

1. Summary of Technical Progress

a) All creep specimens were rough machined, heat treated and machined to finish dimensions. The heat treatment comprised of a solution anneal in air at 1725°F for one hour, a water quench, and aging in air at 1225° ± 5°F for 25 hours. Aged hardness was Rockwell C33-35. An analysis of the test specimen, in weight percent, was as follows:

C	Ni	Co	Ti	Zr	Al	Mn	Si	Ingot No.
0.01	22.5	Bal	2.15	0.95	0.28	0.32	0.15	AC232

b) Two eight-liter-per-second Varian, vac-ion pumps and power supplies were received and tested on a mock-up capsule assembly (see First Quarterly Report NASA-CR-54354, Figure II-3). Pressures of 4×10^{-8} torr at 1100°F and 2.8×10^{-8} torr at room temperature were measured during checkout.

c) The vacuum creep capsules were slightly redesigned to use electron beam welding throughout for assembly, and the capsules assembled.

d) The first Nivco creep test was started at 65,000 psi and 1100°F. Pressure at the time the samples were stressed was 1.4×10^{-7} torr measured 12 inches from the specimen. The pressure was decreasing when this measurement was made.

2. Discussion

The first Nivco specimen was placed on test at the end of the second quarter. Consequently, there are no creep data available for discussion.

In general, work during the second quarter was concentrated on system reliability and an operational system check out. A brief discussion of this work is included here.

During normal operation of some vac-ion pumping systems, one power supply, operating on standard 115V AC power, is used for each pump. These power supplies, however, are designed so that either one can power two pumps simultaneously. Consequently, an automatic power supply switch-over device was designed and successfully tested under the conditions of a simulated failure of one power supply such that both pumps were run from the remaining power supply. In the event of a service power failure, a battery and inverter were wired to cut in immediately

67

thereby preventing a pressure rise. Performance of both safety devices was verified on the complete test capsule and dummy stainless steel specimen. This system was built and operated continuously for 295 hours before being terminated to begin the testing of the Nivco alloy.

It has been decided that the samples should be run to 0. 40 and 1. 0 percent creep strain in 10, 000 hours instead of 0. 20 and 0. 40 percent. This change is the result of a careful analysis of design data requirements as summarized in the following brief analysis. The total creep of a solid generator rotor is defined as the change in rotor pole tip diameter over the operating life of the machine. Creep, therefore, must be held to as low a value as practicable in order to minimize the amount of clearance that must be provided between the bore seal and rotor. A desirable design target for total integrated creep strain in 10, 000 hours is 0. 20 percent. Using this criterion for example, a 10 inch diameter rotor would require additional running clearance of 0. 020 inch. The localized incremental creep might run from 0. 20 inches to as low as 0. 002 inches in this example because of stress and temperature gradients which exist in different areas of the rotor. These incremental creep strains are then integrated over the rotor diameter to obtain the average value of 0. 20 percent creep strain for the rotor. A thorough design therefore requires creep data at various extensions and at several different temperatures. Creep data will be obtained on Nivco alloy at 0. 40 and 1. 0 percent creep strains. The stresses will be adjusted to obtain these strains in 10, 000 hours at 1000° and 1100°F.

3.   Program for the Next Quarter

    a)   The first test will continue.

    b)   A second creep specimen will be placed on test.

SECTION III

PROGRAM II - HIGH TEMPERATURE
CAPACITOR FEASIBILITY

This program will study the feasibility of building a lighweight capacitor suitable for operation up to 1100°F. It will utilize high-purity dielectric materials and specialized fabrication methods. The ultimate application is in lightweight, high-temperature, power conditioning-equipment suitable for space application.

A. SUMMARY OF TECHNICAL PROGRESS

1) A processing method has been developed for sputtering (CVC, AST-100 Low Energy Sputtering System) noble metal electrodes on both sides of a capacitor substrate at the same time. Two pyrolytic boron nitride capacitors have been made in this manner. Electrical measurements made at room temperature with a General Radio Type 1620-A Capacitance-Measuring Assembly were:

Capacitor	Capacitance and Dissipation Factor at 1 KC	Electrode Diameter and Dielectric Thickness	Electrodes
No. 1 (BN)	78.56 pF 0.000298	0.383 inches 1.12 mils	Platinum (99.9% purity)
No. 2 (BN)	264.136 pF 0.00035	0.700 inches 1.11 mils	PT, 20% Rh (99.9% purity)

2) Boron nitride capacitor No. 1 was cycled four times between room temperature and 1100°F in air with no apparent physical or electrical damage. After thermal cycling, the electrical breakdown strength was determined at room temperature and a value of 10,400 volts/mil (4.1×10^6 volts/cm) was obtained.

3) A small vacuum test furnace was fabricated, set up and checked out in an evacuated (CVC, CV-18 pumping system) glass bell jar. A power input of about 43 watts will maintain a temperature of 1100°F at 1 to 2×10^{-7} torr. The first electrical measurements made in this furnace with a test sample (BN capacitor No. 2) were only partially successful because of a short circuit in the thermocouple.

However, using previous data obtained for a power-input-time-temperature relationship, values for the sample temperature versus measured capacitance at 1100°F (2.2 x 10⁻⁷ torr) can be estimated. On this basis, the total capacitance change was less than one percent and the dissipation factor increased to a value of only 0.00055 at 1100°F.

4) The use of three micron diamond powder, followed by polishing with Linde A, was found to be an effective method of reducing 2-3 mil pyrolytic boron nitride to pin-hole-free one mil wafers (one inch square surface area). Ultrasonic machining was successfully used to cut out circular wafers of one mil boron nitride. In addition, satisfactory cleaning procedures appear to have been established for preparing one mil wafers for electroding.

5) Wafering studies have progressed with good results being obtained with boron nitride and Lucalox. Single crystal sapphire is more difficult to slice into 10 mil wafers. Lapped, five mil sapphire wafers are also difficult to polish uniformly with one surface of the wafer bonded to a plate. A modified technique is being evaluated whereby the wafers can be lapped and polished on both sides at the same time.

6) A variety of lapping and polishing methods using rotating and oscillating laps have been investigated in an effort to eliminate grain pull-outs in thin Lucalox wafers. No definite trend can be established as yet. Plans have been made to evaluate the use of a higher frequency, lower amplitude vibratory lap (Syntron Lapping & Polishing Machine). Another polycrystalline, high-purity aluminum oxide material (hot pressed Linde A) appears promising in terms of obtaining better surface finishes because of its smaller average grain size.

7) High-purity beryllium oxide wafers 5 and 10 mils thick with "as lapped" finishes have been received. The necessary steps are being taken to prepare a working area to lap and polish these materials into suitable substrates for deposition of electrodes.

B. DISCUSSION

1. Pyrolytic Boron Nitride Capacitors

   a. PREPARATION OF WAFER MATERIALS

Twenty, one by one inch square, wafers of "Boralloy" (pyrolytic boron nitride) have been sliced using the methods described in the First Quarterly Report (NASA-CR-54354). This material is comparatively easy to slice into wafers with thicknesses in the range of from 10 to 12 mils using a metal-bonded diamond wheel. Several different size (8 to 15 mils thick and 4 to 6 inches diameter) rubber-bonded silicon-carbide, cut-off wheels have been received. It is planned to evaluate the feasibility of using these wheels to slice pyrolytic boron nitride into thinner wafers with a reduction in kerf loss. A brief trial was made using an 11 mil thick by 5 inch diameter rubber bonded wheel at 3700 rpm. The wheel developed an out-of-round condition after making a 1/8 inch depth of cut. A Norton Company representative was contacted and advised the use of higher wheel rpm's. Further experiments are planned in this direction.

A 1 inch x 1 inch x 1/4 inch block of boron nitride has been sent to Norton Company in Worchester, Massachusetts for evaluation on a new wafering machine that they have recently developed. This machine operates on an oscillating metal blade principle with a feed of abrasive slurry directed at the cutting interface. The blades can be ganged in multiples and can be as thin as two mils. The results of this test should be received in the next two to three weeks. If four mil wafers can be sliced with this machine with a kerf loss of four mils, about 30 wafers can be produced from a 1/4 inch thick block of material.

A somewhat modified technique has been used to lap and polish boron nitride wafers in their final stages of completion. Reduction of the material from the "as-sliced" thickness (10-12 mils) to a thickness in the three to four mil range is not critical. Boron-carbide (600 grit) is used on a glass plate with Dymo lapping fluid (Elgin National Watch Company, Industrial Products Division, Elgin, Illinois). The material is mounted and lapped on successively thinner shimmed plates as described in the first quarterly report. The critical phase of the lapping and polishing process is the thickness reduction and final polishing from four mils to approximately one mil. The techniques being used are still exploratory, however, the best results have been achieved as follows:

71

1) Lap one side of wafer to a final thickness of about 2-1/2 mils using 15 micron diamond on a glass lapping plate.

2) Remove wafers and remount on a plain plate glass holder (4 x 4 inches square, total weight two pounds - three wafers per holder). Mounting is critical to insure that all entrapped air pockets are squeezed out from under the wafers.

3) Lap and polish using six micron diamond on Pre K lap surface until all surfaces are polished uniformly. Scratches are still visible at 100X magnification. (Polishing cloths or lap surfacing materials manufactured by Geoscience Instruments Corporation, New York City, New York.)

4) Final polish with Linde A on Fine K lap surface.

5) Reverse mount and repeat step 3 until a thickness of approximately 1-1/2 mils is achieved.

6) Repeat step 4 until a thickness of one mil is obtained.

Dymo lapping fluid was used in all the above operations. The quality of the final polished surface using Linde A (0.3 micron particle size) is good but a few very fine scratches can still be observed. The cause of these scratches is probably due to abrasive contamination from previous polishing and lapping operations. It is planned to evaluate Linde B (0.05 micron particle size) as a final polishing material as well as other lap surfacing materials and extra precautions will be taken to insure that larger abrasive particles are removed when transfer is made to the next lapping or polishing step. In addition, a vibratory lapping and polishing machine (Model LP-01) manufactured by Syntron Company has been ordered and final polishing with this machine will be investigated. All lapping and polishing operations described in this report were done on a Mazur Lapping and Polishing Machine (Model LP-2, Westinghouse Scientific Equipment Department, Pittsburgh, Pennsylvania) with lap surfacing materials (Fine K and Pre K) manufactured by Geoscience Instruments Company.

Mounting of boron nitride wafers is a precise operation particularly after the material has been reduced to two mils in thickness. If the wafer is not mounted flat against the mounting plate or if air pockets greater than about 1/16 of an inch in diameter remain between the wafer and plate surface, high sections or bulges develop and the material will wear away completely or will be reduced to very thin

sections when an attempt is made to achieve an overall one mil thickness. Pressure bonding with Teflon coated or covered weights will be tried in the future to overcome this difficulty.

b. ULTRASONIC CUTTING AND CLEANING

A Sheffield Cavitron, Model 200B-5 was used to cut out 3/4 inch diameter disks of one mil thick boron nitride. The 1 x 1 inch square wafers were mounted (Pyseal wax, Fisher Scientific Company) on a plate glass square with a glass microscope slide waxed to the top of the wafer. An ultrasonic tool with an inside diameter of 3/4 inches was used to cut through the bonded sandwich assembly. The disk of boron nitride was then removed by heating the waxed plate. Satisfactory results were obtained using this technique. The wafers had very sharp and clean edges.

The final cleaning procedure used to prepare the wafers for attachment of electrodes is as follows:

1) Remove mounting wax by boiling in trichloroetylene for five minutes followed by 30 seconds ultrasonic agitation. Rinse three times with clean trichloroethylene with 30 seconds ultrasonic agitation during each rinse.

2) Rinse three times with clean methyl alcohol.

3) Rinse three times with clean acetone.

4) Dry - Boil in Alconox solution (1g per 250 ml of deionized water) followed by 30 seconds ultrasonic agitation.

5) Pour off Alconox solution and rinse in flowing de-mineralized water for 30 minutes (Barnstead Demineralizer Cartridge, Mixed Resin type).

6) Pour off water and rinse with six washes of clean Acetone.

Fisher Spectranalyzed Methanol and Acetone and Reagent Grade Trichloroethylene were used. The lot analysis for each of these solvents is shown in Table III-1.

c. SPUTTERED ELECTRODES

The fixturing used to sputter alloy electrodes of 20 percent rhodium 80 percent platinum on a 3/4 inch diameter x 1.11 mil thick pyrolytic boron nitride wafer is shown in Figure III-1 (BN Capacitor No. 2). This assembly is located within an 18 inch diameter glass bell jar. All the essential parts and their functions are identified in Figure III-1.

73

TABLE III-1. Lot Analysis of Fisher Spectroanalyzed Solvents Used to Clean Capacitor Wafers

Acetone	Lot #750564
Density (g/ml)	0.7853
Boiling range	56.0-56.3°C
Residue after evaporation	0.000%
Acidity (as CH_3COOH)	0.002%
Alkalinity (as NH_3)	0.000%
Aldehyde (as HCHO)	P.T.
Methanol (as CH OH)	0.05%
Substances reducing permanganate	P.T.

Trichloroethylene	Lot #750063
Boiling range	86.7-86.9°C
Specific gravity at 25/25 C	1.460
Residue on evaporation	0.0001%
Acidity (as HCl)	None
Alkalinity (as NaOH)	0.000%
Heavy metals (Pb)	0.000005%
Free Halogens	None

Methanol	Lot #750747
Water H_2O	0.05%
Boiling range	64.5-64.8°C
Residue after evaporation	0.0001%
Acetone, aldehydes	0.000%
Acidity (as HCOOH)	0.002%
Alkalinity (as NH_3)	0.0001%

18 INCH PYREX BELL JAR

STAINLESS STEEL TARGET
CONDUCTOR RODS - COVERED
WITH PYREX TUBING TO
PREVENT SPUTTERED MATERIAL
FROM REACHING COATING AREA
- NEGATIVE VOLTAGE APPLIED

OPENING IN WATER-COOLED
JACKET SURROUNDING
TUNGSTEN EMITTER FILAMENT

HOLE FOR ADDITION OF
SECOND TARGET ASSEMBLY

RUBBER HOSE CONNECTIONS -
FOR WATER COOLING FILAMENT
HOUSING

UP

DOWN

ANODE PLATE - POSITIVE VOLTAGE
APPLIED TO CREATE GLOW
DISCHARGE

ARGON INLET - COPPER TUBE
SURROUNDED BY PYREX TUBING

PLATINUM - 20% RHODIUM 3 MIL
FOIL TARGETS - SUBSTRATE IS
RAISED INTO POSITION BETWEEN
TARGETS DURING DEPOSITION

CAPACITOR SUBSTRATE -
SANDWICHED BETWEEN GLASS
MASKS - SHOWN IN LOWERED
POSITION.

ROD - EXTENDING FROM ROTARY,
PUSH-PULL FEED THROUGH

STAINLESS STEEL COVER PLATE

CONTROLLED LEAK
VALVE

TO ARGON TANK

RIGHT ANGLE GEAR DRIVE

FEEDTHROUGH RING - ON 24 INCH
STAINLESS STEEL BASE PLATE
OVER PUMPING SYSTEM (LN$_2$
BAFFLE, 6" DIFFUSION PUMP,
15 CFM MECHANICAL PUMP)

FIGURE III-1.   Three Element Sputtering Assembly and Associated
Fixturings

75

The sputtering power supply, necessary feed-thrus and accessory items comprise the AST-100 Low Energy Sputtering Unit manufactured by Consolidated Vacuum Corporation. The bell jar is evacuated by a CV-18 pumping system made by the same company.

This unit is equipped as follows:

1) Six inch diffusion pump (Convalex 10 fluid)

2) Liquid nitrogen baffle (BCN-61A)

3) Welch 15 cfm mechanical pump

4) Pirani gauge, 2 station (GP 145)

5) Ionization gauge (GIC-110A)

6) Two push-pull rotary seals

7) Work heater power supply and two kva filament power supply.

8) Twenty-four inch diameter stainless steel baseplate with a variety of feed-thru seals.

The capacitor substrate is located between two glass microscope slides that have coincident holes ultrasonically drilled into each slide to mask off a small margin (approximately 0.025 inches around the circumference of the disk. The major area of the disk is exposed on both surfaces to the bombarding metal atoms sputtered from the target. Aluminum clips are used to clamp the two glass slides together and to hold the capacitor wafer in proper orientation with respect to the holes in the glass. Initial alignment of the capacitor disk is tedious and it is planned to countersink a shallow depression (approximately 0.001 inch deep) around each hole on one of the glass masks. This depression should permit the capacitor disks to be easily placed in precise and fixed registration with respect to the mask holes. It is essential, however, to maintain intimate contact between the mask and substrate surfaces to achieve sharp and well defined margins. Ordinary soda line glass microscope slides have been used for masks, however, it is planned to use either alkali free content glass masks (Corning 7059) or pyrolytic boron nitride masks in the future to minimize any possible contamination from impurities that may be sputtered from the masks.

The AST-100 sputtering system is a three element unit as compared to a conventional two element sputtering geometry using only a cathode and anode. In the conventional system, the cathode must

76

perform a dual function by providing a source of electrons to maintain a glow discharge or plasma as well as providing a source of material which is to be deposited on the substrate. The AST-100 system is a recent development using a separate hot-filament electron source for gas ionization at pressures as low as 5×10^{-4} torr and separate ion targets to provide the source material for deposition. The major advantages of the system as compared to conventional sputtering are:

1) Control over deposit dimensions and composition,

2) Flexibility - a wide range of materials can be deposited and variety of target and substrate geometries can be used, and

3) Adherence - improved film adherence is obtained because of the higher arrival energy of sputtered atoms and a capability to pre-clean the substrate in a glow discharge prior to deposition.

The flexibility of the system is a particular advantage. For example, it would not be possible to sputter electrodes simultaneously on both sides of a capacitor wafer with a conventional two-element system.

The sputtering process used to deposit platinum-rhodium alloy electrodes on pyrolytic boron nitride wafers is as follows:

1) Register substrate between glass masks, clamp, and position substrate holder on rotary, push, pull feed-thru arm as shown in Figure III-1.

2) Evacuate bell jar to $\sim 5 \times 10^{-7}$ torr with CV-18 pumping system.

3) Activate tungsten filament (~ 48 amperes)

4) Back-fill bell jar with Argon and adjust chamber pressure to approximately three microns. (Argon Analysis: Less than 10 ppm or oxygen, 5 ppm of hydrogen, 40 ppm nitrogen and a dew point of <-80°F.)

5) Set anode voltage control to ~ 70 percent full scale.

6) Turn on anode switch and adjust anode current to 3.5 amperes. A glow discharge will appear. The discharge phase is maintained for about 30 minutes to clean the target and substrate surfaces.

7) With the substrate in a lowered position (as shown in Figure III-1) apply 900 volts to the target (Pt-20% Rh alloy, 3 mil foil, Englehard Industries, Baker Platinum Division, Purity 99.9%). Voltage is applied to the target for 15 minutes.

8) Raise substrate-mask assembly as shown by the arrows in Figure III-1 so that the substrate is positioned equidistant ($\sim 3/4$ inches) from each target face. Voltage (900 volts) is then reapplied to the target and sputtering is maintained for 30 minutes at a chamber pressure of approximately one micron. During the sputtering phase, the magnet coil is energized with 3.5 amperes to achieve a high plasma density (increased deposition rate) in the vicinity of the target and substrate.

It is planned to make a number of refinements in the sputtering process described above as the program progresses. These include:

1) Film thickness determination as a function of target material, target to substrate distance, plasma density, target voltage and chamber pressure.

2) Additional fixturing to permit sputtering from a pure rhodium target followed by an over layer of platinum. Ultra-high-purity target materials will be used with purities of 99.99 percent or better. A tabulation of source materials is shown in Table III-2.

3) Utilization of higher-purity masking materials and an improved substrate mounting and registration scheme as discussed previously.

4) The use of ultra-pure argon for chamber back-fill in combination with an ultra-pure transfer regulator. A typical analysis for this type of argon available from Air Reduction Company is as follows:

Purity	99.9995 min. vol. %
Impurities:	
Nitrogen	5 ppm
Oxygen	1 ppm

TABLE III-2. Availability of Ultra High Purity Noble Metals

Metal	Source	Purity	Forms	Price and Comments	
Platinum	Englehard Industries	99.95% 99.99%	foil, wire, etc.	$5.75/gram $5.91/gram	Quote 3/9/65
	Advanced Research Materials Co.	99.999%	single crystal rods	$215 for 1/4 inch dia. x 1 inch long	Quote 4/16/65
	Atomergic Chemicals Co.	99.999%	wire, sheet, foil	Catalog listing	
	Materials Research Corp.	99.99%	foil 3 x 3 x 3 mils	$200	Quote 3/24/65
	Leytess Metal & Chemical Corp.	99.99% min 99.999% min	foil 2 x 2 x 2 mils foil 2 x 2 x 2 mils	$54.60 $118.20	Quote 3/18/65
	Lights Organic Chemicals, Metals & Elements	99.999%	---	$336/10 grams	Quote 3/17/65
Rhodium	Englehard Industries	99.9%	foil, wire, etc.	$14.70/gram	Quote 3/9/65
	Materials Research Corp.	99.99%	foil, 3 x 3 x 3 mils	$250	Quote 3/24/65
	Atomergic Chemicals Co.	99.999%	wire, sheet, foil	Catalog listing	
	Advanced Research Materials Co.	99.999%	single crystal rods	E. B. Zone Refined	Quote 4/16/65
	Leytess Metal & Chemical Corp.	99.9%	foil 2 x 2 x 1 mil	$59	Quote 3/18/65
	Lights Organic Chemicals, Metals & Elements	99.999%	---	$336/10 grams	Quote 3/17/65
Platinum - 20% Rhodium Alloy	Englehard Industries	99.9%(Rh) 99.99%(Pt)	foil, wire, etc.	$6.42/gram	Quote 3/9/65
	Materials Research Corp.	99.99%	foil 3 x 3 x 3 mils	$200	Quote 3/24/65

Hydrogen	1 ppm
Carbon Dioxide	0.5 ppm
Hydrocarbons	0.5 ppm
Dew Point	-110°F

d. SINGLE LAYER CAPACITOR ELECTRICAL MEASUREMENTS

(1) Capacitor No. 1

The first single layer capacitor made from pyrolytic boron nitride was coated with sputtered pure platinum (99.9 percent) electrodes for preliminary evaluation. The electrode diameter was 0.383 inches. Electrodes were sputtered onto a 1/2 inch wide strip of lapped and polished boron nitride that varied in thickness from 1-1/4 to 1-1/2 mils (micrometer measurement). A calculated average thickness of 1.12 mils was obtained based on the measured capacitance at 1 KC, the electrode diameter and a dielectric constant of 3.4 using the formula:

$$T = \frac{KA}{4.45\,C}$$

where:

T = thickness (inches)
K = dielectric constant
A = electrode area (inches^2)
C = measured capacitance (pico farads)

Table III-3 shows the measured capacitance and dissipation factor at 1 KC. Also shown are the results of a d-c resistance measurement and voltage test made before and after thermal cycling. As noted, the capacitor appeared to be unaffected by thermal cycling in air to 1100°F, both physically and electrically.

Following the thermal cycling test, the d-c voltage breakdown strength of this capacitor was determined. The test was performed at room temperature with the capacitor immersed in Dow Corning Electronic Grade Silicone Oil. Voltage was increased at a rate of about 500 volts per second to 7,000 volts and held at this level for five minutes. The voltage was then increased until breakdown occurred. At 13,000 volts the power supply (DC Power Supply, Model PSP 30-5, Research-Cottrell, Inc., Electronics Division, Bound Brook, New Jersey) relay tripped indicating a short circuit or a current flow in excess of 10 milliamperes. No indication of leakage current was detectable

TABLE III-3. Preparation and Evaluation of Pyrolytic Boron Nitride Capacitor No. 1

Sample	Preparation	Capacitance at 1 KC, Room Temperature(a)	Dissipation at 1 KC, Room Temperature(a)	Insulation Resistance at 500V d-c, Room Temperature(b)	Voltage Test	Thermal Cycling	Remarks
Pyrolytic Boron Nitride Capacitor No. 1	1) Sliced wafer from 1 x 1 x 1/8 inch block(d) 2) Lapped to approximately 1.5 mil 3) Cleaned 4) Sputtered platinum(c) electrodes in argon partial pressure. Electrode diameter 0.383 inch	78.56 pF	0.000298	10^{15} ohms	withstood 1000V d-c before and after thermal cycling	1) Sample placed in cold furnace on thin Al$_2$O$_3$ slab-heated to 1100°F 2) Withdrawn from hot furnace - cooled 3) Inserted into 1100°F furnace - withdrawn 4) Repeat 3, two additional cycles	No evidence of electrode agglomeration or lifting from substrate after thermal cycling (800X magnification)

(a) - Capacitance and Dissipation Factor measured with a General Radio Type 1615-A Capacitance Measuring Assembly (Digital Readout)

(b) - Insulation resistance measured with a Keithley Multi-Range Electrometer, Model 610B

(c) - Platinum foil target, Englehard Industries, 99.9% Purity

(d) - "Boralloy" Pyrolytic Boron Nitride, High Temperature Materials, Inc., Lowell, Mass.

on the power supply milliammeter at any voltage level up to 13,000 volts. After resetting the power supply relay, voltage could be reapplied with no leakage current indication until 13,000 volts was reached. At this voltage level the dielectric punctured permanently.

Examination of the capacitor electrodes showed several areas where the platinum had vaporized. A section near the center of the capacitor was blackened and a hole was visible. The volts per mil breakdown voltage was calculated at 10,400 (4.1 x 10^6 volts/cm) based on the minimum measured thickness. This value in terms of volts per mil or volts per cm is about 2-1/2 times higher than the value reported for thicker pyrolytic boron nitride of same vendor and purity (10 to 20 mils thick, Table III-1, first quarterly report.

(2) Capacitor No. 2

The second completed pyrolytic boron nitride capacitor was processed as previously described with platinum-rhodium alloy electrodes. Three substrate disks were originally started, however, two of these disks were rejected after the final polishing and ultrasonic cutting operations because of a deep surface scratch on one disk and a torn edge on the other. However, the quality of the surface finish on the electroded disk was significantly improved over the first test capacitor evaluated (BN Capacitor No. 1).

The capacitance and dissipation factor of this capacitor has been measured at room temperature and over a temperature range up to approximately 1100°F in a vacuum at 1 to 2 x 10^{-7} torr. Unfortunately, precise temperature measurements were not possible during this first test run because of a short circuit in the thermocouple (caused by twisted thermocouple leads). The short circuit was not evident until the system had been evacuated and power was applied to the furnace winding.

Figure III-2 shows a cut away view of the test furnace which was designed to be used within the same glass bell jar system used for sputtering electrodes. The capacitor is placed on top of a columbium disk as shown in Figure III-2. Several trial runs were made without a test sample in the furnace to outgas the parts. A heating curve for one of these runs is shown in Figure III-3. A d-c power supply was used to energize the furnace winding since it was felt that there would be less 60 cycle interference during capacitance measurements. There appears to be
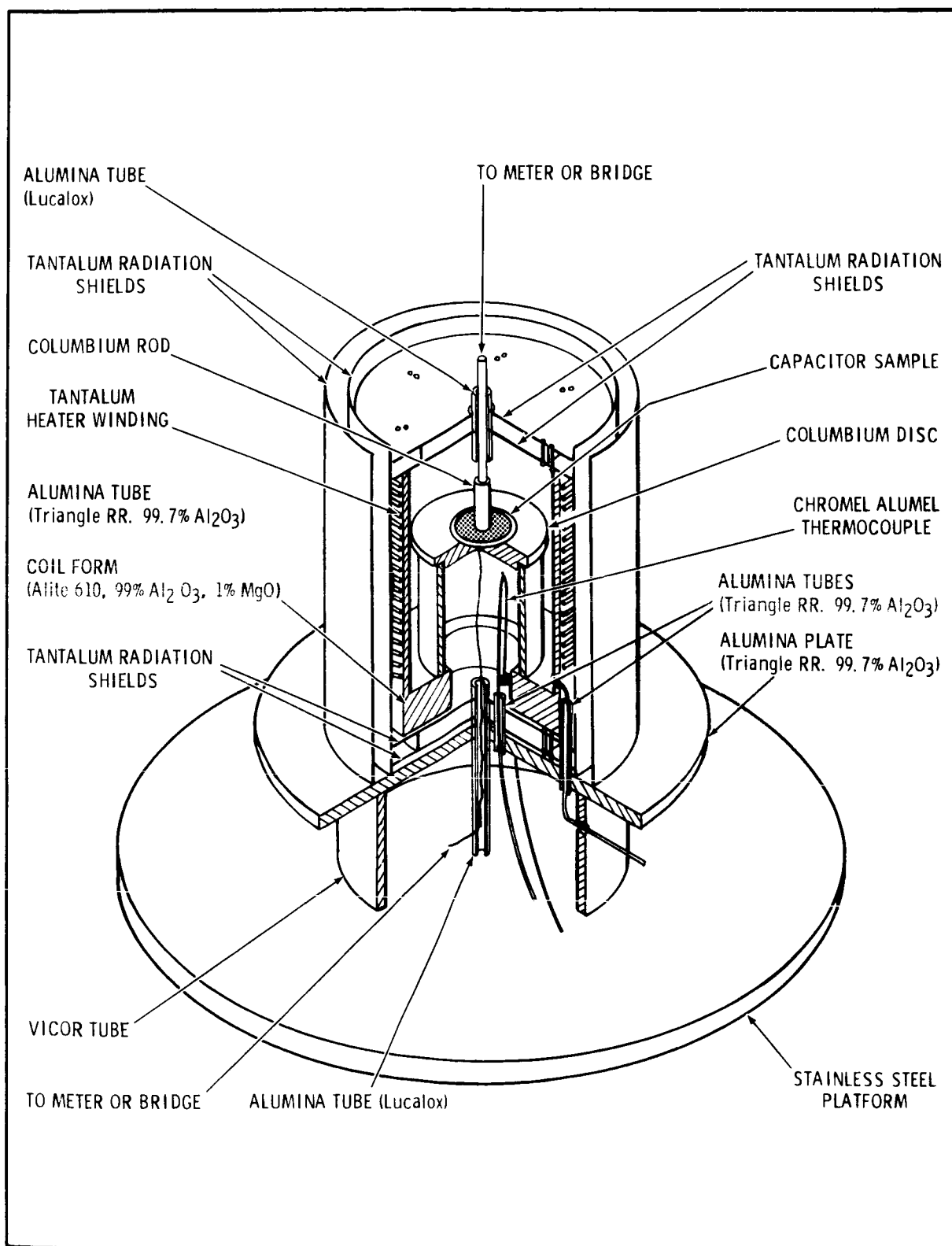
FIGURE III-2.   Cut Away View of 1100°F Vacuum Furnace Constructed
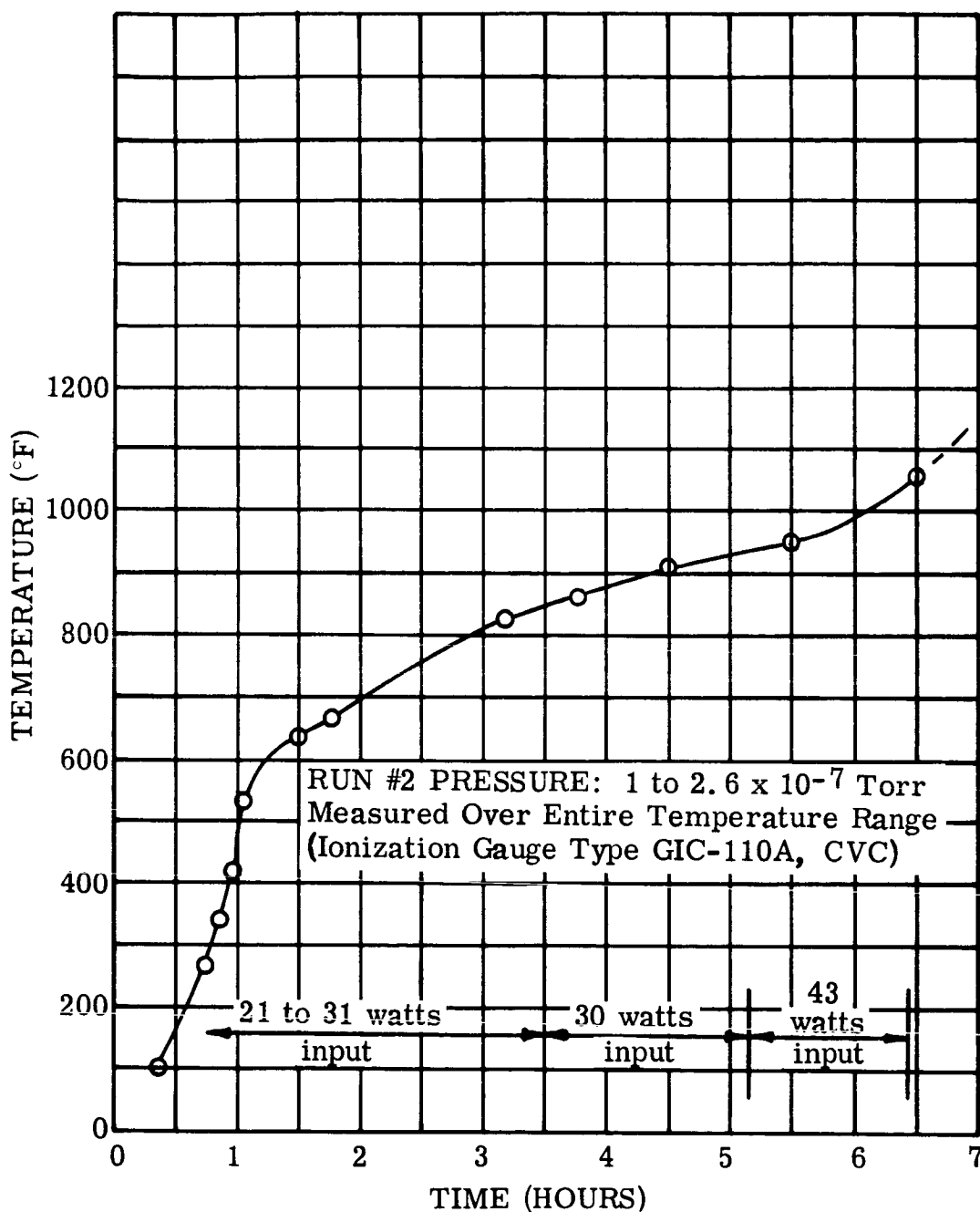For Electrical Testing of Single Layer Capacitors

83

FIGURE III-3. Temperature Vs. Time and Power Output for Vacuum Test Furnace (Figure III-2) Located Within Pyrex Bell Jar of CV-18 Vacuum System

Figure III-3. Temperature Vs. Time and Power Output for Vacuum Test Furnace

no difficulty in achieving a consistent vacuum level in the low 10^{-7} torr range when the furnace is heated in the 1100°F temperature range.

Based on previous heating runs with a functional thermocouple (Figure III-3) it appears that a power input of about 43 watts applied for 1/2 to 1 hour will result in a furnace temperature somewhat greater than 1100°F. Figure III-4 shows the results, subject to temperature estimates, of the capacitance and dissipation factor values obtained with the test capacitor located in the furnace as shown in Figure III-2. Dotted lines are drawn between room temperature values and the values measured in the vicinity of 1100°F. Intermediate points cannot be located with any degree of accuracy. The capacitance temperature coefficient is negative with a maximum change of about one percent. The dissipation factor measured at about 1100°F is as low or lower than the values obtained for many low-loss, conventional capacitors at room temperature. Based on these preliminary results, one would expect that this type of pyrolytic boron nitride capacitor would perform very well at 1100°F or higher in the audio frequency range. By way of a cursory comparison, Figure III-5 shows a typical set of curves for capacitance change and dissipation factor of a Teflon capacitor, Type 43, made by the Texas Capacitor Company. It is claimed that this capacitor will operate up to 200°C with excellent performance without derating. It appears that the dissipation factor of the Teflon capacitor from about 167 to 393°F (75 to 200°C) is almost an order of magnitude higher than boron nitride over a far greater temperature range (room temperature to 1100°F). In addition, the change in capacitance of the Teflon capacitor up to 393°F (200°C) is about four percent whereas the change in capacitance of the pyrolytic boron nitride capacitor is only about one percent up to 1100°F. A further comparison with a mica capacitor (ref. 1) designed for operation at 932°F (500°C) shows that the capacitor (Figure III-6) has a dissipation factor at 500°C (1 KC test frequency) of 0.1 (10 percent) which is almost three orders of magnitude greater than the value obtained for the pyrolytic boron nitride capacitor at the same frequency and approximate temperature range.

All capacitance measurements were made with a General Radio Type 1620-A bridge assembly using a three terminal measuring technique. The assembly consists of a Type 1615-A capacitance bridge with six digit capacitance readout and four digit dissipation factor readout, a Type 1311-A Audio Oscillator and a Type 1232-A tuned amplifier and null detector.

85

PYROLYTIC BN CAPACITOR NO. 2 – TEST RUN NO. 1

Electrodes: PT, 20% RH, 0.700 inch diameter
Dielectric Thickness: 1.12 Mils, Calculated using K – 3.4
Measurements made in vacuum at 1.6 to 2.3 x 10^{-7} torr
GR Type 1670 - A Bridge Assembly at 1 kc
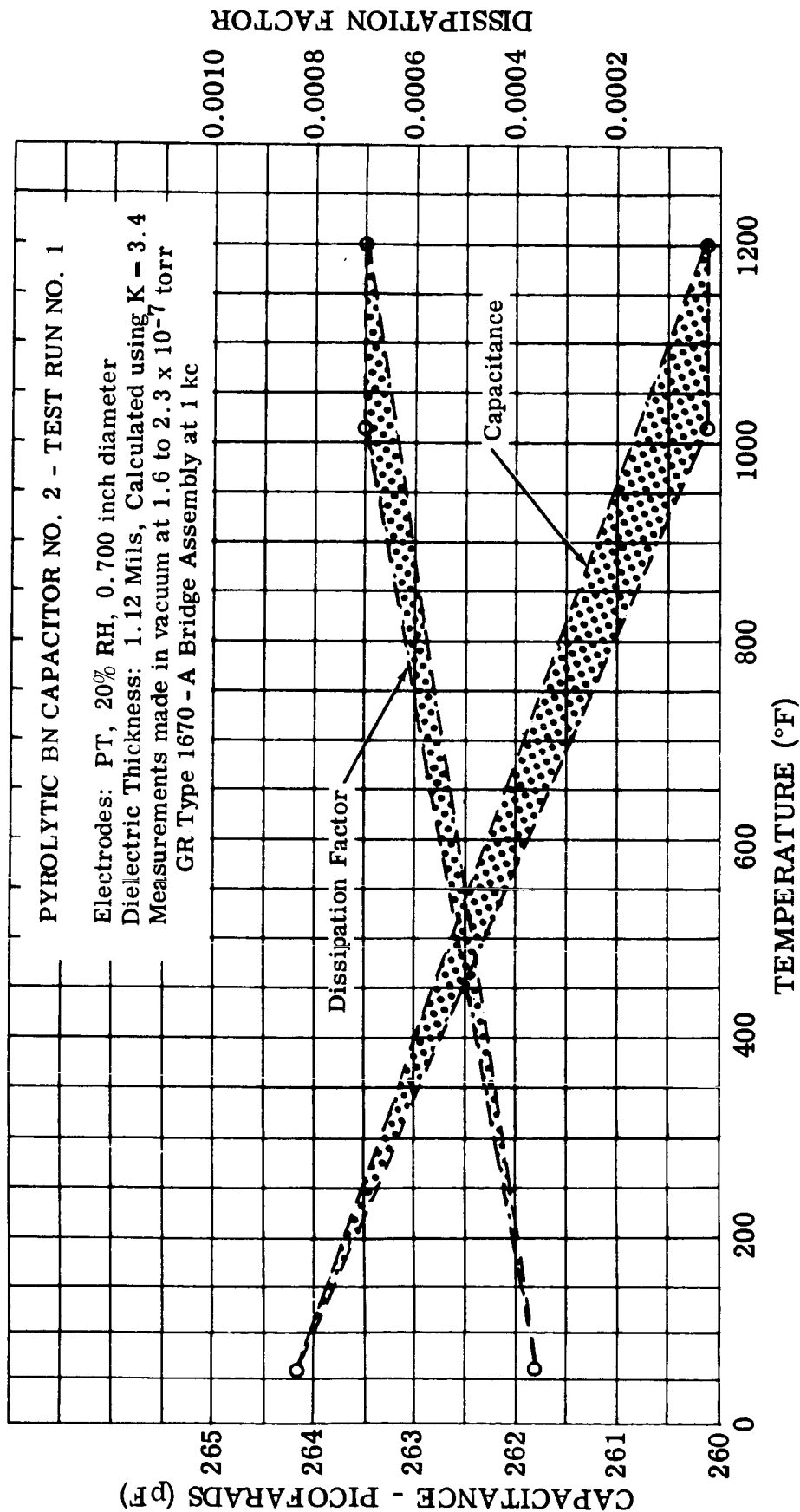
FIGURE III-4. Capacitance and Dissipation Factor Vs. Estimated Temperature
of Pyrolytic BN Capacitor No. 2

Figure III-4. Capacitance and Dissipation Factor Vs. Temperature
Pyrolytic BN Capacitor

FIGURE III-5. Texas Capacitor Co. Teflon Capacitor Type 43, Capacitance and Dissipation Factor Vs. Temperature to 392°F (200°C). Data From Company Bulletin, Page 21. Test Frequency Not Given. Curve Shown for Comparison Purposes. See Text Page 85.

Figure III-5. Capacitance and Dissipation Factor Vs. Temperature of Teflon Capacitor

87
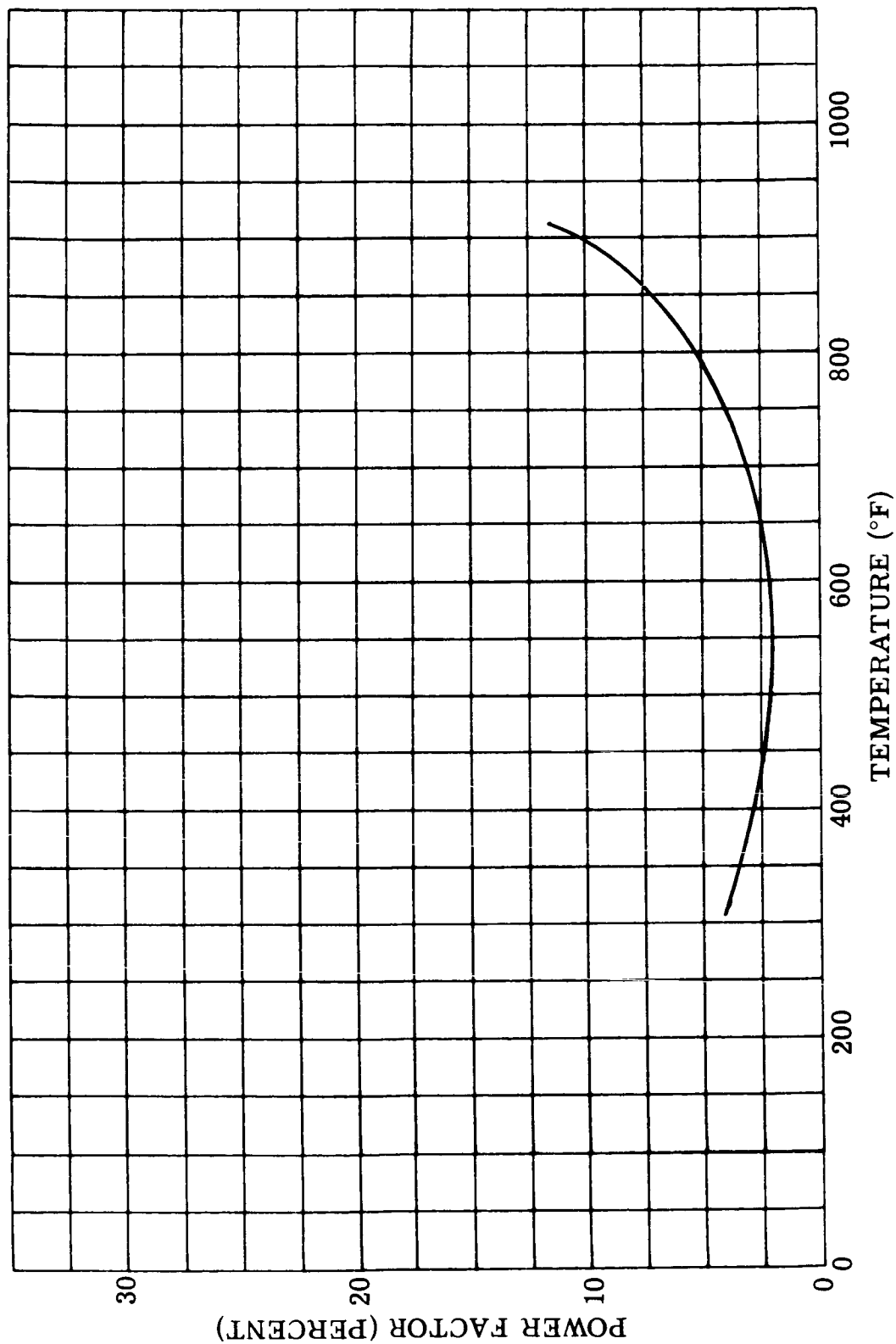
FIGURE III-6. Typical 1 kc Power Factor Variation for 500°C (932°F) Mica Capacitors (General Electric Co.) Note: Power Factor Approximate Dissipation Factor at Values Less Than 10%. Curve Shown for Comparison Purposes. See Text Page 85.

Figure III-6. Typical Power Factor Variation Vs. Temperature for 1 kc Mica Capacitors

It is planned to make another test run with this capacitor to verity the temperature capacitance relationship more precise. In addition, the d-c resistivity will be measured versus temperature and d-c voltage breakdown will be determined at 1100°F.

2. Lucalox, Sapphire and Beryllium Oxide Capacitor Wafers

A number of exploratory lapping and polishing methods were tried in an effort to eliminate grain pull outs over the entire surface of 3/4 inch diameter Lucalox (Al_2O_3) wafers (4 to 6 mils thick). These methods and the results are:

a) Polishing on a rotating glass lap plate (eight inch diameter plate at 575 rpm) using 9, 6 and 3 micron diamond. The sample was wax bonded to a steel disk that weighed 50 grams. Grain pull-outs were evident at 400X magnification and the disk edges were chipped.

b) A series of variations of the techniques outlined in Table III-3 of the first quarterly report were evaluated. Different vibration settings were tried, glass lap plates with one and three micron diamond were used, softer lap surfaces (Pre K and Fine K) with smaller diamond abrasive were tested and the effect of light and heavy weights were studied. No definite trend could be established. Some grain pull outs were still visible at 400X magnification. Most of the holes left by vacant grains were one to two mils wide and estimated to be about 1/2 mil deep. It appears therefore, that these wafers can be tested with sputtered electrodes provided a minimum overall thickness of about four mils is used.

A recent paper (ref. 2) presented at the American Ceramic Society 1965 Annual Meeting dealt with the lapping and polishing of difficult materials such as Lucalox. The authors reported that Lucalox with a surface area of about two cm^2 was polished with no visible pull outs using a Syntron Lapping and Polishing Machine. A nylon lap surface was used with one micron diamond. Six hours of lapping were required to produce the desired surface finish. Since these results are promising it was decided to obtain a Syntron polisher with Westinghouse funds for further evaluation of Lucalox four mil disks.

Four aluminum oxide disks 0.375 inch diameter by 0.015 inch thick prepared by a hot pressing technique developed on a previous contract (ref. 3) were lapped to five mils using 6 micron diamond on a glass lap plate. The original material used for these hot pressings was Linde A aluminum oxide. The average grain size

of this material is on the order of 1/3 the size of Lucalox grains. After lapping to 5 mils, the surfaces were examined at 400X magnification. In comparison with Lucalox, the surface depressions in the hot pressed material appeared to be significantly reduced. It is planned to polish these disks on the Syntron machine.

A sapphire boule (Crystal Products Department, Linde Company) was sliced and mounted on a glass plate using the same methods and equipment described in the first quarterly report for wafering Lucalox stock material. The boule had a diameter of approximately 1 inch and was about 3-1/2 inches long. Slices were made at right angles to the long or growth direction.

A five inch diameter by 0.016 inch thick metal bonded diamond wheel (Type D220-N100M 1/8, Norton Company) was tried with poor results. This wheel would not cut through the boule in a straight line. A 0.035 inch thick, resinoid bonded diamond wheel (Type DIAIR, DIM-N100B1/4) was tried with considerable success. Wafers about 15 mils thick were sliced. Seven of these wafers were lapped to six mils using 400 grit boron carbide, 30 micron diamond and 15 micron diamond (in that order) on a glass plate with Elgin Watch Company (Dymo) lapping fluid.

Several attempts were made to prepolish these wafers with nine and six micron diamond on Fine K lap surfaces. The wafers were bonded to a holding plate. In one instance, an excessive amount of weight was applied and the wafer cracked. When a lighter weight was used another wafer could only be polished around its outer circumference. These results indicate that the wafers have a slight warpage apparently due to non-uniform surface stresses resulting from previous machining operations.

As a means of solving this difficulty, it is planned to lap both wafer surfaces at the same time. A fixture has been designed which will permit both surfaces of a wafer to be lapped and polished between two (top and bottom) lapping plates. This arrangement has been evaluated using the Mazur Lapper and it appears to work satisfactorily. Different thickness metal shims with an arrangement of punched holes have been obtained. The wafers will be placed in the holes (about 1/8 inch larger in diameter than the wafer) with a floating lap placed on top. The floating lap is contained by a retaining ring bonded to the vibrating base lap plate. It is also planned to determine, by x-ray techniques, the precise crystallographic orientation of the next boule that is sliced.

The beryllium oxide wafer materials identified by specific types, size, purity and source as "on order" in the first quarterly report have all been received. One group of wafers are lapped to 10 mils (Consolidated Ceramics Corporation) and the other group of hot pressed wafers received from Atomics International are lapped to 5 mils in thickness. For purposes of comparative electrical evaluation it will be necessary to lap and polish these wafers to the four mil thickness range. The best lapping and polishing techniques that are developed for the other dielectric wafer material will be used for BeO. It is planned to start preparing these wafers for attachment of electrodes during the next few weeks.

C. PROGRAM FOR NEXT QUARTER

1) Preparation of single crystal and polycrystalline Al_2O_3 and BeO wafers with polished surfaces in the two to six mil thickness range will continue.

2) Pyrolytic boron nitride single layer capacitors will be completed.

3) Refinements in the sputtering process will be started and sputtered electrodes of platinum and rhodium will be applied to capacitor wafers of Lucalox, single crystal sapphire and BeO.

4) Electrical evaluation of single wafer pyrolytic boron nitride capacitors will be completed and testing of Al_2O_3 and BeO capacitors will be started.

SECTION IV

PROGRAM III - BORE SEAL DEVELOPMENT AND COMBINED MATERIAL INVESTIGATIONS UNDER A SPACE-SIMULATED ENVIRONMENT

The bore seal effort under Task 1 will evaluate promising ceramic-metal sealing systems in potassium and lithium vapor at temperatures from 1000° to 1600°F for 2000 hours. Elevated temperature seal strength and vacuum tightness will be determined. A four-inch diameter bore seal loaded with potassium will be incorporated in a stator design and evaluated in a 5000 hour endurance test at temperature and in a high-vacuum environment. This test will confirm data determined on smaller geometries.

Two five-thousand hour tests will be run under Task 2 on a stator which typifies the construction of an inductor alternator or a motor. The first will be run between 800 and 1000°F temperature. The second test will be run with a bore seal at temperatures between 1100 to 1600°F. All will be tested at high vacuum (greater than 10^{-8} torr) under electric and magnetic stresses.

A transformer and two solenoids under Tasks 3 and 4 will be similarly tested under high vacuum and at elevated temperature. The purpose will be to evaluate the combined effects of electric and magnetic stresses, and high vacuum on combinations of materials suitable for application in advanced space electric power systems. One solenoid test will be under d-c excitation and the other under intermittent excitation so the effects of an invariant electric stress can be investigated.

The design features incorporated into the stator, transformer and bore seal were defined in detail in Appendixes A, B, and C of the First Quarterly Report (NASA-CR-54354).

A.   TASK 1 - BORE SEAL DEVELOPMENT

1.   Summary of Technical Progress

   a)   The chamber for alkali metal loading and for electron beam
        welding was checked out and has attained a pressure of 4. 4
        x 10^{-6} torr at room temperature.   The dual vacuum furnaces
        for test capsule environmental exposure were checked and
        attained pressures of 3 x 10^{-9} torr when empty.   Elevated
        temperature testing of the equipment was started.

   b)   Six outgassing tests on several alkali-metal resistant ceramics
        have been completed.

   c)   The active-metal brazing study was initiated.   Active metal
        brazing alloys which were received in the foil form were found
        to have higher oxygen content than the powdered form.

2.   Discussion

   a.   FACILITY CONSTRUCTION AND CHECK-OUT

   The modification of the vacuum chamber for alkali-metal loading
   and electron beam welding has been completed.   A schematic
   diagram of the system identifying individual parts is shown in
   Figure I V-1.   A schematic of the liquid metal transfer line and
   associated valving is shown in Figure I V-2.   Photographs of the
   vacuum loading facility, the Brad Thompson Industries electron
   beam welder, and a close-up of the alkali metal hot-getter con-
   tainer with the right-end chamber entry are shown in Figures
   I V-3, I V-4, and I V-5.   During the testing and check-out operations,
   a vacuum of 4. 4 x 10^{-6} torr was attained with the chamber cold, dry
   and empty.   During one typical sequence of simulated operating
   conditions, the following changes in pressures were noted.   In and
   out movement of the manipulators reduced the pressure to 1. 1 x
   10^{-5} torr.   After the electron beam welder drive motor was on for
   15 minutes the pressure stabilized at 1. 9 x 10^{-5} torr.   With full in
   and out movement on both left and right manipulators, the pressure
   rose to 3. 5 x 10^{-5} torr but returned to 2 x 10^{-5} after 10 seconds.
   Lateral manipulator movement had no effect on the chamber pres-
   sure.   While welding stainless steel capsules (not outgassed) with
   the electron beam welder at 150 watts, the pressure rose to 6. 3 x
   10^{-5} torr.   The pressure returned to 2 x 10^{-5} torr within two
   minutes after the beam was turned off.   After some minor modifi-
   cations, electron beam welding of the columbium-1% zirconium
   corrosion test capsules will be started.
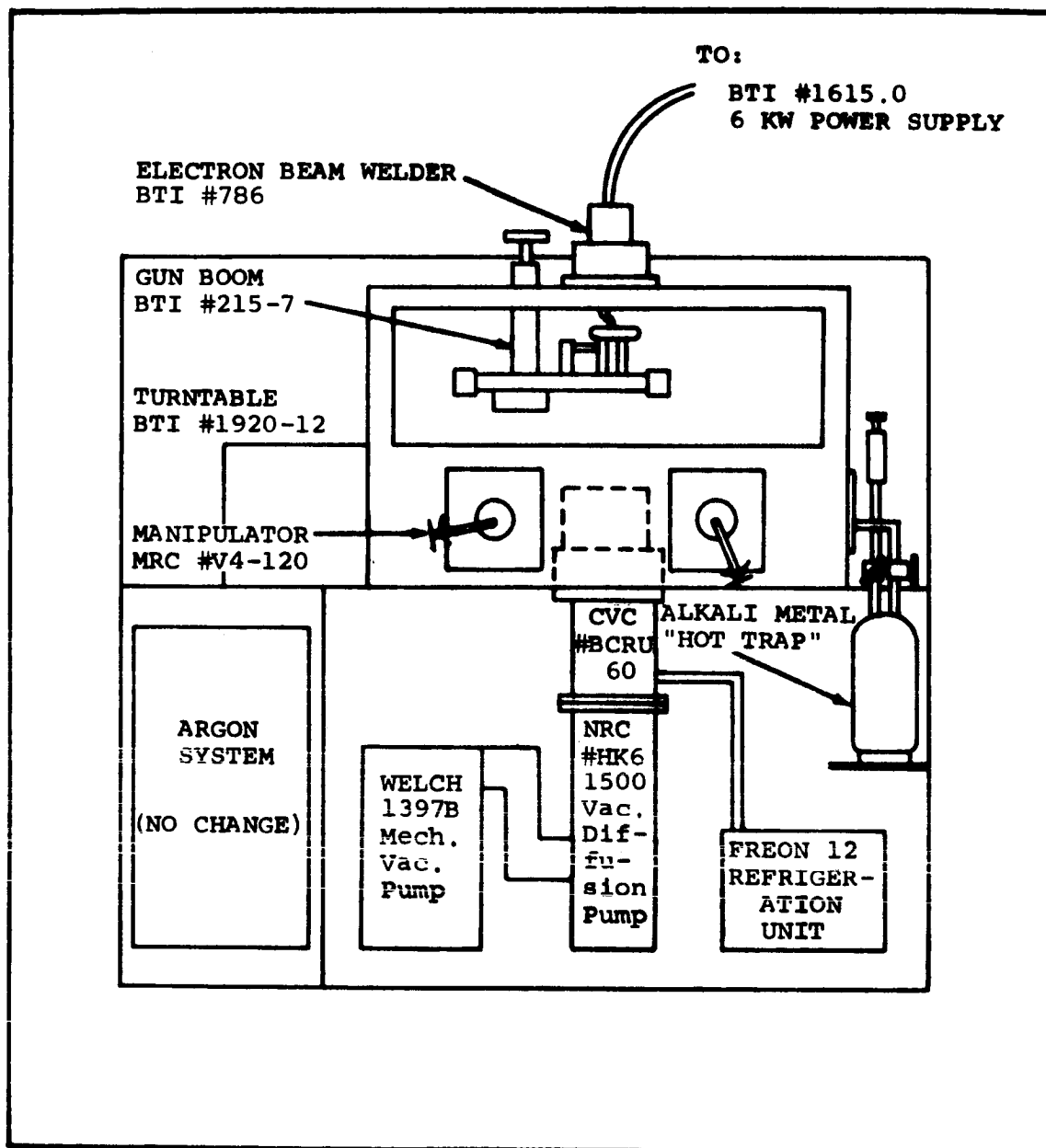
FIGURE IV-1. Schematic of the Capsule Fabrication and Loading Equipment

95
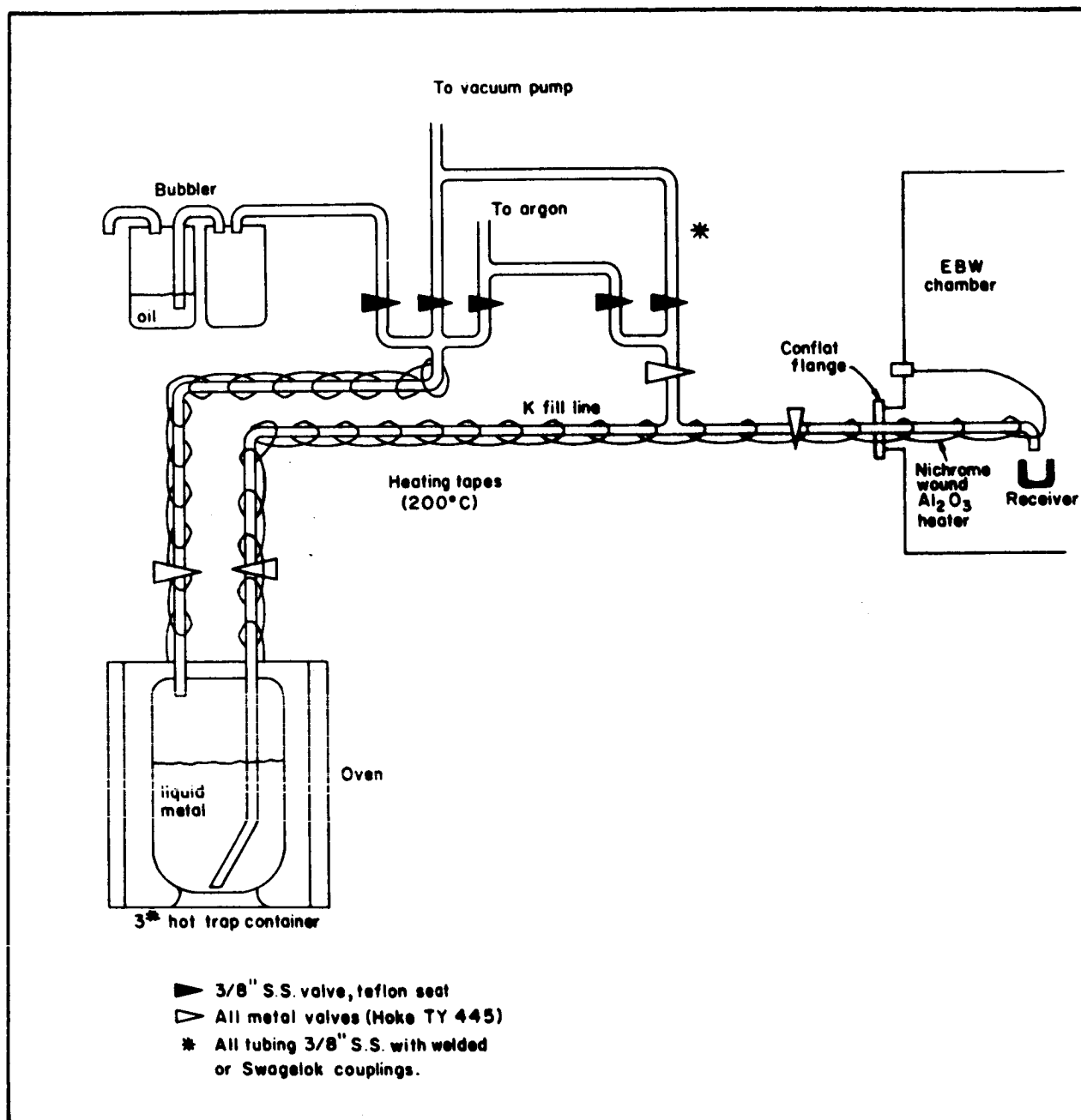
FIGURE I V-2. Schematic of Liquid Metal Transfer System
for the Vacuum Loading Chamber
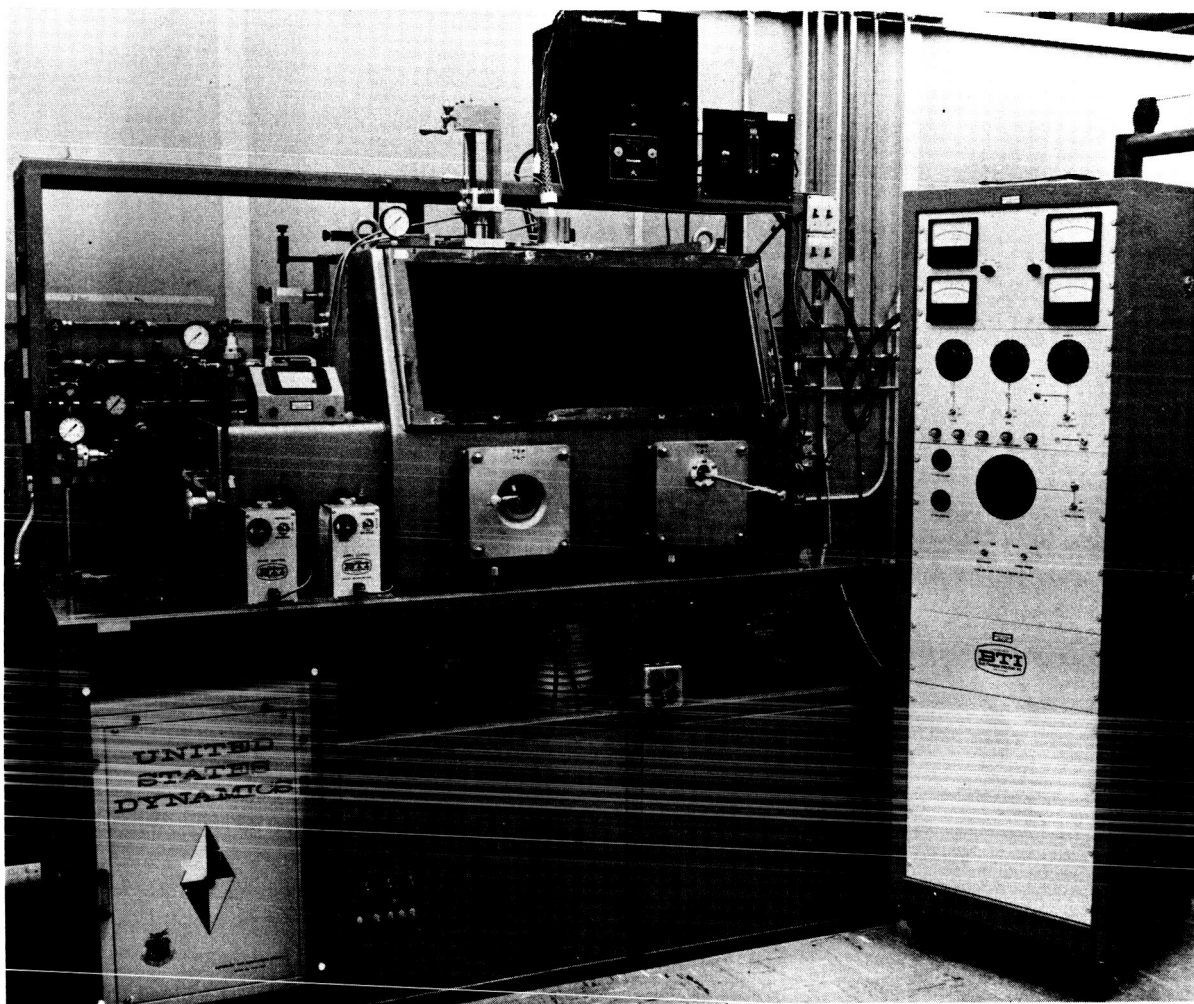
FIGURE I V-3.   Vacuum Chamber and Power Supply For
Capsule Loading and Welding
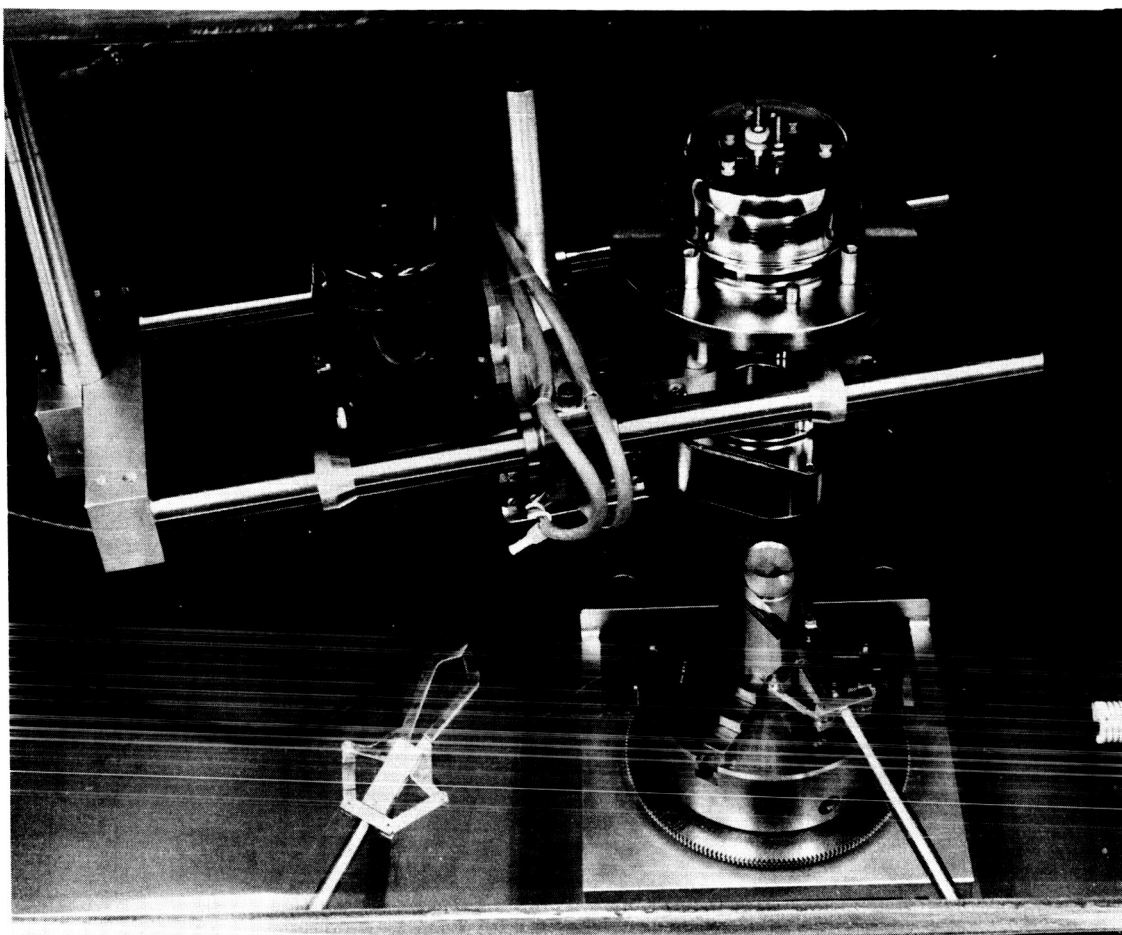
FIGURE IV-4. View Through Vacuum Chamber Window Showing Electron Gun and Positioning Boom, Turntable, and Manipulator With Capsule

98
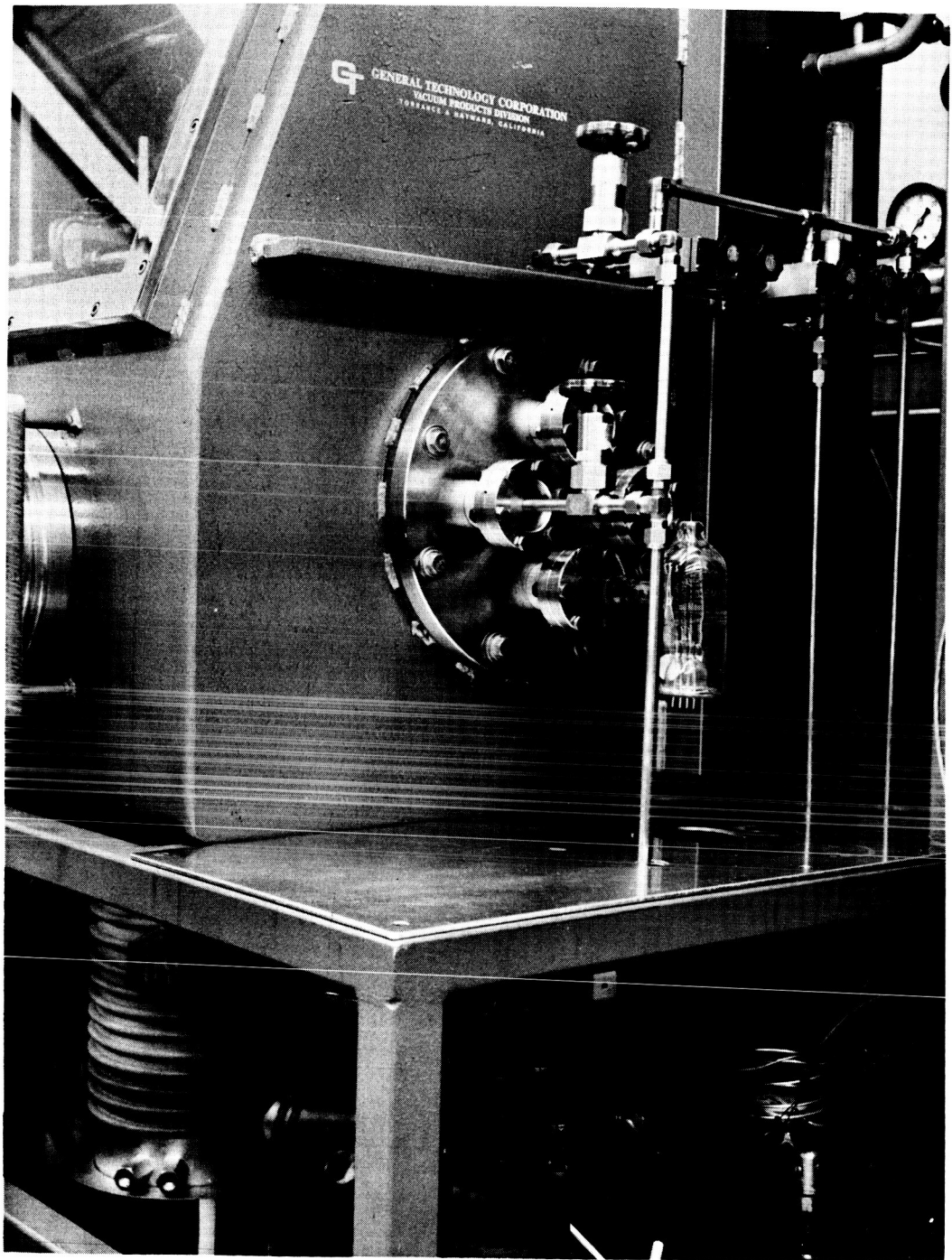
FIGURE I V-5.   Right End of Vacuum Chamber Showing Liquid Metal Hot
Trap Container Below Table and Transfer Line and
Valving Above Table.   Heating Tape on Transfer
Lines Removed for Photography.

An ion pumped, dual vacuum furnace system will be used to carry out the 500 and 2000 hour capsule exposure tests at 1000 and .1600°F. The individual components on the dual system are called out on the schematic diagram shown in Figure IV-6. A schematic of the resistance heated tantalum element furnace is shown in Figure IV-7. A photograph of the dual furnace equipment is shown in Figure IV-8.

During initial testing, the furnaces attained a vacuum of 3×10^{-9} torr when empty. Bakeout of the system had not been completed during this check-out test.

b. CERAMIC OUTGASSING STUDY

Alumina and beryllia ceramic bodies are normally fabricated by sintering the appropriate materials, in compacted powder form, in an oxidizing atmosphere for 1/2 to 3 hours at temperatures in the 2700 to 3100°F (1500 to 1700°C) range. Dissolved, chemisorbed, and occluded oxygen-containing gases (H_2O, CO, CO_2) are therefore released by the ceramics during subsequent treatment or use at elevated temperatures. Previous work at Eitel-McCullough (ref. 1) on alumina and sapphire outgassing has shown that cleaning and heat treating procedures on "as-received" ceramics also markedly affect the outgassing rate and the composition of the gas volume evolved.

The outgassing studies cited consisted of heating the samples from temperature T_1 to temperature T_2 in a vacuum furnace, collecting the evolved gases and then analysing them with a mass spectrometer. The method was useful in determining the total evolved gas content and composition for the T_1 to T_2 heat treatment. Subsequently, a technique and associated instrumentation were developed at Eitel-McCullough which offered the additional advantage of discrimination between surface absorbed gas and bulk outgassing. The technique consists of dropping the prepared sample into a precisely controlled, pre-conditioned vacuum furnace held at the test temperature. Selected m/e (mass to charge) ratios corresponding to the predominant gases are cyclically monitored as well as the overall fluctuations in furnace pressure. The pumping rate of the system for each gas component is known and outgassing rates and total evolved gas volumes can thus be determined. As the test sample rapidly rises to the furnace temperature, the outgassing curve goes through three distinct pressure peaks corresponding to:

1) Surface gases disturbed by sliding the sample into the furnace.

2) Surface gas desorption from the sample.

100
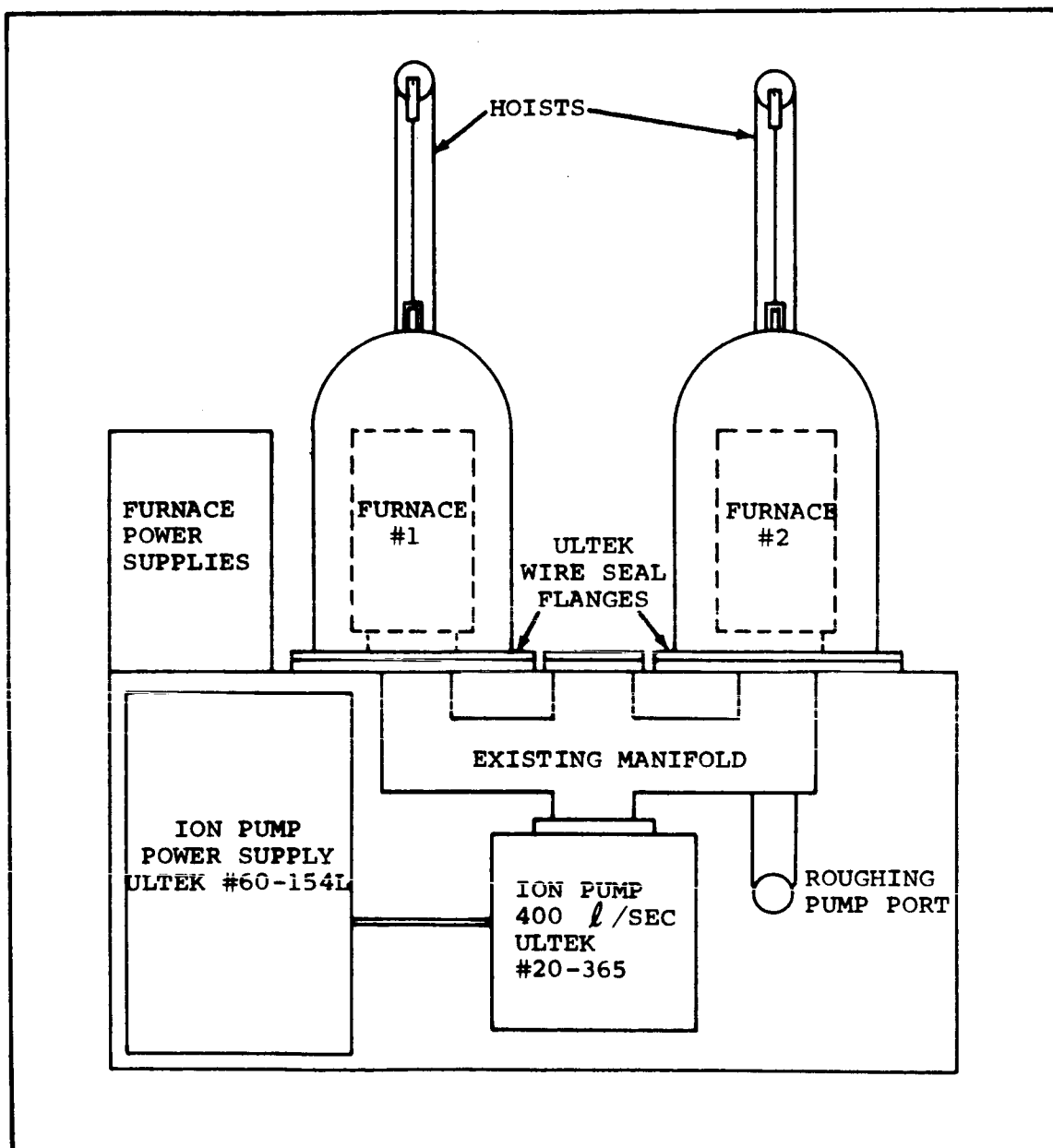
FIGURE IV-6. Schematic of Dual Vacuum Furnace Modifications
Using Ion Pumping
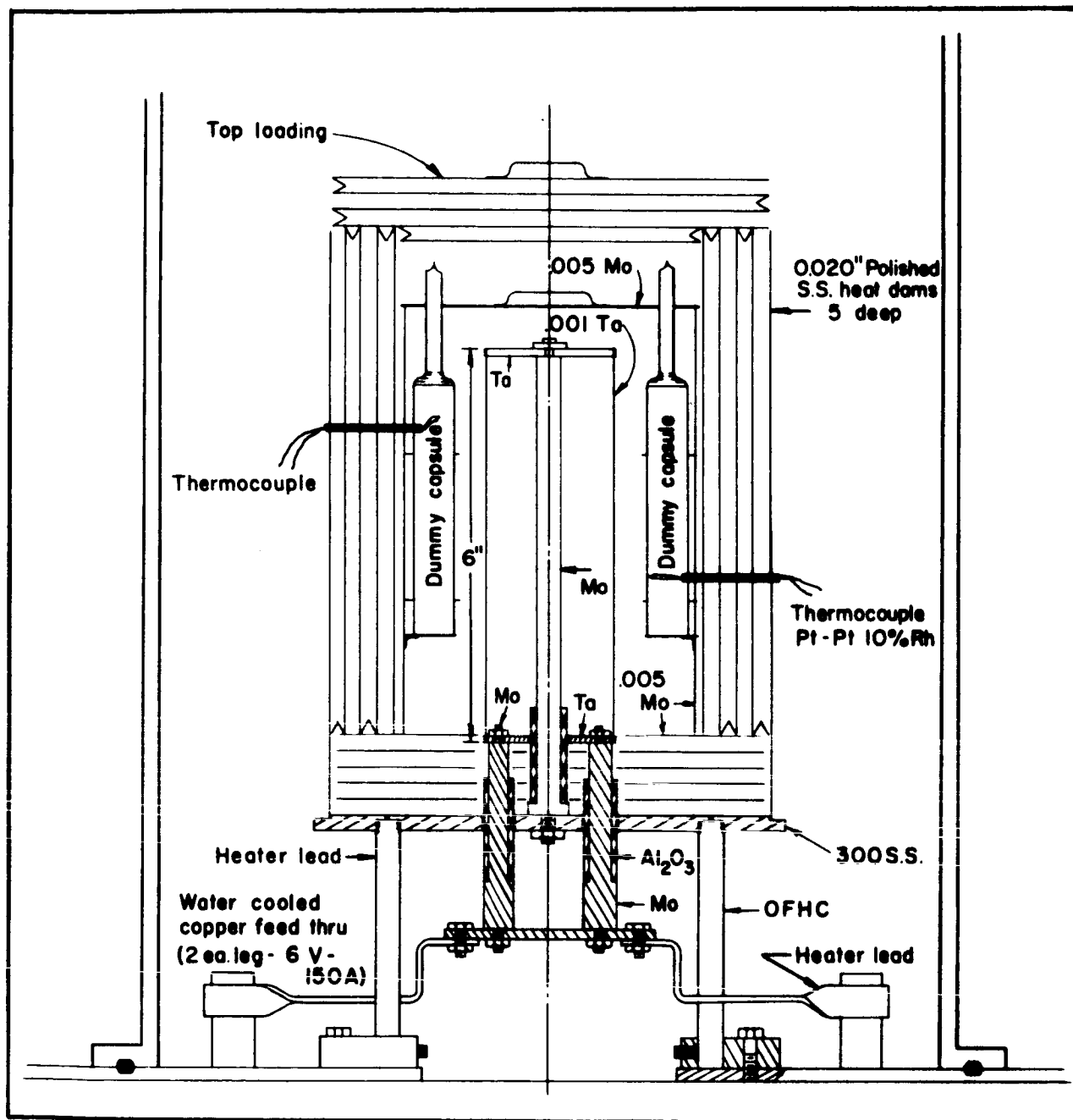
FIGURE IV-7. Schematic of Tantalum Element Vacuum Furnace Used in 1000° and 1600°F Capsule Exposure Tests. Dummy Capsules Contain Thermocouples Used to Monitor Temperature

102
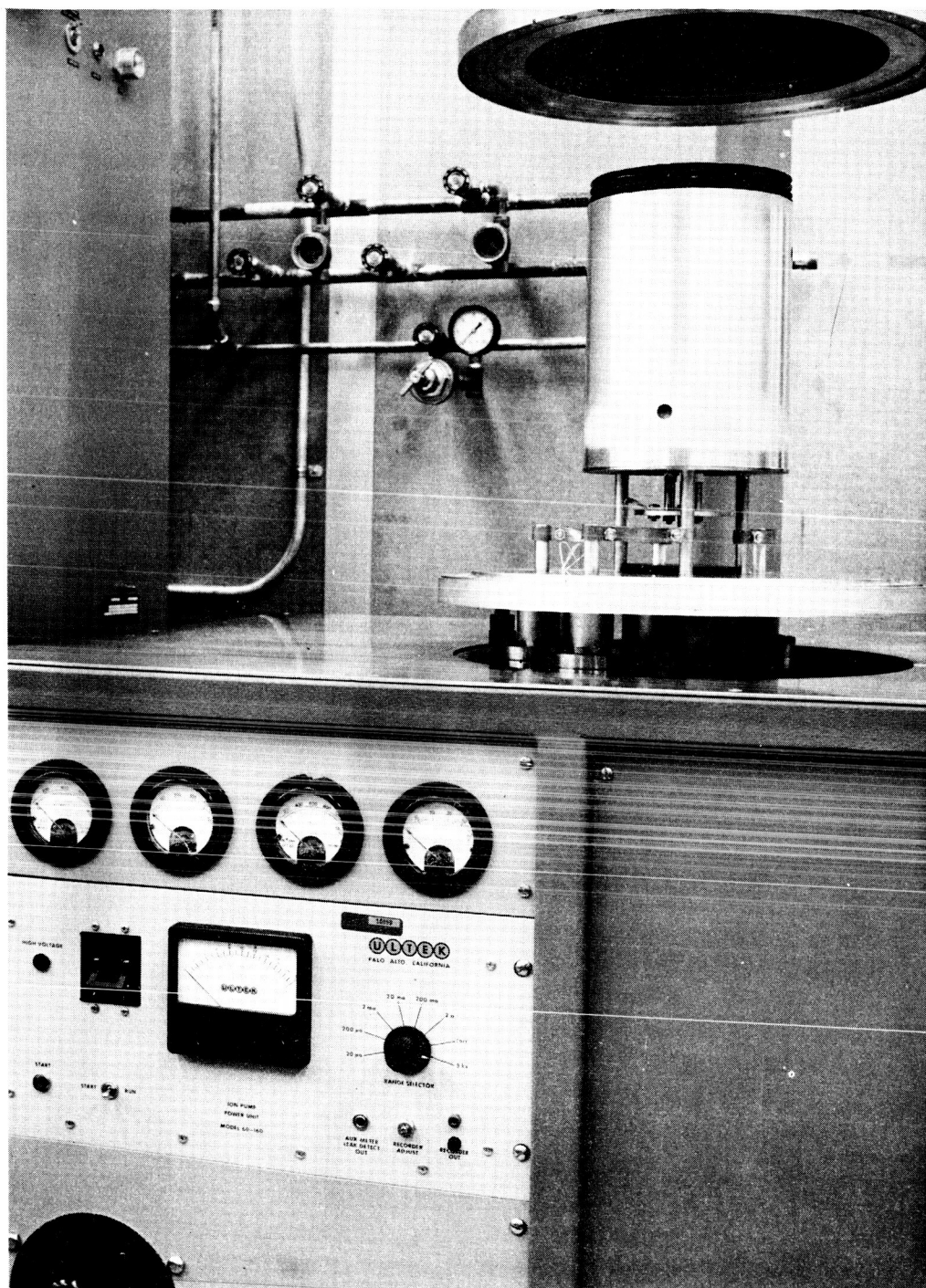
FIGURE IV-8. Close up of Dual Vacuum Furnace Equipment

3) Diffusing gases from the bulk of the sample.

The tails of the pressure peaks overlap but the peaks themselves are quite distinct. The third and last peak represents the bulk gases which are of greatest interest in this work. They are the gases which will diffuse out during operation of the bore seal and introduce oxygen into potassium vapor. The surface gases can be eliminated with proper system preparation. The third peak (for each gaseous component) rises rapidly and falls off exponentially corresponding to the increasing diffusion path of the gases from the interior of the sample.

The residual bulk outgassing rates of similarly fabricated and sintered ceramics will be similar. For this study, ceramic materials which were representative of different fabrication and sintering procedures were chosen. The three materials selected for this series of measurements and the systems they represent are:

1) Sapphire, single crystal 100 percent alumina; essentially no grain boundaries, no voids.

2) Lucalox, sintered polycrystalline 99. 8 percent alumina; with grain boundaries, but almost no voids.

3) Thermalox 998, sintered polycrystalline 99. 8 percent beryllia; with grain boundaries and voids.

The beryllia and Lucalox are representative bore seal ceramics and the sapphire is a control which will give an indication of the importance of grain boundaries and voids to residual outgassing. These three materials are not sintered (or flame fusion grown in the case of sapphire) in the same atmosphere. Therefore, useful comparisons and conclusions on manufacturing processes can also be made with the outgassing rate data obtained.

The specific sample preparation and test distribution for the out-gassing study is shown in Table IV-1. The 1832°F vacuum firing and the 2597°F firing in 70%N_2-25%H_2 are normal firings given to all ceramics on this program prior to vacuum brazing. The out-gassing tests will be continued for 20 minutes or until outgassing falls below detectable limits (background magnitude) corresponding to a partial pressure of below 5×10^{-8} torr.

TABLE IV-1. Test Distribution for Ceramic Outgassing Measurements

Ceramic	Nominal Composition	Outgassing Test Temperature	Ceramic Precondition				
			(a) As Received	(b) Vacuum Fired	(c) Clean and Vacuum Fired	(c) Clean and Vacuum Fired	(d) Clean and Vacuum Fired
Sapphire (Linde)	Single Crystal 100% Al₂O₃, Essentially Zero Porosity	1000°F 1600°F	X X	X X	X X	X X	X
Lucalox (G.E.)	Sintered 99.8% Al₂O₃, Essentially Zero Porosity	1000°F 1600°F	X	X	X X	X X	X X
Thermalox 998 (Brush)	Sintered 99.8% BeO 2-5% Porosity	1000°F 1600°F	X	X	X X	X X	X X

(a) - Precondition 1. After dye check and ceramic cleaning procedures (see Appendix A).
(b) - Precondition 2. Dye check and ceramic cleaning plus 10 minutes at 1832°F at less than 5 x 10-6 torr.
(c) - Precondition 3. Dye check plus ceramic cleaning plus 30 minute fire at 1425°C in 75% N₂-25%H₂; 100°F dew point plus 10 minutes at 1832°F at 5 x 10-6 torr.
(d) - As in (c) above except 120 minutes vacuum fire at 2192°F at less than 5 x 10-6 torr.

105

To date, the sapphire and Lucalox with preconditions 1, 2, and 3 (see Table IV-1) have been evaluated. Total gas volume evolved from the sapphire samples is summarized in Table IV-2. These data are now being evaluated and the gas species will appear in the Third Quarterly Report.

c. OTHER CERAMIC MATERIALS

There are two new Brush Beryllium Company BeO bodies available.

1) A 99.8% BeO body containing <50 ppm silicon as SiO_2, 0.1% MgO.

2) A 99.9% BeO body containing <50 ppm silicon as SiO_2, and approximately 0.05% MgO.

It is believed that the MgO addition to the BeO bodies does not seriously affect their corrosion resistance based upon thermodynamic considerations and it helps "processing" to a denser body. Both of these ceramic bodies are comparable in price being twice as expensive as the <100 ppm silica standard 99.8% BeO body. Some comments on their properties follow.

The densities of "low-silica" Thermalox 998 and "low-silica" 999 are quite similar with 998 ranging from 2.85 to 2.94 and is generally 2.90, while Thermalox 999 ranges from 2.82 to 2.90 and is generally 2.86. The normal strength of the 998 body, pressed to size, is 25,000-30,000 psi. The samples formerly supplied were cut from larger blocks, where the method of processing would a slight affect on strength reduction. The same characteristics hold for the 999 body.

Brush Beryllium Company can now supply the "low-silica" 998 body with a modulus of rupture above 30,000 psi on special order. They cannot, as yet, do this on the 999 body, although they believe that it will be technically feasible. All of the other properties are said to be similar to those previously given for the standard 998 body (<100 ppm SiO_2). On the basis of this information, the "low-silica" 998 body will be investigated.

Yttria ceramic in the form of modulus of rupture bars (0.1 inch x 0.1 inch x 1.0 inch) and 25 rings (0.35 inch OD x 0.50 inch wall x 0.1 inch) have been ordered from the Coors Porcelain Company. Their attention has again been drawn to the fact that silica content of less than 100 ppm is required and that the bodies be vacuum tight with a porosity of less than six percent.

106

TABLE IV-2. Total Gas Evolved from Sapphire Samples with Various
Preconditioning and Outgassing Temperatures

Precondition	Run No.	Outgassing Temperature	Sample Weight	Sample Area	Gas Evolved (torr liter/g)
1. After dye check and ceramic cleaning procedures	20	1000°F	0.264g	1.16 cm^2	40×10^{-4}
	21	1600°F	0.264g	1.16 cm^2	54×10^{-4}
2. Dye check plus ceramic cleaning procedure plus 10 minutes at 1832°F at less than 4×10^{-6} torr	18	1000°F	0.250g	1.12 cm^2	11×10^{-4}
	19	1600°F	0.269g	1.17 cm^2	20×10^{-4}
3. Dye check plus ceramic cleaning plus 30 minutes at 2597°F in 75%N_2-25%H_2 with 100°F dew point before 10 minutes at 1832°F at less than 5×10^{-6} torr.	13	1000°F	0.264g	1.17 cm^2	3.5×10^{-4}
	14	1600°F	0.264g	1.17 cm^2	6×10^{-4}

It is anticipated that the neutron activation technique will be employed for the non-destructive determination of silica in bore seal ceramics. This method of analysis, performed by the General Atomics Division of General Dynamics Inc. , is capable of determining silicon to several parts per million.

d. ACTIVE METAL BRAZE ALLOY FOILS

The oxide content of the ceramic-braze interface resulting from oxides in the braze alloy, from occluded atmospheric gases in the braze alloy, and from reactions of the braze alloy with the ceramic substrate, represents a potentially vulnerable area in the overall ceramic-metal seal system. The oxides of columbium and of the zirconium, titanium, and vanadium in the braze material are much less stable in alkali metal vapor than the metals themselves, while nitrogen or nitrides accelerate corrosion by lithium. The contributions of the three oxygen (and nitrogen) sources mentioned above can be controlled in a seal by the following methods:

1) Oxides (or nitrogen) in the braze alloy can be controlled by using pre-analyzed material, low in oxygen and nitrogen.

2) Occluded atmospheric gases in the braze alloy can be controlled by storing in protective atmospheres and by limiting the surface area of the alloy; for example, using sheet material versus coarse powder versus fine powder, etc.

3) Reaction of the braze alloy with the ceramic (reduction of the BeO or Al_2O_3) can be controlled by the selection and relative concentrations of the active materials and by the brazing temperature and cycle used.

The alloys used on this program are made from high purity raw materials, and the initial melted buttons have relatively low oxygen and nitrogen contents (100 to 700 ppm). The current procedures for controlling braze application and brazing cycle are given in Appendix A. The remaining means of oxygen and nitrogen control is controlled by the physical form of the braze alloy. The active metal brazing work reported previously (ref. 2) utilized powdered alloys exclusively.

For this program, selected single element, high-purity foils were ordered. Active-metal alloys, which had shown usefulness in alkali metal vapor (ref. 2) and which had exhibited sufficient ductility in the original comminution at Battelle Memorial Institute to warrant a rolling attempt, were also ordered in foil form.

108

A compilation of data obtained on the interstitial content of representative button, powder and foil braze materials is given in Table I V-3.

The alloying, comminution and rolling process was carried out by Battelle Memorial Institute.

Brazing alloy foils were prepared by conventional pack rolling techniques at elevated temperatures and final room temperature rolling to size. Two of these materials were on hand in the form of melted buttons (the method of melting is described later), the third alloy was prepared in the form of a 50-gram button from virgin material. The buttons were machined, placed in picture frame-type mild steel packs, painted with chrome oxide to prevent reactions between pack and core, and sealed by electron-beam welding to insure removal of the bulk of the nitrogen and oxygen. During the initial rolling sequence, which was accomplished at 1472°F (800°C), it was noted that the pack containing the 40Zr-30Ti-30V alloy was reduced 66 percent and the core reduced 58 percent when the pack ruptured. The initial rolling of the pack containing the 50Ti-30Zr-20V alloy ruptured after it was reduced 87 percent and the braze alloy core was reduced 83 percent. An examination of the cores at this stage of fabrication revealed some edge cracks and the remains of a solidification pipe in the 40Zr-30Ti-30V alloy. The 50Ti-30Zr-20V core appeared to be in excellent condition.

After trimming the edges of the cores to remove all evidence of cracking and to obtain regular shapes, the cores were placed into new packs as before but with cover plates 0.130 inch thick. The 40 weight percent zirconium alloy pack was then reduced to 0.055 inch with an average core thickness of 0.030 inch. The 50 weight percent titanium alloy pack was rolled to 0.035 inch with an average core thickness of 0.007 inch. These braze alloy cores were vapor blasted, belt sanded, and then cold-rolled on a four-high mill to 0.002 inch foil. Rolling was terminated at this point as no further reduction in thickness was noted after repeated passes through the rolls. Further reduction of the material might be possible by vacuum annealing and pack rolling, however, it should be noted that there is no assurance that this would not yield wrinkled and torn material of little value.

The alloy containing 56 weight percent zirconium, 28 weight percent vanadium, 16 weight percent titanium was prepared in much the same manner as the aforementioned materials. However, a 50-gram button of the alloy was prepared from virgin melting stock. The analyses of the melting stock is shown in Table I V-3. After melting six times (by the inert-gas nonconsumable arc-melting

TABLE IV-3. Interstitial Content of Selected Braze Materials
in Button, Powder and Foil Form

Material	Form	Oxygen (ppm)	Nitrogen (ppm)
Be [a]	--	2500 [b]	200
Th [a]	--	600	60
Ti [a]	--	180	20
Y [a]	--	2000-4000	100
Zr [a]	--	0-360	6-36
V [a]	--	784	270
56Zr-28V-16Ti	Melted button [c] Powder [c] Foil [c]	580 620 1700	100 120 1000
75Zr-6Be-19Cb	Melted Button Powder	520 960	97 98
65V-35Cb	Melted Button Powder	900 990	260 260
50Ti-30Zr-20V	Powder Foil	710 2600	(f) (f)
40Zr-30Ti-30V	Powder Foil	(f) 1300	(f) (f)
V [d]	Foil	1600	320
Zr [e]	Foil	850	25

(a) - Typical analyses supplied by Battelle Memorial Institute on raw materials
used in preparation of active alloy braze materials which they supplied.
(b) - as BeO
(c) - The powder and foil were from a different melt than the button.
(d) - Foil supplied by Battelle.
(e) - Foil supplied by Wah Chang.
(f) - Not determined

All analyses except those materials marked (a) were made by Westinghouse R & D
Center. Oxygen by vacuum fusion; nitrogen by modified Kjeldahl.

technique) at 400 amps for 30 seconds per melt utilizing a water-cooled tungsten-tipped electrode, the button weighed 49.90 grams. This represents a loss of 0.2 percent during melting. The tungsten tip exhibited a weight gain of 0.02 grams as a result of this melting cycle. Experience indicates that there is little or no contamination due to tungsten in the button and an alloy of the same composition as the charge to the furnace results under these conditions. After melting, the button was cleaned with a shaper, put in a pack, and rolled. Pack rolling was accomplished at 1650°F with reductions of 10 percent per pass. When the braze alloy core was removed from the pack, it was approximately 0.015 inch thick. The core was vapor blasted, belt sanded, and cold rolled to 0.002 inch thick foil.

It is evident from the analyses shown in Table IV-3 that the use of foil versus powder to minimize oxygen and nitrogen in the braze area will depend largely on the ability to roll foils without oxygen pickup and, as indicated by the rolling information given, even more elaborate techniques will be required to do this. At this point in time, even though application of braze alloys in the form of foil is simpler and more reproducible, it appears that the use of powdered material will result in a lower oxygen content in the braze area. The use of single element low oxygen content foils may prove feasible and limited work will be carried out to investigate that possibility.

An order has been placed for titanium, zirconium and vanadium as one mil foil from Materials Research Corporation (MRC). The oxygen content of these materials is 300 ppm. MRC uses electron beam zone refined ingots as their starting material. Beryllium foil, one mil thick, has been received from the Beryllium Corporation. This material is expected to have a maximum oxygen content of 100 ppm.

Yttrium (0.004 inch) and thorium (0.001 inch) foils have been received from Battelle Memorial Institute. The oxygen content of this material is approximately 3000 ppm. It appears that yttrium foil cannot be obtained in a purer form. This material was used on the initial experiments which are reported in Section IV. A. 2. d. Additional material has been ordered.

e.   ACTIVE METAL BRAZING

Yttrium braze alloy studies were commenced by brazing three mil yttrium metal foils, obtained from Battelle, to Cb-1Zr and beryllia or alumina CLM-15 tensile test pieces. Good mechanical seals were obtained with brazing cycles at 2550°F with a vacuum of 1 x 10^{-4} torr

at that temperature. However, leak checks showed the alumina sample to have a micro-leak while the beryllia sample indicated a gross leak.

A piece of yttrium metal foil was placed on an alumina substrate and processed under the same conditions as above. Despite the fact the yttrium melts at 2680°F, a firm mechanical bond was established between the yttrium and the alumina member, indicating that considerable reduction of alumina had taken place.

Two samples of yttrium-6% Cb braze alloy (using Y and Cb-1Zr shims) on BeO and Al_2O_3 plaques were processed at 2550°F in vacuum as above. Although neither alloy melted, it was noted that the reaction had proceeded much further on the alumina plaque than on the beryllia plaque; indicating that reduction of alumina to aluminum occurs more readily than beryllia to beryllium, and the consolidation of the braze alloy must be due to solution of aluminum in the braze alloy. These results might be expected, considering the relative thermodynamic stability of Al_2O_3 and BeO. The above braze was tested on a Cb-1Zr plaque. Only partial melting took place under the same conditions where melting took place on the ceramic plaques. In order to investigate the effect of the zirconium from the Cb-1Zr alloy on this braze alloy, a eutectic melt of 54Y-46Zr with a melting point of 2525°F was used to join a Cb-1Zr washer to Al_2O_3. A good mechanical seal was · obtained. However, difficulty was experienced in evacuating the seal which indicates a poor hermetic seal. The alloy foils had melted down adequately, but the braze appeared to be granular and porous.

Although the yttrium brazes appear promising for use in alkali metals because the oxide formed at the ceramic to metal interface is thermodynamically stable, control of excessive oxide formation may be a problem from the standpoint of joint integrity. This would be especially true if fabricated parts were stored for some length of time before use where even trace quantities of oxygen were available. Further investigation of the yttrium bearing braze alloys for ceramic to metal seals is expected to clarify their limitations.

3. Program for the Next Quarter

    a) Complete the initial check-out operation of electron-beam welder and load capsules with potassium and lithium. Complete the check-out of the dual vacuum furnace equipment.

    b) Complete ceramic outgassing study.

    c) Initiate screening tests on the yttria and low SiO_2-Thermalox 998 in Cb-1Zr capsules.

    d) Complete the preliminary screening of new braze alloys.

B. TASK 2 - STATOR AND BORE SEAL

1. Summary of Technical Progress

a) All stator materials have been received except for a few ceramic parts (Al_2O_3) and thermocouples. Delivery of these items is expected in early June.

b) The Varian thermal vacuum chambers and control console were received early in May.

c) All stator component manufacturing information has been released and parts are in manufacture.

d) Anadur insulated rectangular nickel-clad silver wire was received in May. Anadur is a refractory-oxide-filled glass fiber coating processed by Anaconda.

e) An aluminum oxide interlaminar insulation was applied to 125, 8 mil thick Hiperco 27 laminations (8 inch OD). The insulated laminations were made into a large Rowland Ring magnetic sample to evaluate the effectiveness of the plasma arc sprayed stack.

f) An electron beam welding technique was developed for use if needed in assembling the laminations into stator stacks. This method increases core losses by only five to ten percent as compared to 25 to 40 percent in cores which were inert-gas tungsten-arc welded.

2. Discussion

Figure IV-9 is a cutaway view of the stator assembly which shows the primary features of the design. The main magnetic frame is made from a Hiperco 27 (27Co-Fe) forging and the laminations are held in place in the frame by a magnetic ring which is also made from a Hiperco 27 forging. The stack consists of Hiperco 27 laminations 0.008 inch thick with a 0.0003 inch thick sapphire-like interlaminar insulation coating of plasma-arc sprayed Linde A compound (Al_2O_3). The stator is representative of one of the two stator stacks of a 15 kva, 12,000 rpm inductor generator and of the stator of a 12 horsepower, 12,000 rpm induction motor. The a-c stator has 36 teeth and slots which are proportioned approximately the same as those of an operating generator or motor.

The a-c stator winding is similar to that in a three-phase generator or motor stator. The winding is divided into three sections of twelve turns each. The overlapping of the sections is similar to that which occurs
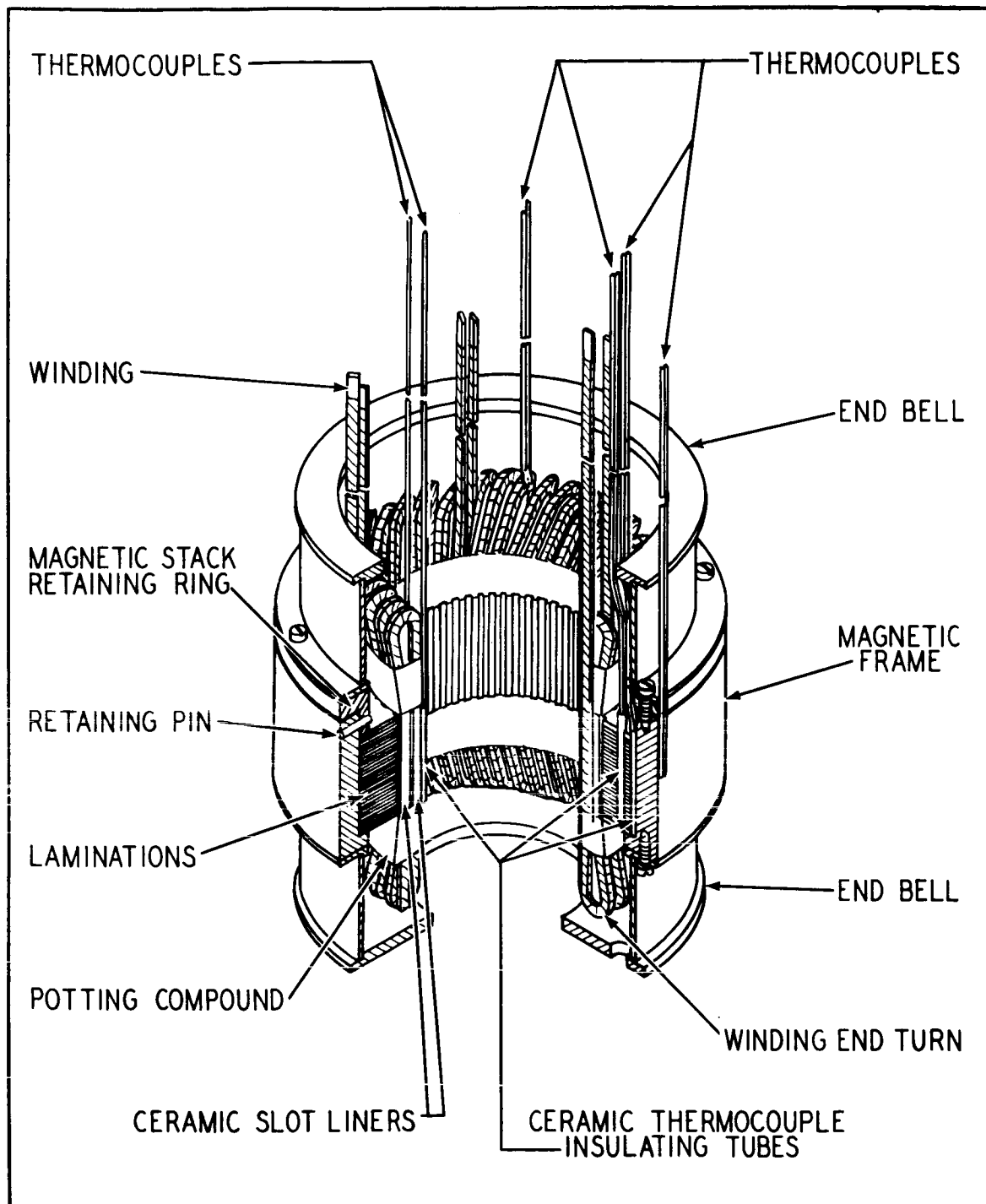
FIGURE IV-9. Cutaway View of Stator Without a Bore Seal

115

between the phases of a generator or motor winding. Thus, it is possible to make potential tests between windings and from winding to ground.

Stator ground insulation and insulation between turns was designed to withstand 500 volts d-c. The stator winding will be tested at this voltage before installation in the vacuum furnace.

Rated frequency of the stator is 400 cps. This frequency was chosen because it is a standard power system frequency where other comparative data are available and because it represents the approximate frequency where advanced space electric motors will operate.

The design of the stator was such that testing could be done at any frequency up to at least 1600 cps if desired. The losses in the stator when current is passed through the winding is the $I^2 R$ plus a small amount of core loss. At a frequency higher than 400 cps, there will be a slight increase in losses, but at 1600 cps, this increase will be less than ten percent.

Conductor wire is nickel-clad (20 percent of cross-section) silver coated with a six mil thick layer of Standard Anadur, a refractory-oxide-filled electrical glass fiber. Slot insulation is provided by ceramic (99% Al_2O_3) U-shaped channels (slot liners), spacers, and wedges. W-839, a zirconia base potting compound, is used to fill voids around the conductors in the slot liners and extends about half-way to the end turns to provide winding support.

Two thermocouples are installed in the slots in each winding. Additional pairs of thermocouples are located in the stack, between the stack outside diameter and the housing, on the outside diameter of the housing and on winding end turns. Hollow Al_2O_3 tubes are used as thermocouple insulators in the slot and stack areas.

The stator end bells are made from Hastelloy Alloy B which is a non-magnetic material having a thermal expansion coefficient very similar to that of Hiperco 27. Average thermal expansion coefficient for Hiperco 27 from 72° to 1100°F is 6.14 x 10^{-6} inches/inch-°F while the coefficient for Hastelloy Alloy B from 72° to 1200°F is 6.7 x 10^{-6} inches/inch-°F.

All materials and purchased parts for the stator assembly are either on hand or promised for delivery early in June. All the information required for the manufacture of components has been completed and issued to the shop. Manufacture of stator components was initiated in May and will be concluded in July.

Two thermal vacuum chambers and the associated control console were received from Varian Associates early in May. Provisions have been

116

made for installing the furnaces in the laboratory. The chambers were tested at Varian prior to shipping. Performance was excellent and pump-down was rapid. Pressures in the 10^{-11} torr range were obtained at room temperature and pressures in the 10^{-9} torr range were attained with a furnace temperature of over 2400°F when the furnace was clean, dry and empty.

A composite specification covering the cleaning of components and clean handling and assembly techniques for the stator assembly has been drafted in preliminary form and is being reviewed. Existing cleaning specifications have been defined when applicable and adequate, and new requirements have been specified as needed.

In general, all parts will be specifically cleaned except Anadur coated wire, potting compound and Al_2O_3 parts. These parts will be "cleaned" by bakeout to set the Anadur insulation. After cleaning each component it is to be stored in a plastic bag filled with dry Nitrogen and containing a desiccant. After the cleaning operation parts shall be handled only with clean, lint free gloves. Gloves shall also be used for handling all internal vacuum chamber and furnace parts. All specimen subassembly and assembly operations shall be performed at the "clean" bench using parts that have been cleaned previously and properly stored. The "clean" bench to be used constitutes a laminar air flow work station according to Federal Standard No. 209, "Clean Room and Work Station Requirements, Controlled Environment," and meets Class 10,000 of that specification.

The plasma-arc sprayed alumina interlaminar insulation described earlier was actually developed for the 1400°F test samples, but it has performed so well it will be used on the 1100°F samples. This alumina insulation is required since the aluminum-orthophosphate normally used is stable only at temperatures to 1100°F. Plasma-arc application of the ultra-fine Linde A alumina as interlaminar insulation would have been impossible without using a special fluidized feeding device developed previously by Westinghouse. Basically this device consists of a 48 inch long, 2-1/2 inch diameter tube with alumina powder at the bottom. Argon carrier gas passes through this alumina and up the tube to the gun carrying a fine mist of Al_2O_3 with it. A flexible coating 0.0003 inch thick is applied by this method. An eight inch diameter Rowland Ring made of Hiperco 27 alloy was insulated by this method and magnetically tested. Core-loss tests have verified that the alumina interlaminar insulation has a core loss (e.g. 30 watts/pound at 100 kilolines/inch^2 at room temperature and 400 cps) similar to laminations insulated with aluminum orthophosphate. The ring was then electron-beam welded and retested to determine what effect this method of joining laminations would have on performance. The d-c magnetization curves, core loss and volt-amperes/pound are shown in Figures IV-10, IV-11, and IV-12 in the as-plasma sprayed and as-plasma sprayed and electron-beam welded conditions.

FIGURE IV-10. DC Magnetization Curves as a Function of Induction at 400 cps for a Plasma Arc Sprayed Alumina Insulated Hiperco 27, 0.008 Inch Thick Laminated Core Before and After Electron Beam Welding
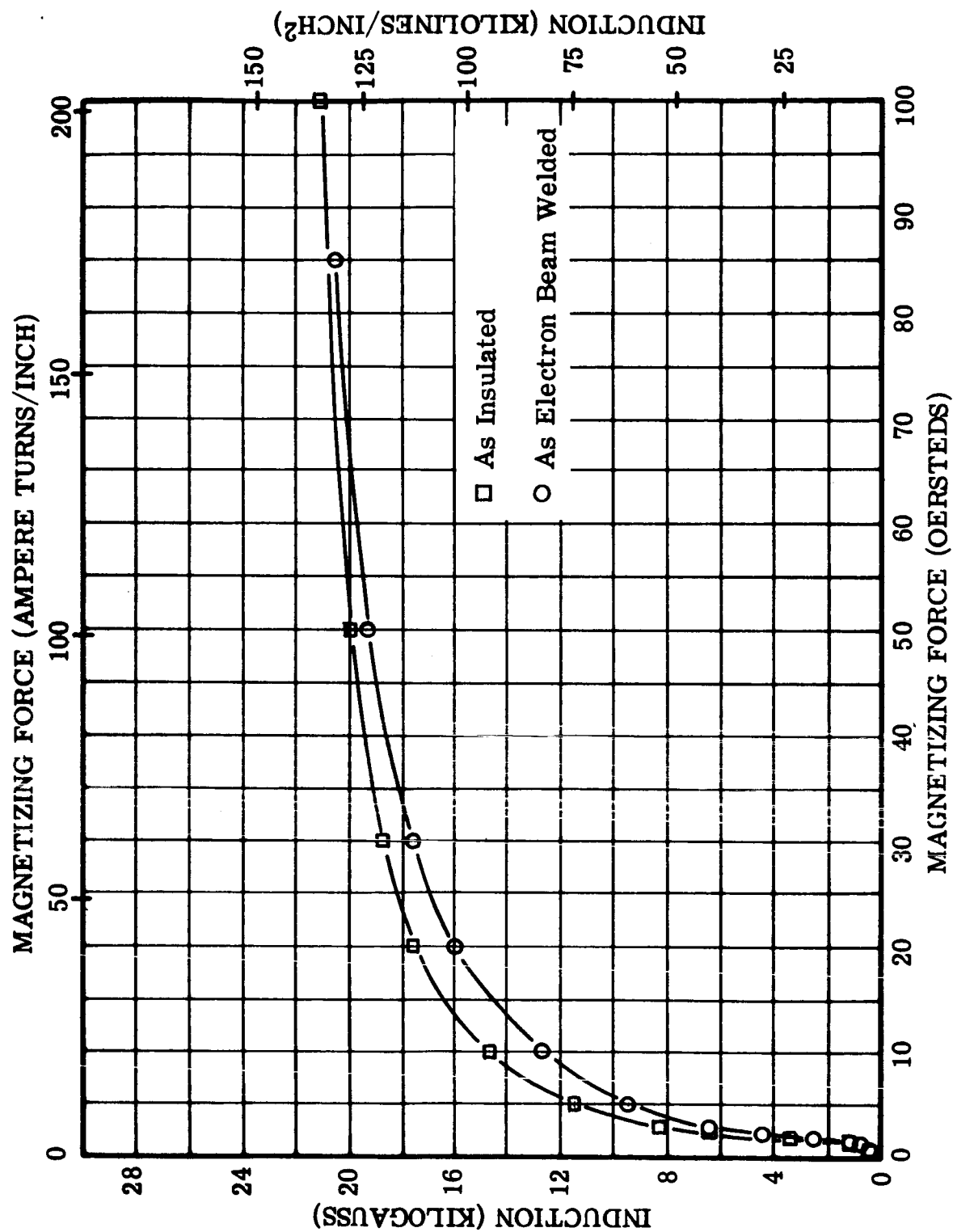
Figure IV-10. D-C Magnetization Hiperco 27 Before and After Electron Beam Welding

118

INDUCTION (KILOLINES/INCH²)

CORE LOSS (WATTS PER POUND)

INDUCTION (KILOGAUSS)

□ As Insulated

O As Electron Beam Welded
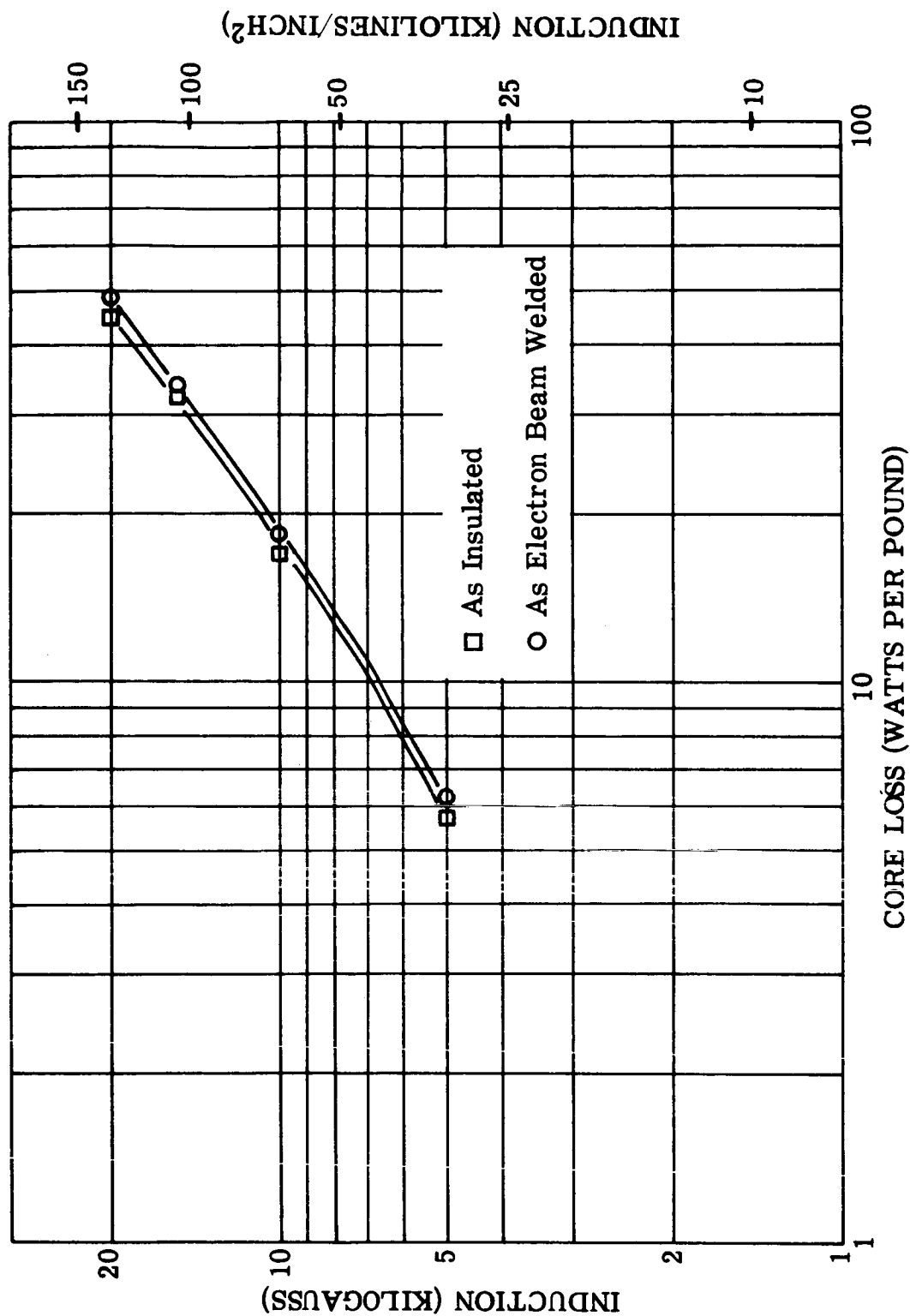
FIGURE IV-11.   Core Loss as a Function of Induction at 400 cps for a Plasma Arc Sprayed Alumina Insulated Hiperco 27, 0.008 Inch Thick Laminated Magnetic Core Before and After Electron Beam Welding

Figure IV-11.   Core Loss, 400 cps, Hiperco 27 Before and After Electron Beam Welding

119

FIGURE IV-12. Exciting Volt-Amperes Per Pound at 400 cps for a Plasma Arc
Sprayed Alumina Insulated Hiperco 27, 0.008 Inch Thick
Laminated Magnetic Core Before and After Electron
Beam Welding
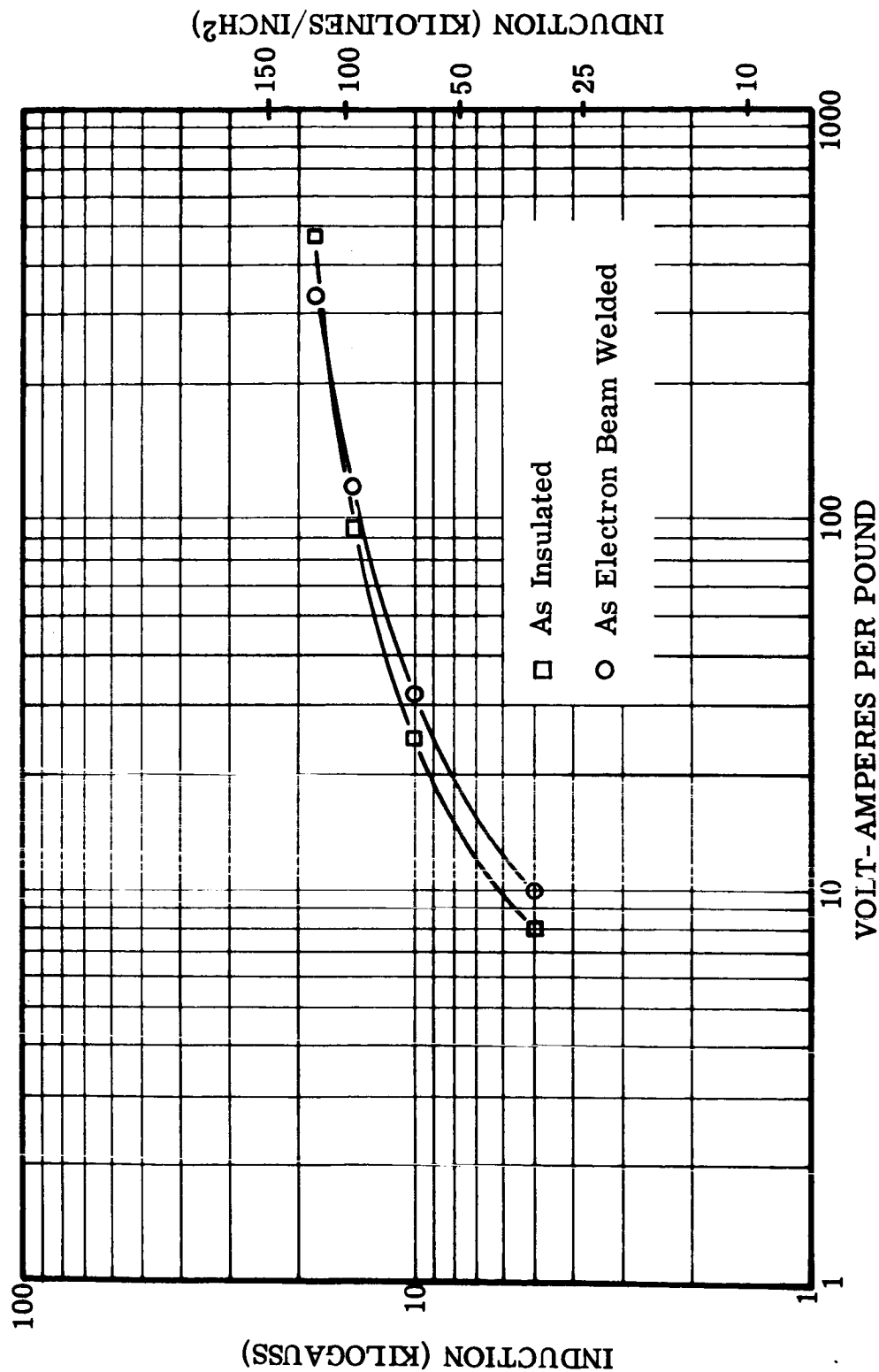
Figure IV-12.   Exciting VA, 400 cps, Hiperco 27 Before and
After Electron Beam Welding

Normal electrical degradation for TIG (Tungsten Inert Gas) welded Hiperco 27 stacks may approach 50 percent. However, the data using electron-beam welding show only 10 percent degradation at the lower inductions and suggests this as one possible method of joining stacked laminations with a minimum of magnetic property degradation.

3. Program for Next Quarter

    a) Complete the manufacture of stator component parts.

    b) Issue final material cleaning and clean assembly specifications.

    c) Complete furnace installation and check-out.

    d) Assemble the stator specimen and conduct bench tests for baseline data.

    e) Define thermal vacuum chamber operating procedure, criteria for terminating the test and a procedure for cleaning the chamber in the event it becomes contaminated.

    f) Begin a 5000 hour high-vacuum, 1100°F hot-spot test on the stator specimen.

    g) Continue the design of a bore seal for use in a second stator test.

C. TASK 3 - TRANSFORMER

1. Summary of Technical Progress

a) Hiperco 27 lamination stock 0.008 inch thick has been sent to a vendor for punching E-I core forms.

b) Anadur insulated nickel-clad silver wire for the primary and secondary windings was received late in May.

c) A fixture to support the transformer in the furnace was designed and is being manufactured.

d) Delivery of the Al_2O_3 parts which form the winding spool and end plates has been delayed approximately one month. These parts are being expedited.

e) A heat transfer calculation was made to obtain an approximation of the temperature gradient from the transformer core to the outside of the windings.

f) A simple, fluxless, argon atmosphere thermocouple-to-feed-through brazing technique was developed to bring thermocouple leads through the vacuum chamber wall. Sample joints have been mass spectometer leak checked and found to be vacuum tight. A vacuum tube grade braze alloy (72Ag-28Cu) was used in these joints.

2. Discussion

Figure IV-13 is a cutaway view of the vacuum furnace which shows two solenoids and the transformer installed in the furnace hot zone. Winding leads and thermocouple leads from the specimens are carried upward through holes in the top heat shields and then directed to their respective feedthroughs in the chamber wall. Some representative leads are shown in the figure. A total of eight winding leads and 24 thermocouple leads are carried through the chamber wall.

The vacuum chamber is of double wall construction with baffles between the walls to channel cooling water flow. The chamber top cover is also double-walled to provide a path for cooling water.

Figure IV-14 is a cutaway view of the transformer which shows the basic design features. The core is made from E-I style Hiperco 27 alloy laminations 0.008 inch thick with plasma-arc sprayed alumina as the inter laminar insulation (same as used on stator laminations). The windings

122
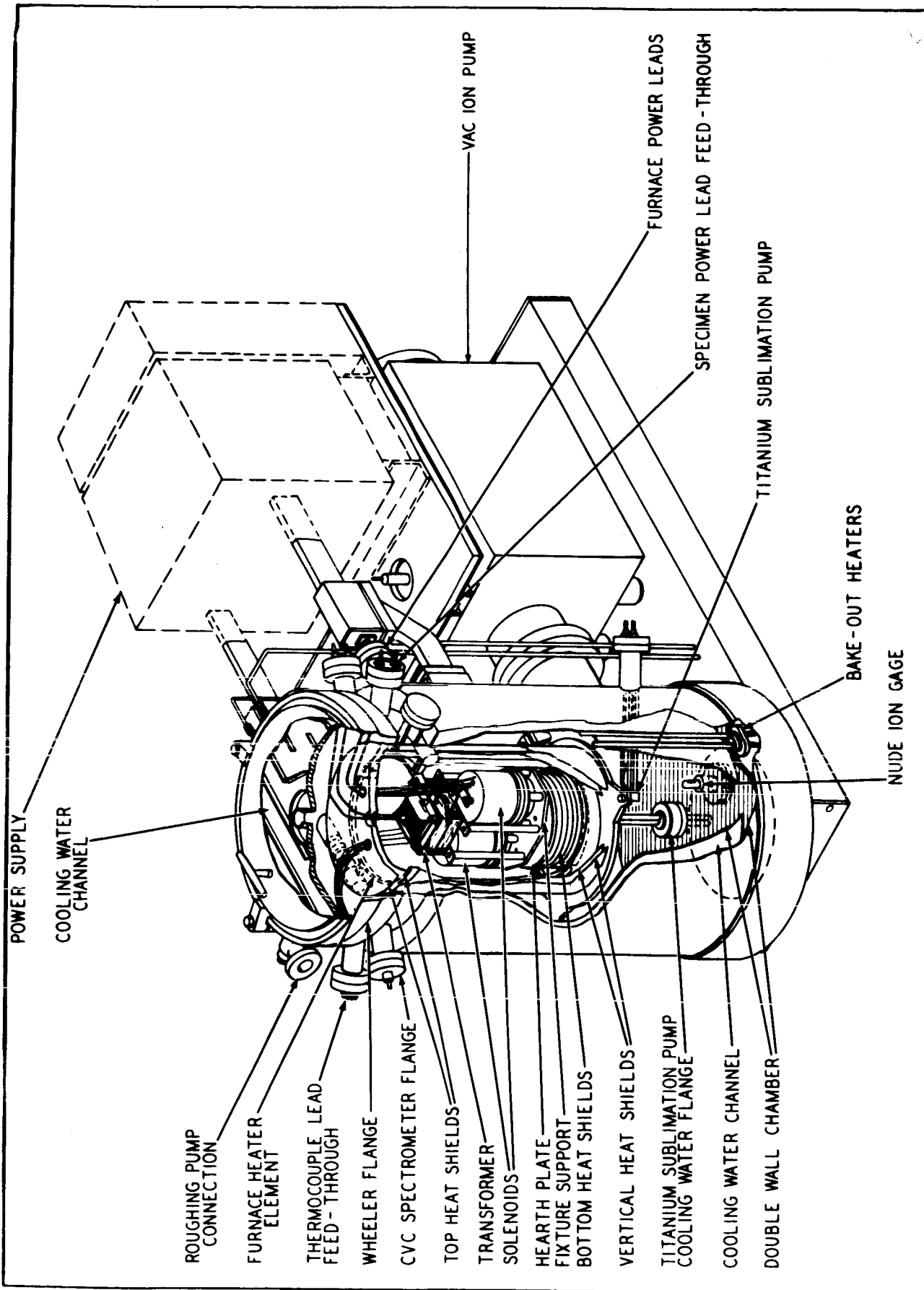
FIGURE IV-13. Cutaway View of a Vacuum Furnace Showing Installation of Two Solenoids and a Transformer

123
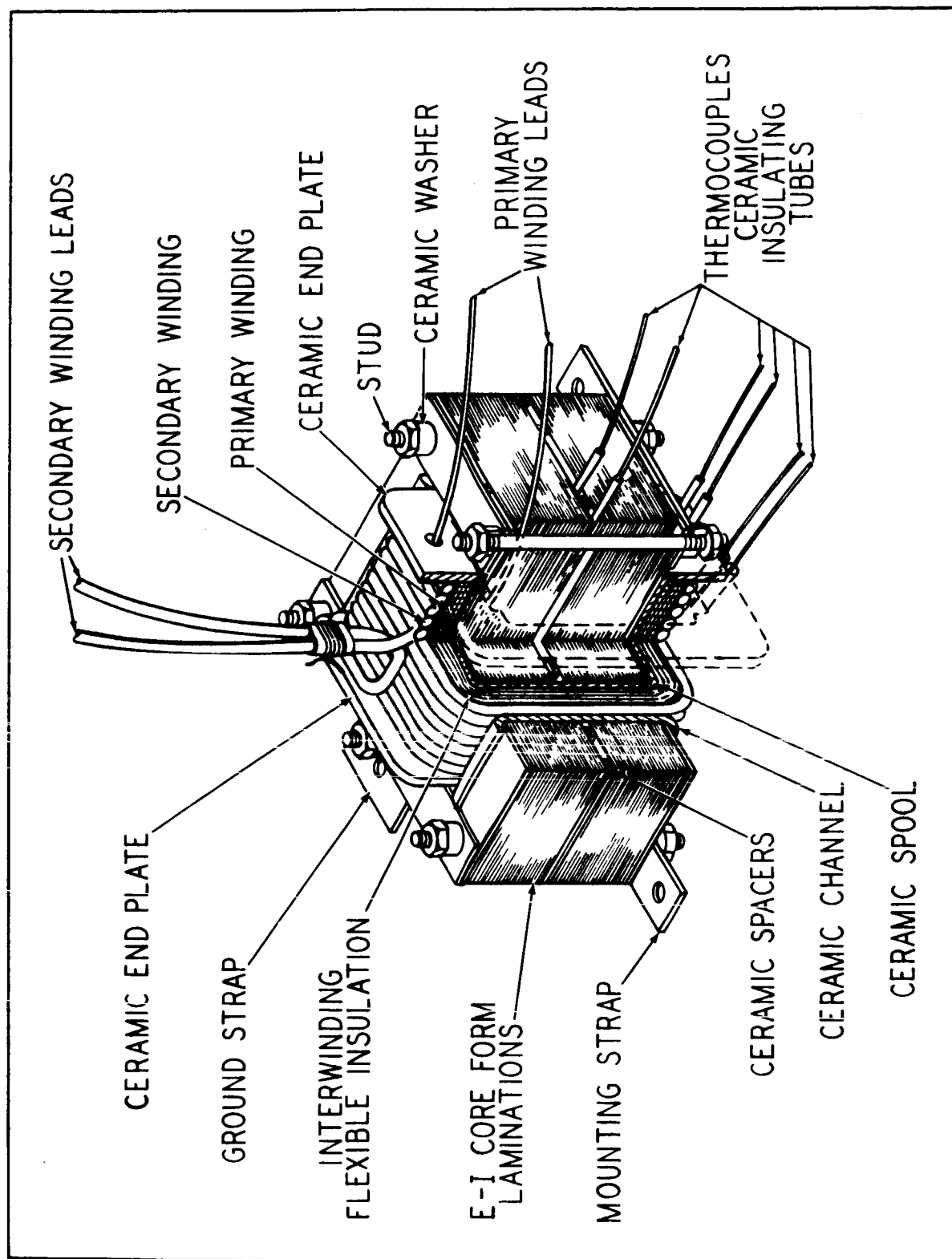
FIGURE IV-14. Cutaway View of Transformer

Labels: SECONDARY WINDING LEADS, SECONDARY WINDING, PRIMARY WINDING, CERAMIC END PLATE, STUD, CERAMIC WASHER, PRIMARY WINDING LEADS, THERMOCOUPLES, CERAMIC INSULATING TUBES, CERAMIC END PLATE, GROUND STRAP, INTERWINDING FLEXIBLE INSULATION, E-I CORE FORM LAMINATIONS, MOUNTING STRAP, CERAMIC SPACERS, CERAMIC CHANNEL, CERAMIC SPOOL

124

are formed around a ceramic (Al_2O_3) spool which provides insulation between the windings and the center leg of the core. Alumina end plates and channels provide insulation between the winding ends and sides and the laminations. Non-magnetic Hastelloy Alloy B strips are used outside the laminations to provide lamination support. The laminations and support strips are held together by through studs, ceramic washers, and lock nuts.

Pairs of thermocouples are installed between the primary winding and ceramic spool and between the two windings. The stack has been divided into two halves by ceramic strip spacers so that four thermocouples can be buried in the core.

This transformer design is rated at 1 kva at 400 cps with 600 volts on the primary winding and approximately 30 volts at the secondary winding. A frequency of 400 cps was chosen because of the availability of a reliable power source for the 5000 hour test at the rated conditions. The transformer can be operated at higher frequencies with little change in losses, provided the voltage is maintained at rated value. This single-phase transformer provides the technology for a three phase transformer having the same phase voltage which, when coupled in a wye network with a full-wave rectifier system, would provide 1400 volts d-c.

A heat transfer calculation was made to estimate the temperature gradient occurring from the laminated core to the outside of the secondary winding. For calculation purposes it was assumed that the windings and wire insulation had a square cross-section and that there was face-to-face contact between the wire insulation and the flexible insulation between layers. These assumptions resulted in a ΔT approximation of 47°F. The apparent thermal conductivity value used was based on tests run in vacuum under NAS3-4162 to obtain transverse heat flow across round insulated conductors mounted between two flat plates. The transformer thermocouples are placed so as to measure actual temperature changes across the accessible part of the windings.

It has been anticipated that construction of the transformer winding could be initiated before the end of May. However, subcontractor difficulties in forming the Al_2O_3 spool and end plates used to insulate the windings from the core has resulted in a projected delivery delay of approximately one month for these parts. Improvement in delivery dates is being attempted. The Anadur insulated nickel-clad silver wire for both primary and secondary windings was received late in May.

A composite specification covering the cleaning of components and clean handling and assembly techniques for the transformer assembly has been prepared in preliminary form and is being reviewed. The same overall requirements apply here as were mentioned earlier in the stator discussion.

3. <u>Program for Next Quarter</u>

a) Complete the manufacture of transformer component parts.

b) Issue final material cleaning and clean assembly specifications.

c) Assemble the transformer specimen and conduct bench tests for base-line data.

d) Define thermal vacuum chamber operating procedure, criteria for terminating the test if necessary, and a procedure for cleaning the chamber in the event it becomes contaminated.

e) Begin 5000 hour high vacuum 1100°F hotspot test on the transformer assembly.

D. TASK 4 - SOLENOID

1. Summary of Technical Progress

a) Material for manufacturing two Hiperco 27 (27Co-Fe) solenoid housings has been rough machined from forging stock.

b) Anadur-insulated nickel-clad silver wire for the solenoid winding was received late in May.

c) All ceramic (Al_2O_3) components used in the solenoid design were received late in May.

d) A heat transfer calculation was made to obtain an approximation of the temperature gradient from the inside diameter of the solenoid winding to the outside diameter of the solenoid housing.

e) A fixture to support the solenoids in the furnace was designed and is being manufactured.

2. Discussion

Figure IV-13, presented earlier, shows the two solenoids installed in a vacuum furnace along with one transformer assembly. Each solenoid is instrumented with eight thermocouples which are located to give the maximum amount of temperature information during the 5000 hour test. Pairs of thermocouples are located at the inside diameter of the winding, at the halfway point radially in the winding, between the winding outside diameter and the housing inside diameter, and on the housing outside diameter.

Figure IV-15 is a cutaway view of the solenoid showing the location of the coil leads and thermocouple leads. A weight of three pounds is suspended on the plunger, and when the solenoid is actuated the weight is lifted approximately 0.050 inch and held in that position. The solenoid magnetic housing, cover and plunger are made from Hiperco 27 forged material. The coil is wound on an alumina spool which provides insulation between the winding and the plunger and housing center core. Alumina end plates insulate the sides of the winding from the housing and cover. Bearing surfaces for the plunger consist of an alumina guide rod at one end of the plunger and an alumina bushing at the opposite end.

Electrically the solenoid design is rated at 1530 ampere turns with 28 volts d-c applied to the winding at 1100°F.

127

THERMOCOUPLES

COIL LEADS

CERAMIC END PLATE

GUIDE ROD
RETAINER

MAGNETIC
HOUSING

CERAMIC
GUIDE ROD

POTTING
COMPOUND

CERAMIC SPOOL

PLUNGER

COIL

CERAMIC
END PLATE

MAGNETIC
COVER

PLUNGER
STOP PLATE

POTTING
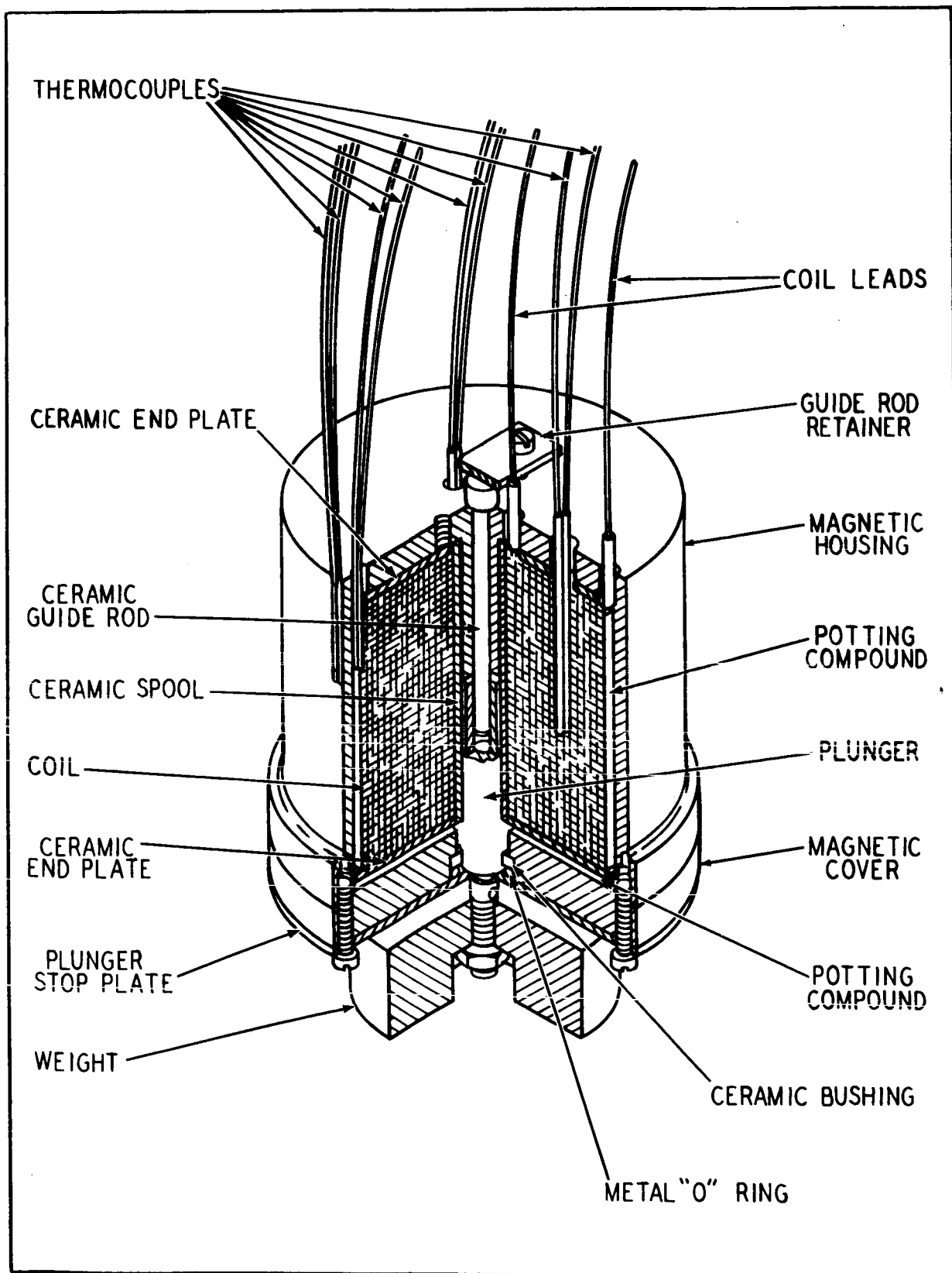COMPOUND

WEIGHT

CERAMIC BUSHING

METAL "O" RING

FIGURE IV-15.   Cutaway View of Solenoid

128

All Al_2O_3 components used in the solenoid design were received late in May. The insulated nickel-clad silver wire was also received late in May. Winding of the solenoid coils can be started as soon as a special winding arbor tool is available. This tool is being manufactured and completion is promised by the second week in June.

A heat transfer calculation was made to obtain an approximation of the temperature gradient that will occur across the winding when the solenoid is actuated. For calculation purposes it was assumed that the wire and wire insulation had a square cross-section and that there was face-to-face contact between layers of the winding. It was further assumed that 28 volts d-c would be applied to actuate the solenoid but that seven volts d-c would hold the plunger in position after actuation. These assumptions resulted in a ΔT approximation of 2°F. The apparent thermal conductivity value used was based on tests run in a vacuum under NAS3-4162 to obtain transverse heat flow across round insulated conductors mounted between two flat plates. During the 5000 hour high vacuum, high temperature test, temperature gradients will be obtained at several holding voltages to obtain as much thermal conductance information as possible.

A composite specification covering the cleaning of components and clean handling and assembly techniques for the solenoid assembly has been prepared in preliminary form and is being reviewed. The same overall requirements apply here as were discussed earlier in the stator section.

3. Program for Next Quarter

   a) Complete the manufacture of solenoid component parts.

   b) Issue final material cleaning and clean assembly specifications.

   c) Assemble the two solenoid specimens and conduct bench tests for base-line data.

   d) Define a thermal vacuum chamber operating procedure, criteria for terminating the test if necessary, and a procedure for cleaning the chamber in the event it becomes contaminated.

   e) Begin a 5000 hour high-vacuum 1100°F hot-spot test on two solenoid assemblies.

SECTION V

REFERENCES

Section II
Program I - Magnetic Materials for High-Temperature Operation

References for Task 1 - Optimized Precipitation Hardened Magnetic Materials for High Temperature Application

1. Bozarth, R. M., Ferromagnetism, D. VanNostrand Co., Fig. 5-77, p. 162; Fig. 5-80, p. 165, 1951.

2. Preuss A., A Dissertation, Magnetic Properties of Fe-Co Alloys at Different Temperatures, Univ. Zurich, 1912.

3. Elmen, G. W., Magnetic Alloys of Iron, Nickel and Cobalt, J. Franklin Institute, v. 207, p. 583, 1929.

4. Pshchenkova, G. V., A. D. Skokov, The Temperature Dependence of Magnetic Induction in Fe-Co Alloys, Physics of Metals and Metallography, USSR, v. 14, p. 797, 1962.

5. Decker, R. F., R. R. DeWitt, Trends in High Temperature Alloys, Journal of Metals, v. 17 No. 2, p. 139, 1965.

6. Decker, R. F., S. Floreen, Precipitation from Substitutional Iron Base Austenitic and Martensitic Solid Solutions, Symposium; Precipitation from Iron Base Alloys, Intersc. Div., John Wiley, in press.

7. Decker, R. F., R. B. Yeo, J. T. Eash, C. G. Bieber, Maraging Steels, Materials in Design Engineering, May 1962.

8. Decker, R. F., J. T. Eash, A. J. Goldmann, 18% Nickel Maraging Steel, Trans. ASM, v. 55, p. 58, 1962.

9. Floreen. S., R. F. Decker, Maraging Steel for 1000°F Service, Trans. ASM, v. 56, p. 403, Sept. 1963.

10. Sadowski, E. P., Development of 12% Nickel Maraging Steel, **ASM, Metals Engrg.**, v. 5, p. 56, 1965.

11. Kueser, P. E., Magnetic Materials Topical Report, NASA-CR-54091, Contract NAS 3-4162, 1964.

12. Detert, K., Investigation of the Transformation and Precipitation Processes in 15% Maraging Steel, **Trans. ASM,** to be published.

13. Kase, T., On the Equilibrium Diagram of the Iron-Cobalt-Nickel System, **Tohoku University Sci. Rept.**, v. 16, p. 491, 1927.

14. Floreen, S., and G. R. Speich, Some Observations on the Strength and Toughness of Maraging Steels, **Trans. ASM,** v. 57, p. 714, 1964.

15. Hansen, M., **Constitution of Binary Alloys,** McGraw Hill, 1958.

16. Freche, J. C., R. L. Ashbrook, I. J. Klima, Cobalt Base Alloys for Space Power Systems, **J. Metals,** v. 15, p. 928, 1963.

17. Cochardt, A., Die Anwendung des Magneto-Mechanischen Effectes für Legierungen mit Hoher Dämpfung und Festigkeit, **Z. Metallkunde,** v. 50, p. 203, 1959.

18. Schramm, J., Das Dreistoffsystem Nickel-Kobalt-Aluminium, **Z. Metallkunde,** v. 55, p. 403, 1941.

19. Detert, K., G. Pohl, Untersuchung über die Ausscheidungsvorgänge in Nickel-Kobalt Legierungen mit Aluminium-Titan Zusätzen, **Z. Metallkunde,** v. 55, p. 35, 1964.

20. Detert, K., G. Pohl, Untersuchungen über die Ausscheidungsvorgänge in Co-Ni Legierungen mit Al and Ti Zusätzen, **Z. Metallkunde,** in press.

21. Hagel, W. C., H. J. Beattie, High Temperature Aging Structures in γ' Hardened Austentic Alloys, **Trans. AIME,** v. 215, p. 967, 1959.

22. Mihalisin, J. R., R. F. Decker, Phase Transformations in Nickel-Rich Nickel-Titanium-Aluminum Alloys, **Trans. AIME,** v. 218, p. 507, 1960.

23. Pfiefer, W. A., Levitation Melting, A Survey of State-of-the-Art, **J. of Metals,** v. 17, p. 487, May 1965.

References for Task 2 - Investigation for Raising the Alpha to Gamma
Transformation Temperature in Cobalt-Iron Alloys.

24. Preuss, A., A. Dissertation, Magnetic Properties of Fe-Co Alloys
at Different Temperatures, Univ. Zurich, 1912.

25. Pschenkova, G. V., A. D. Skokov, The Temperature Dependence of
Magnetic Induction in Fe-Co Alloys, Physics of Metals and
Metallography, USSR, v. 14, p. 797, 1962.

26. Chen, C. W., Soft Magnetic Cobalt-Iron Alloys, Cobalt, v. 22,
March 1964.

27. Hansen, M., Constitution of Binary Alloys, McGraw Hill, 1958.

References for Task 3 - Dispersion-Strengthened Magnetic Materials for
Application in the 1200-1600°F Range.

28. R. T. Phelps, E. A. Gulbransen, and J. W. Hickman, "Electron
Diffraction and Electron Microscope Study of Oxide Films Formed
on Metals and Alloys at Moderate Temperatures," Ind. Eng. Chem.,
v. 18, June 14, 1946, p. 391.

29. E. A. Gulbransen and K. F. Andrew, "The Kinetics of the Oxidation
of Cobalt," J. Electrochem. Soc., v. 98, No. 6, p. 241, June 1951.

30. A. Preece and G. Lucas, "The High-Temperature Oxidation of Some
Cobalt-Base and Nickel-Base Alloys," J. Inst. Metals, v. 81, p. 219,
1952-53.

31. C. A. Phalnikar, E. B. Evans, and W. M. Baldwin, Jr., "High
Temperature Scaling of Co-Cr Alloys," J. Electrochem. Soc.,
v. 103, No. 8, pp. 429-438, August 1956.

32. D. W. Bridges, J. P. Baur, and W. M. Fassell, Jr., "Effect of
Oxygen Pressure on the Oxidation Rate of Cobalt," J. Electrochem.
Soc., v. 103, pp. 614-618, 1956.

33. B. Fisher and D. S. Tannhauser, "The Phase Diagram of Cobalt
Monoxide at High Temperatures," J. Electrochem. Soc., v. 111,
pp. 1194-1196, 1964.

34. F. R. Morral, "Identification of Corrosion Products on Cobalt and Cobalt Alloys," Corrosion, v. 18, No. 11, pp. 421t-423t, November 1962.

35. F. R. Morral, "Informative Abstracts on Corrosion of Cobalt and Cobalt Alloys," Cobalt Information Center, Battelle Memorial Institute.

36. E. A. Gulbransen, R. T. Phelps, and J. W. Hickman, "Oxide Films Formed on Alloys at Moderate Temperatures," Ind. Eng. Chem., v. 18, p. 640, October 15, 1946.

37. J. W. Hickman and E. A. Gulbransen, "Electron Diffraction Study of Oxide Films Formed on Alloys of Iron, Cobalt, Nickel and Chromium at High Temperatures," Metals Tech., v. 13, No. 7, pp. 1-26, October 1946, TP 2069.

38. E. Aukrust and A. Muan, "Thermodynamic Porperties of Solid Solutions with Spinel-Type Structure: II. The System Co_3O_4-Fe_3O_4 at 1200°C," Trans. Met. Soc. AIME, v. 230, No. 6, pp. 1395-1399, October 1964.

39. E. Aukrust and A. Muan, "Activities of Components in Oxide Solid Solutions: The Systems CoO-MgO, CoO-MnO, and Co-"FeO" at 1200°C," Trans. Met. Soc. AIME, v. 227, No. 6, pp. 1378-1380, December 1963.

40. Brazing Manual, American Welding Society, 1963, p. 62.

41. W. H. Chang, "A Dew Point-Temperature Diagram for Metal-Metal Oxide Equilibria in Hydrogen Atmospheres," Welding Journal, v. 35, No. 12, pp. 662-s to 624-s, December 1956.

42. A. Preece and G. Lucas, "The High-Temperature Oxidation of Some Cobalt-Base and Nickel-Base Alloys," J. Inst. Metals, v. 81, p. 219, 1952-53.

43. C. H. Lund and H. J. Wagner, "Oxidation of Nickel and Cobalt Base Superalloys," DMIC Report 214, March 1, 1965, p. 3.

44. W. C. Hagel, "The Oxidation of Iron, Nickel, and Cobalt Base Alloys Containing Aluminum," paper presented at the 2nd International Congress on Metallic Corrosion sponsored by the National Association of Corrosion Engineers, New York, N. Y., March 11-15, 1963.

45. J. S. Wolf and E. B. Evans, "Effect of Oxygen Pressure on Internal Oxidation of Nickel-Aluminum Alloys," Corrosion, v. 18, No. 4, pp. 129t-136t, April 1962.

46. N. Komatsu, L. J. Bonis, and N. J. Grant, "Some Features of Internal Oxidation of Dilute Copper and Nickel Alloys for Dispersion Strengthening," Powder Metallurgy, Ed. by W. Leszynski, Interscience Publishers, pp. 343-358, 1961.

47. O. Preston and N. J. Grant, "Dispersion Strengthening of Copper by Internal Oxidation," Trans. Met. Soc. AIME, v. 221, No. 1, pp. 164-172, February 1961.

48. M. H. Lewis, R. H. Seebohm and J. W. Martin, Powder Metallurgy, No. 10, pp. 87-107, 1962.

49. A Gatti, "Iron-Alumina Materials," Trans. Met. Soc. AIME, v. 215, pp. 753-755, October 1959.

Section III
Program II - High Temperature Capacitor Feasibility References

1. Dummer, G. W. A., H. M. Nordenburg, Fixed and Variable Capacitors, McGraw-Hill Book Company, Inc., 1960, p. 180.

2. Myers, S. L., H. W. Stetson, "A New Technique for Diamond Polishing Alumina (Al_2O_3) Ceramics, "Presented at 67th Annual Meeting, American Ceramic Society, May 1965.

3. Snavely, W. H., "High Temperature Alkali Metal Resistant Insulation," AFAPL-TR-62-22, March 1965.

Section IV
Program III - Bore Seal Development and Combined Material
Investigation under a Space-Simulated Environment

References for Task 1 - Bore Seal Development

1. Waits, R. K. and Harra, D., "The Outgassing of Alumina Ceramic Sapphire and Kovar," TR-22 for Sandia Corporation, March 1960.

2. Kueser, P. E. et al, Bore Seal Technology, NASA-CR-54093, Contract NAS 3-4162, 1964.

APPENDIX A

SPECIFICATIONS AND PROCEDURES

APPENDIX A

SPECIFICATIONS AND PROCEDURES

1. ### Dye Check Procedure

   A. **OBJECTIVE:**

   To aid in the inspection of incoming raw ceramics for chips, scratches, pits, pocks, cracks, porosity, etc.

   B. **PROCEDURE:**

      1) Dip in Rhodamine B solution.

      2) Hot tap water rinse.

      3) Two methyl alcohol rinses.

      4) Dry and inspect.

2. ### Ceramic Cleaning Procedure

   A. **OBJECTIVE:**

   The purpose of this procedure is to assure that all foreign matter is removed from ceramic rings and cylinders prior to metallizing or brazing.

   B. **PRECAUTIONS:**

   After this cleaning procedure has been started, ceramic parts shall not be handled with the bare hands. Regular Wilson Natural Latex Industrial gloves are to be used. Air hoses are not to be used for drying ceramic parts. Routing tags and other identification tags should not be placed where the ink, dye, or other substances from them might contaminate the ceramic parts. The practice of stacking ceramics one on the other must be avoided as this tends to chip and otherwise damage them.

C. PROCEDURE:

1) Immerse the ceramic for 15 to 20 minutes in detergent solution "A" (Triton X100) which is maintained at a temperature of $131° \pm 5°F$ ($55° \pm 3°C$).

2) The ceramic parts should be rotated or agitated several times during the period of immersion.

3) Remove the parts from the detergent solution and scrub with a nylon brush and detergent solution. Step 3 applies to the larger (3-4 inch diameter) size ceramic cylinders.

4) Rinse the ceramic part thoroughly in hot running water.

5) Rinse the ceramic part thoroughly in running de-ionized water.

6) Rinse the ceramic part in a shallow container of acetone by rotating the part on its side. NOTE: Discard the acetone after rinsing each ceramic part (large ceramic parts only).

7) Rinse in fresh acetone as in Step 6. This acetone may be used as the first acetone rinse for the next ceramic.

8) Place the ceramic on clean tissue and allow to thoroughly dry. NOTE: If the parts are to be stored, they should be wrapped in a double thickness of tissue. Large ceramic parts should be wrapped individually.

3. Procedure for the Application of Active Metal Brazing Alloy

A. OBJECTIVE:

To increase uniformity of braze joint thickness.

B. PROCEDURE:

1) Clean and/or fire all required parts by appropriate cleaning procedure and store in suitable containers to maintain cleanliness until use.

2) Utilize clean work area for assembly. For large assemblies which require over five minutes to prepare, use a laminar-flow assembly bench.

3) Utilize clean assembly techniques, clean gloves, finger cots, tools and jigs, clean and dust free work surface, etc.

4) Apply braze alloy to joint area by method 4a) or 4b) below.

    a) Powder form: Suspend powder ($<$ 50 mesh) in Butyl Methacrylate lacquer.

        360g Butyl Methacrylate (Lucite #44)
        1500g Butyl Alcohol (C.P.)
        1500g Butyl Acetate (C.P.)

    Apply evenly to appropriate ceramic surface(s) with small spatula at approximately 0.5g per square inch, as determined by experience.

    b) Foil form: Cut foil (normally 0.001-0.003 inch thick) to exact seal area geometry, or as dictated by foil thickness and experience. Place in seal area. Tack in place with methacrylate lacquer (see 4a), if necessary.

5) Assemble ceramic and metal parts for brazing in appropriate clean braze jig and put weights in position if required. Normally, molybdenum or tungsten weights are to be used. Record the type and size of weights in the Brazing Log Book.

6) Place jigs containing unbrazed assemblies in vacuum brazing furnace chamber and check part alignment and weight position before closing furnace.

7) Record alloy form and weight used in the Brazing Log Book.

4. Vacuum Brazing Procedure

A. OBJECTIVE:

To insure reproducibility of the brazing cycle.

B. PROCEDURE:

1) Load the vacuum furnace with the same number and distribution of parts and jigs as was used in the original time-temperature determination for a specific alloy.

2) Close the furnace, bell jar, etc., and slowly raise temperature, keeping pressure below 5×10^{-5} torr.

3) Fill out Brazing Log Sheet and maintain time, temperature and vacuum log.

4) Hold the temperature for 10 minutes at 200°F below brazing temperature to allow the furnace to reach equilibrium at 1×10^{-5} torr.

5) Increase the temperature rapidly to the brazing temperature and hold for five minutes. Monitor the temperature closely.

6) Allow the parts to cool to 400°F or less in vacuum, then back-fill with helium.

7) Allow the parts to cool 15 minutes in helium before opening the furnace.

8) Complete Brazing Log information.

5. Tentative Alkali Metal Loading Procedure

The welding of the columbium-1% zirconium capsules and loading of these capsules with test assemblies and with potassium and lithium will be carried out under vacuum in a chamber with appropriate fixtures and accessories.

The chamber is a General Technology Model Mark 5A modified to accommodate the special accessories for electron beam welding and alkali metal loading. The evacuation system consists of a 15 cfm Welsh forepump Model No. 1397B, and 1500 liters/sec diffusion pump NRC Model No. HK6 with a Freon 12 cooled chevron ring baffle CVC Model No. BCRU60.

The welding equipment consists of a BTI (Brad Thompson Industries) 6 kw power supply and electron beam gun (BTI No. 786). The gun is mounted on a support boom (BTI No. 215-7) providing X, Y, and Z translation; the X motion being power driven. A modified power driven, variable speed turn-table (BTI No. 1920-12) and manipulators (MRC No. V4-120) complete the modified handling apparatus.

The alkali metal transfer plumbing has been modified from that used in loading under pure argon. The major change is in the transfer line between the external valve and the alkali metal receiver inside the chamber (see Figure

140

IV-10). Prior to loading alkali metal into the test capsules, the alkali metal will have been Zr hot-trapped at 1400°F for 24 hours.

The capsules, test samples, lids and all other parts which could contact the alkali metal or capsule interior will have been fired to approximately 1300°F in a vacuum of better than 1×10^{-5} torr; then cooled, let down to a helium atmosphere, and transferred into the loading chamber just prior to the loading operation.

The freshly hot trapped alkali metal is then flushed through the transfer line into a receiver cup on a pedestal and the excess allowed to flow into the over-flow cup directly below the receiver cup. A recently vacuum-fired 1 cc Cb-1Zr cup is then placed on the receiver pedestal and partially filled with alkali metal for the corrosion test. The 1 cc cup has small holes to receive the fingers of the manipulator which is used to transfer the cup containing the alkali metal into a test capsule. The ceramic-metal test assemblies which have been previously vacuum fired are then placed in the capsule. The lid which has a radiation shield on the bottom side and a handling hook on the top side is then placed in position.

The purpose of this loading technique is (1) to get all of the potassium (or lithium) into the bottom of the capsule and preclude its sticking to the side walls, and (2) to shield the alkali metal from the electron beam by means of the ceramic-metal assemblies and the radiation shield on the lid. Con-duction of heat down the capsule walls towards the potassium (or lithium) will be dissipated by the electron beam centering fixture. This fixture is designed for easy loading with subsequent firm positioning by means of a manipulator-operable spring-loaded clamp.

After loading and sealing, the top capsule weld will be annealed for one hour at 2200°F, prior to loading into the vacuum furnace for the exposure test.